Heat Transfer in the Thick Thermoset Composites

Proefschrift

ter verkrijging van de graad van doctor
aan de Technische Universiteit Delft,
op gezag van de Rector Magnificus prof.ir. K.C.A.M. Luyben;
voorzitter van het College voor Promoties,
in het openbaar te verdedigen op
maandag 22 februari 2016 om 15:00 uur

door

Lei SHI

Master of Aeronautical and Astronautical Manufacturing Engineering,
Northwestern Polytechnical University, China
geboren te Zhangjiagang, Jiangsu, China

This dissertation has been approved by the

promotor: Prof.dr.ir. R. Benedictus
copromotor: Prof.dr.ir. K.M.B. Jansen

Composition of the doctoral committee:

Rector Magnificus	chairman
Prof.dr.ir. R. Benedictus	Delft University of Technology
Prof.dr.ir. K.M.B. Jansen	Delft University of Technology

Independent members:

Prof.Dr.-Ing. K.U. Schröder	RWTH Aachen, Duitsland
Prof.dr.ir. R. Akkerman	University of Twente
Prof.dr. S.J. Picken	Delft University of Technology
Prof.dr.ir. R. Marissen	Delft University of Technology
Dr. H. Luinge	TenCate Advanced Composites

This research was funded by the China Scholarship Council (CSC).

ISBN: 9789462954595

Cover design by Lei Shi

Printed in the Netherlands by Uitgeverij BOXPress || Proefschriftmaken.nl

To my family

Summary

Nowadays we are witnessing the emergence of many new advanced materials such as the composite materials used in aerospace and off shore industries. One of the trends in this area is the exploration of the possibility of manufacturing large composite structures that aims to replace the traditional metallic structural materials. However, with the increase of the size of the composite products, also the difficulty of manufacturing increases. Moreover, for thick thermoset composites, the size not only influences the mechanical properties in the completed products, but also the core temperature overshoot generated during the manufacturing has to be well-controlled.

For glassfiber reinforced epoxy composites, it is known that the curing reaction heat is a main factor that causes a significant temperature overshoot during cure. Therefore, a thermo-chemical model consisting of the heat transfer equation coupled with cure kinetics was then established to evaluate the temperature distributions in the composites.

In order to model the heat transfer process, material properties such as the density, thermal conductivity, heat capacity and cure kinetic parameters of the resin and composite have to be studied and determined. A global fitting method was introduced to find the solution of the cure kinetic parameters in the full experimental temperature range. As a low thermal conductive material, this composite cannot dissipate the reaction heat in time and is heated up inside-out quickly. This part of the work can give us a clear view of the thermal behavior in thick composites and helps us to understand the magnitude of the temperature overshoot created in the core.

In this thesis, the research work can be divided into three parts: analytical modeling, numerical modeling and experimental validation. First of all, an analytical model of the core temperature rise was derived based on a thermo-chemical model. An 1D transient heat transfer equation was then established to evaluate the temperature distributions through the thickness of the composite. Here the study only focused on the moment when it reached the maximum

temperature in the core. By using a non-dimensionalization process, the governing equation was finally transferred in a second order differential equation with a single dimensionless number. This dimensionless number revealed the relationship between the core temperature, and the curing temperature applied to the mold, the thickness of the composite and the cure kinetics of the resin. This resulted in a critical dimensionless number as well as a critical thickness above which the processing is impossible without an uncontrolled temperature overshoot in the thick thermoset composites during manufacturing.

Secondly, a numerical study was performed to predict the temperature distributions as well as the degree of cure. Here a 3D heat transfer model was built up that can provide more accurate predictions. In order to simulate the cure kinetics, a coefficient form partial differential equation (PDE) was added into the heat transfer model. The results showed that the temperature in the core first increased to the maximum value and then decreased to its initial value which had the same trend as its reaction heat. Furthermore, because of the temperature gradient through the thickness, it also created a large gradient in the degree of cure which may result in undesired residual stresses.

Finally, experimental validation was carried out to verify the thermo-chemical model. The vacuum infusion process (VIP) was used for manufacturing the composites. The experiments mainly focused on composites whose thickness excesses the critical values mentioned above. It was found that the infusion time has to be taken into consideration for these thick composites to improve the accuracy of the numerical solutions. Both of the numerical and experimental results showed that the maximum temperature in the thick composites will increase with the curing temperature as well as the thickness.

Samenvatting

Tegenwoordig zien we veel nieuwe geavanceerde materialen hun weg vinden naar de luchtvaart-, ruimtevaart- en offshore-industrie. Een van de trends op dat gebied is de verkenning van de mogelijkheid om grote composieten onderdelen te produceren met als doel de vervanging van traditionele metalen constructiematerialen. Maar met toenemende grootte van de composieten onderdelen, wordt ook de productie lastiger. Bovendien beïnvloedt de grootte voor dikke thermoharder composieten niet alleen de mechanische eigenschappen van het eindproduct, maar moet ook de temperatuurpiek in de kern worden gecontroleerd.

Van glasvezel versterkte epoxy composieten is het bekend dat de reactiewarmte ten gevolgde van de uitharding een van de hoofdoorzaken is van de lokale temperatuurpiek gedurende uitharding. Daarom is er een thermisch-chemisch model ontwikkeld dat bestaat uit de warmteoverdrachtsvergelijking gekoppeld aan de uithardingskinetica om de temperatuurverdeling te evalueren.

Om het warmteoverdrachtsproces te modeleren dienen materiaaleigenschappen zoals dichtheid, thermische geleiding, warmtecapaciteit en de parameters van de uithardingskinetica te worden bestudeerd en bepaald. Een globale passingsmethode is geïntroduceerd om de oplossing van de parameters van de uithardingskinetica over het gehele experimentbereik te vinden. Als laag thermisch geleidend materiaal , kan dit composiet de reactiewarmte niet binnen afzienbare tijd dissiperen en warmt het intern snel op. Dit deel van het werk kan ons een duidelijk beeld geven van het thermisch gedrag in dikke composieten en helpt ons om de grootte van de kerntemperatuurpiek te begrijpen.

Het onderzoekswerk in deze thesis kan in drie delen worden gesplitst: analytisch modelleren, numeriek modelleren en experimentele validatie. Ten eerste, een analytisch model van de kerntemperatuurtoename was afgeleid op basis van een thermisch-chemisch model. Een eendimensionale dynamische warmteoverdrachtsvergelijking was toen ontwikkeld om de temperatuurverdeling

over de dikte van het composiet te bepalen. Hierbij heeft de studie zich alleen gericht op het moment waarop de maximumtemperatuur van de kern bereikt werd. Door een proces van dimensieloos maken te gebruiken is de bepalende vergelijking uiteindelijk omgezet naar een tweede-orde differentiaalvergelijking met een enkel dimensieloos getal. Het dimensieloos getal toont de relatie tussen de kerntemperatuur, de uithardingstemperatuur van de mal, de dikte van het composiet en de uithardingskinetica van de hars. Dit resulteerde in zowel een kritiek dimensieloos getal als een kritieke dikte waarboven het verwerking onmogelijk is zonder een ongecontroleerde temperatuurpiek in de dikke thermoharder composieten gedurende de productie.

Ten tweede is er een numerieke studie uitgevoerd om de temperatuurverdeling als wel de uithardingsgraad te voorspellen. Een driedimensionaal warmteoverdrachtsmodel was opgebouwd dat accuratere voorspellingen kan leveren. Om de uithardingskinetica te simuleren is er een partiele differentiaalvergelijking in coëfficiëntvorm toegevoegd aan het warmteoverdrachtsmodel. De resultaten tonen een temperatuur in de kern die eerst toeneemt tot de maximumwaarde en dan afneemt tot de beginwaarde en dit is een zelfde trend als de reactiewarmte. Bovendien creëert de temperatuurgradiënt door de dikte een grote gradiënt in de uithardingsgraad welke kan zorgen voor ongewenste interne spanningen.

Ten slotte is er experimentele validatie uitgevoerd om het thermisch-chemisch model te verifiëren. Het vacuüminfusieproces werd gebruikt om de composieten te produceren. De experimenten waren vooral gericht op composieten met een dikte groter dan de eerder genoemde kritische dikte. Het bleek nodig te zijn om de infusietijd onderdeel te maken van het model om de nauwkeurigheid van de numerieke simulatie te verbeteren. Zowel de numerieke als de experimentele resultaten laten zien dat de maximumtemperatuur in dikke composieten toeneemt met zowel de uithardingstemperatuur als met de dikte.

Contents

1

Introduction

1.1 Applications of thick composites

In the past decades, composite materials and technologies have been extensively used in the aerospace, wind energy industry and offshore works. Compared to traditional materials, composite materials offer significant advantages not only in the term of weight saving, but also in the mechanical performance, durability and cost. Typically, common composite products are thin layer laminated structures with a typical thickness of 2-20 mm. The products include airplane components (fuselage, wing sets and tails), ship bodies and bicycle frames, etc. As limited by the manufacturing technologies, these products are usually moulded in small pieces and then assembled which generally involve a number of spars and shells. These kinds of structures need additional gluing or mechanical joints that can become the potential weak points resulting in defects and cracks. However, thick walled composites can avoid the above mentioned manufacturing of many smaller, thin walled components as well as the necessary joining process. It is therefore not only more efficient to make thick walled components, but also reduces the number of potential weak spots and therefore is expected to increase the reliability.

Another important reason of manufacturing thick composite is driven by the increase of the product size. Currently the industry starts to explore the possibility of making large composite structures which can be found in the latest generation of aircraft structures. These large and thick components were used to replace the traditional metallic materials and meet the requirements under the most extreme conditions. With the increase of the size of the aircrafts, the dimension of the structural parts also becomes very large. The commercial aircraft Airbus 380 made extensive use of composite materials, for example, the centre wing box, the wing

ribs, and the rear fuselage section (see Figure 1.1). The thickness of the composite material at the major force loading positions was approximately 45 mm and even more than 160 mm at the joints [1].

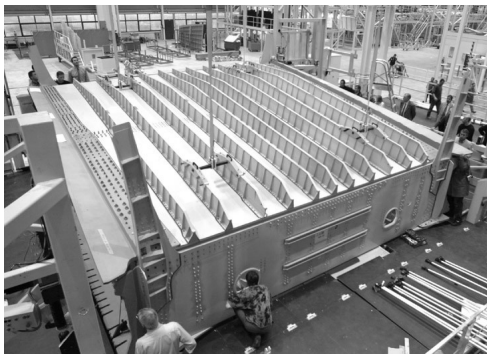

Figure 1.1 Composite center wing box of A380 airplane.

Also for wind turbine blades, nowadays thick walled composites are widely used. In early times, wood was used as the basic structure material in windmill blades. As the blades get larger, glass fiber reinforced composite materials start to dominate this field due to its high strength and low price. For wood windmills, the size of the blade is about 10 m in diameter. Whereas the largest wind power product, the Siemens SWT-6.0-154 wind turbine, has a rotor diameter of 154 meters. The blades were made of glassfiber reinforced epoxy composites (GFRE) as 75 m long [2].

Figure 1.2 Manufacturing of a wind turbine blade.

As shown in Figure 1.2, the root of this blade was up to 2 m in diameter with an extremely thick wall about 100 mm. The whole blade was manufactured in one piece using a closed mould process. The epoxy resin was injected under a vacuum and cured at a high temperature in the mould.

The challenge for manufacturing thick thermoset composite is, however, to control the heat generated during the manufacturing. The thicker the part, the more difficult it is to prevent the core from overheating. In fact, this interaction between laminate thickness, processing conditions and material properties forms the main topic of this thesis.

1.2 Manufacturing of thick thermoset composites

Thick thermoset composites can in principle be fabricated using a wide variety of manufacturing processes. For a particular part the process depends on the part size, material type, production volume, tool costs, quality requirements, and of course, the mechanical, electronic as well as chemical performances. The type of process should be selected well before the manufacturing in order to accomplish a high-quality production.

Different to metal processes, most of the composite products were built up using an incremental material manufacturing process. It means that the materials were laid up into a mold with the shape of the final structure in the form of fiber tows, tapes or fabric sheets. Generally, the minimum thickness of carbon-fiber fabrics is about 0.1 mm [3]. Considering that the thickness of composite products usually ranged from several millimeters up to hundreds of millimeters. Thus, a practical part may consist of a large number of layers which are oriented in different directions to achieve the desired structural performances.

The most common techniques used for thick composites manufacturing include Autoclave Molding, Prepreg Compression Molding (PCM), Resin Transfer Molding (RTM), Vacuum Infusion Process (VIP) [4-6]. Filament winding is also a widely practiced technique for large-scale components. However, it is currently more used for ‘thin’ vessel products like high-pressure containers [7, 8].

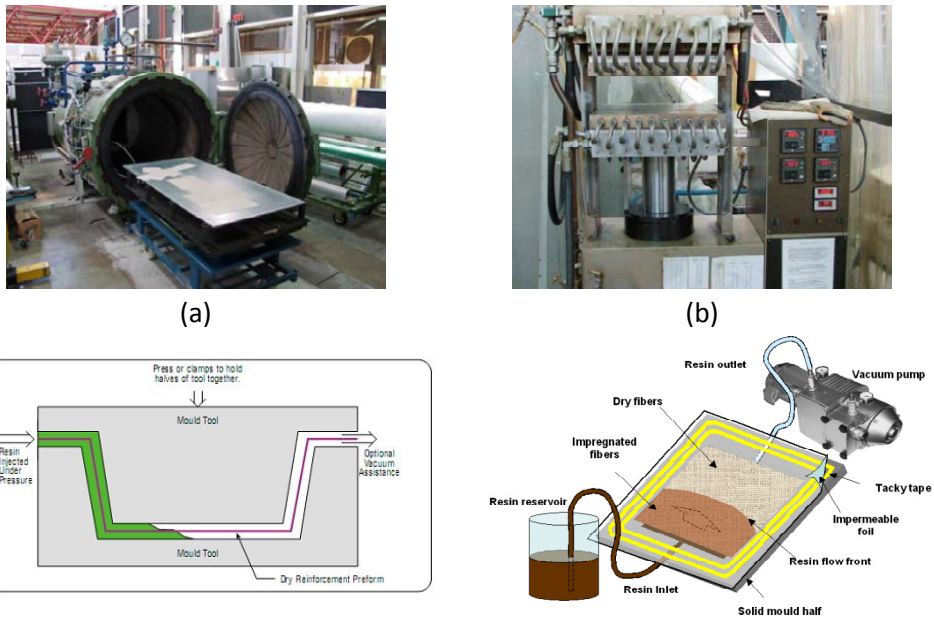

Figure 1.3 (a) Autoclave; (b) Flat hot plate press for PCM process; (c) RTM mold; (d) VIP set-up.

Most autoclaves are temperature and pressure controlled ovens that allow programmed heating and pressurization cycles. They are widely used for curing high-quality aircraft components under controlled conditions not only for single parts but also for assemblies. The assemblies can be bonded together during the heat curing cycle. Appling pressure is to ensure the bonding and curing of the parts occur properly. It is obvious that the dimension of the parts determines if it can be cured in the autoclave oven. A large composite part like an airplane fuselage needs a huge chamber to contain it. In 2010 a new autoclave was applied to cure the fuselage shell of the Airbus A350 XWB which was up to 17.8 m long and 5.6 m wide. It has a usable length of 21 m and a usable diameter of over 7 m [9].

In the PCM process, a prepreg is commonly used which is a composite sheet in which the reinforcement has been pre-impregnated with resins and is ready to be placed in a mold without requiring additional resin. According to the resin system, there are two types of prepregs: thermoset prepregs and thermoplastic prepregs.

In practice, the thermoset prepregs such as carbon/epoxy or glass/epoxy prepregs, are the most popular in industry. Since the resin is partially cured with the reinforcement, the prepreg must be stored in a freezer prior to use. When the composite structure is built up in a mold, it usually requires temperature and compression load to finish the complete polymerization. As opposite to thermoplastic prepregs, cured thermoset composites have a fixed shape and cannot be remolded or reshaped.

Compared with the PCM process, RTM uses dry fiber preforms without resin. By placing the dry reinforcement material inside a mold, any combination of material and orientation can be used including three-dimensional fabrics [10]. When the mold is closed and resin is injected into the mold, the dry fibers are wetted by the resin. Finally the product is extracted after the resin is cured. This process is also known as the name of Liquid Molding (LM). As well as the VIP process, they all belong to the class of Resin Infusion Technologies (RIT). An important advantage of the RTM process is that the fiber preform can be placed into the mold in any shape with complex structures. Due to the support of the cavity, the geometry of the product can be controlled very precisely [11].

The VIP process uses an open mold system which is different from RTM [4]. The fiber preform is sealed in a vacuum bag assisted by a mold. The liquid resin fills the mold and wets the fibers because of the pressure difference between the inside and outside of the vacuum bag. Since the applied pressure is relatively low, other materials such as polymers or composites can be used to replace the metal mold. However, a metal mold is often used because of its excellent surface finish. In the VIP process, because of the flexible surface of vacuum bag, the extra resin infused into the laminate will be pressed out which can greatly improve the fiber-resin ratio to obtain a fiber volume fraction about 45-55% [6, 12]. In this thesis, the VIP process is used for manufacturing the thick thermoset composites.

1.3 Defects in thick composites

For the thick composites, it is difficult to reach the same quality as the thin composites. In many instances, the defects are found such as laminate deformation, cracks in the matrix, delamination between the layers, etc. Though it

could also occur in mechanical processes, but most of these defects happen at the stage of manufacturing the laminates.

1.3.1 Deformation

In industry, dimensional accuracy is always required to meet the shape tolerances. However, all manufacturing processes have their own defects, such as fiber wrinkling, thickness variation, spring-forward and warpage [5, 13-15]. For the composite parts, dimensional inaccuracy usually comes from the induced residual stress during cure. Sometimes warpage deformation occurs when a cured composite part is removed from the mold. The main sources of the residual stress and deformation are inherited from the resin cure shrinkage, non-uniform fiber distribution and anisotropic thermal expansion. The spring-forward and warpage of a composite product is shown in Figure 1.4.

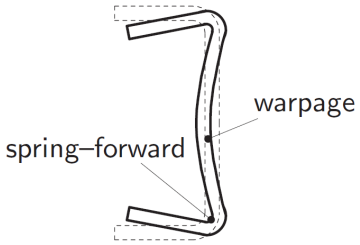

Figure 1.4 Spring-forward and warpage phenomenon in a C-shape composite [15].

As Wijskamp presented that the warpage is mainly caused by a non-balanced stress distribution through the thickness of the composite. However, spring-forward always happens at the corners which is because of the anisotropic material properties [15]. Fernlund also studied on the spring-in phenomenon using the C-shaped and L-shaped hollow composite parts and he found that the spring-in phenomenon is affected by many factors, including the cure cycle, tool surface, part geometry as well as lay-up directions of the fibers. He introduced a numerical model to calculate the stress transferred between the part and tool based on a large deformation solution technique [5]. In order to reduce the spring-in angles, Teoh used a multi-stage curing technique (MSC) to improve the dimensional accuracy for the curve-shaped composites [14].

1.3.2 Microcracks

The first form of damage in a laminate is probably the matrix microcracks [16]. Moreover, most of these microcracks happen at the interlaminar interface or in [0/90] plies which is caused by the non-uniform strain distribution between the fiber-fiber or fiber-matrix. For a thick laminate, multiple cracking processes have been observed in the experiments. For a conventional manufacturing process, heat energy is usually transferred to the laminate through conduction from the surfaces to the center. Because of the low thermal conductivity of the glassfiber reinforced composites, a temperature gradient is always created which finally leads to an outside-in curing of the laminate. As a result, the outer layers shrink and stiffen first. If the core then cures and shrinks, the outer layers are put in compression whereas the core itself is in tension. It is this tension stress in the core which may eventually result in the observed matrix cracking. Thostenson presented that the microcracks were found in a 24.5 mm thick glass/epoxy laminate manufactured by an autoclave process [17], as shown in Figure 1.5. A practical solution for reducing the temperature gradient is to apply a lower curing temperature and heating rate although this results in an excessive curing time.

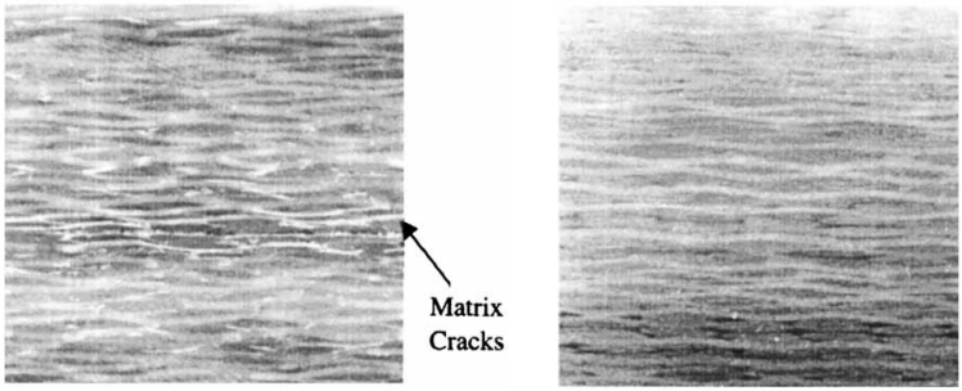

(a) (b)

Figure 1.5 Cross-section view of a composite part. (a) Matrix cracks in the conventional autoclave-processed laminate [17]; (b) no visible crack in a microwave-processed laminate.

Compared to the conventional heating systems, microwave heating transits energy volumetrically by an electromagnetic field which is more moderate. The penetration depths of microwave radiation for glassfiber composites can be over 30 cm [18, 19]. It can be used to heat and cure most of the thermoset resin systems without special requirements. The most important thing is that microwave heating results in an inside-out curing process which can greatly reduce the internal residual stress and curing time.

For an inside-out curing process, Bogetti and Pillai mentioned that the surface temperature initiates the cure reaction first and then exothermic reaction accelerates the cure and creates a cure-front that sweeps the laminate from inside towards to the outside [20, 21]. Consequently, the core reaches gelation before the surface. Though the surface is heated up before the core, the reaction heat in the center may become dominant such that the resin cure front moves from inside to outside. As a result, it will avoid creating the microcracks during cure and reduce the process-induced residual stresses. However, the problem of temperature overheating in the core for an inside-out curing process is larger than that for a conventional outside-in curing process.

1.3.3 Temperature overshoot

For the manufacturing process, the most important phase change is the polymerization or curing of the resin system. During the curing process, molecules are crosslinked to form a large 3D network [22]. For all thermosets, heat is generated during the curing reaction. This exothermic behavior is a large problem for the manufacturing of thick composite products, since it can lead to undesired delamination or even degradation of the core.

Generally, thermoset resins need a minimum temperature to activate the polymerization. Therefore, the resin has to be heated up to a certain temperature. At the same time, the reaction exotherm creates additional heat in the laminate. If this additional heat is concentrated but cannot be conducted fast enough to the mold, then it may lead to an overheating of the core. This overheating risk therefore limits the reliable manufacturing of the thick thermoset composites.

Figure 1.6 shows a temperature overshoot in a GF/Epoxy composite during the curing process.

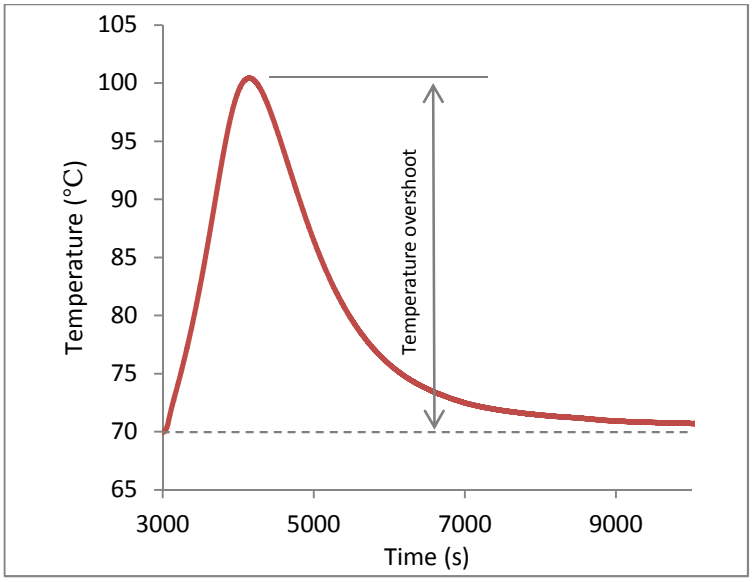

Figure 1.6 Temperature overshoot in the core of a 32 mm thick GF/Epoxy composite curing at 70 ℃.

Figure 1.6 shows that a temperature overshoot is created in a 32 mm thick GF/Epoxy composite part which is cured at 70 ℃ using the VIP process. The temperature in the core is approx. 30.4 ℃ higher than the surface. For a thicker composite or at a higher curing temperature, the temperature overshoot can become higher. As a result, this temperature overshoot in the core will create a extreme temperature gradient in the composite and cause a different curing rate through the thickness. It is also a main reason that enlarges the no-uniform shrinkage in an anisotropic material and induces the residual stresses and microcracks during cure.

1.4 Basic heat transfer equations

In order to estimate the temperature profiles in the composites, thermal analysis of the curing reaction has to be studied. Based on the theory of energy balance,

many researchers studied on this exothermic curing reaction and presented different heat transfer equations to determine the temperature distribution in the composite [23-35]. As a thermo-chemical model, the mathematical equations are described as a heat transfer model coupled with cure kinetics. By ignoring the influence of resin flow during cure, the energy equation can be written as:

$$\rho_c C_{p_c} \frac{\partial T}{\partial t} = \nabla(k\,\nabla T) + Q \tag{1.1}$$

where ρ_c, C_{p_c}, and k are the density, heat capacity, and thermal conductivity of the composite. T is the absolute temperature in Kelvin. t is the time in the system and Q is the internal heat source per volume in W/m^3 which can be expressed as:

$$Q = \rho_r v_r H_r \frac{d\alpha}{dt} \tag{1.2}$$

where ρ_r is the density of the resin, v_r is the resin volume fraction in the composite, H_r is the total heat generated by the resin during cure in J/g. $\frac{d\alpha}{dt}$ is the reaction rate in $1/s$, depending on the cure kinetics of the resin system. For different resin systems, the mechanisms of the curing reaction are different because of the various types of functional groups in the molecules. For the epoxy resins, the n-th order cure kinetic model and autocatalytic model or their combination model is commonly used (see Table 2.1) [23, 34, 36, 37].

Based on the Equation 1.1 and 1.2, it gives a complete expression of the thermo-chemical energy balance equation as shown below:

$$\rho_c C_{p_c} \frac{\partial T}{\partial t} = \nabla(k\,\nabla T) + \rho_r v_r H_r \frac{d\alpha}{dt} \tag{1.3}$$

Lim and Lee used a 1D heat transfer model to evaluate the temperature distribution in the composite through the thickness [24, 25, 35]. Other researchers also used 2D and 3D models for solving the differential equation according to the required solutions and boundary conditions [20, 28, 38, 39].

However, because of the complex relations between the differential terms, such as the conduction heat term and the parameter of reaction rate $\frac{d\alpha}{dt}$ which is a function of degree of cure α versus temperature and time, it is difficult to solve this nonlinear higher-order partial differential equation. Therefore, there is still no

efficient commercial software to solve this problem directly. In this thesis, the focus is on the through-thickness temperature profile as well as on the prediction of the temperature overshoot and the thermo-chemical model will be solved in the analytical and numerical methods, respectively.

1.5 Thesis outline

The main work of this thesis is to study the thermal behaviors in the thick epoxy-based composites and to predict the temperature profiles and temperature overshoot through the thickness of the composites by using the analytical and numerical methods. Finally, the results are validated experimentally. The outline below shows how these topics are addressed into the different chapters.

Chapter 1: a brief introduction is given about the applications of the thick composites as well as their manufacturing processes. The purpose of this thesis is to study the temperature overshoot problems.

Chapter 2: an overview about the thick thermoset composites is presented. It includes the descriptions about the manufacturing defects during the curing processes and the temperature overshoot phenomenon. In order to study this thermal behaviors, a brief background of the thermo-chemical model and cure kinetics is introduces in this chapter.

Chapter 3: material properties, such as the density, heat capacity, thermal conductivity and cure kinetic parameters are determined by experimental methods. A global fitting method is created to find the reaction rate parameters in the entire temperature range.

Chapter 4: analytical solutions are presented to estimate the core temperature in a curing composite. The dimensionless numbers are used to solve the differential equations which give a great view of the relations between the conduction heat and reaction heat during cure. Moreover, the critical thickness for the manufacturing is defined for ‘thin’ or ‘thick’ composites.

Chapter 5: numerical solutions are carried out in 1D and 3D heat transfer models and both the temperature profiles and degree of cure distributions are obtained to validate the analytical predictions.

Chapter 6: using a vacuum infusion set-up, experimental measurements are carried out for glassfiber/epoxy composites. Temperature profiles are measured and used to validate both the analytical and numerical solutions.

Chapter 7: conclusions including practical guide lines for the manufacturing of thick thermoset composites. A short overview of standard processing conditions is also discussed as well as the expected work to do in the future.

Reference

[1] S. Chen, "Application of composites materials in A380," *Hi-Tech Fiber & Application,* vol. 33, 2008.

[2] Siemens unveils 75 m wind turbine blade [Online].

[3] T. I. Inc., "Carbonfiber Fabrics Dataset," ed, 2005.

[4] A. B. Strong, *Fundamentals of Composites Manufacturing - Materials, Methods, and Applications*: Society of Manufacturing Engineers, 2008.

[5] G. Fernlund, N. Rahman, R. Courdji, M. Bresslauer, A. Poursartip, K. Willden*, et al.*, "Experimental and numerical study of the effect of cure cycle, tool surface, geometry, and lay-up on the dimensional fidelity of autoclave-processed composite parts," *Composite : Part A - Applied Science and Manufacturing,* vol. 33, pp. 341-351, 2002.

[6] K. V. RIJSWIJK, "Thermoplastic composite wind turbine blades - vacuum infusion technology for anionic polyamide-6 composites," PhD, Delft University of Technology, 2007.

[7] L. Zu, "Design and Optimization of Filament Wound Composite Pressure Vessels," PhD Dissertation, Design and Production of Composite Structures, Delft University of Technology, 2012.

[8] L. Zu, "DESIGN AND OPTIMIZATION OF FILAMENT WOUND COMPOSITE PRESSURE VESSELS," PhD, Aerospace Engineering, Delft University of Technology, 2012.

[9] P. AEROTEC. (2009, Autoclave for production of the new Airbus A350 XWB arrives at Premium AEROTEC's plant in Nordenham. Available: http://www.premium-aerotec.com/Binaries/Binary4253/PM_NOR_Autoclave_Aug_09_EN.pdf

[10] A. P. Mouritz, M. K. Bannister, P. J. Falzon, and K. H. Leong, "Review of applications for advanced three-dimensional fibre textile composites," *Composite : Part A - Applied Science and Manufacturing,* vol. 30, pp. 1445-1461, 1999.

[11] J. M. Lawrence, K.-T. Hsiao, R. C. Don, P. Simacek, G. Estrada, E. M. Sozer*, et al.*, "An approach to couple mold design and on-line control to manufacture complex composite parts by resin transfer molding," *Composite : Part A - Applied Science and Manufacturing,* vol. 33, pp. 981-990, 2002.

[12] W. P. Benjamin and S. W. Beckwith, "Resin transfer molding," presented at the SAMPE, 1999.

[13] K. Potter, *Introduction to Composite Products: Design, Development and Manufacture*: Springer Science & Business Media, 1997.

[14] K. J. Teoh and K.-T. Hsiao, "Improved dimensional infidelity of curve-shaped VARTM composite laminates using a multi-stage curing technique - Experiments and modeling," *Composite : Part A - Applied Science and Manufacturing,* vol. 42, pp. 762-771, 2011.

[15] S. Wijskamp, "Shape distortions in composites forming," PhD, University of Twente, 2005.

[16] J. A. Nairn and S. Hu, *Damage Mechanics of Composite Materials*: Elsevier, 1994.

[17] E. T. THOSTENSON and T.-W. CHOU, "Microwave and Conventional Curing of Thick-Section Thermoset Composite Laminates: Experiment and Simulation," *Polymer Composites,* vol. 22, pp. 197-212, 2001.

[18] U. Klun and A. Krzan, "Rapid microwave induced depolymerization of polyamide-6," *Polymer,* vol. 41, pp. 4361-4365, 2000.

[19] E. T. THOSTENSON and T.-W. CHOU, "Microwave processing: fundamentals and applications," *Composite : Part A - Applied Science and Manufacturing,* vol. 30, pp. 1055-1071, 1999.

[20] T. A. Bogetti and J. John W. Gillespie, "Two-Dimensional Cure Simulation of Thick Thermosetting Composites," *Journal of Composite Materials,* vol. 25, March 1991.

[21] V. PILLAI, A. N. BERIS, and P. DHURJATI, "Intelligent Curing of Thick Composites Using a Knowledge-Based system," *Journal of Composite Materials,* vol. 31, pp. 22-51, 1997.

[22] D. J. Walton and J. P. Lorimer, *Polymers*: Oxford Science Publications, 2000.

[23] H. E. Kissinger, "Reaction Kinetics in Differential Thermal Analysis," *Analytical Chemistry,* pp. 1702-1706, 1959.

[24] E. Broyer and C. W. Macosko, "Heat Transfer and Curing in Polymer Reaction Modeling," *AIChE Journal,* vol. 22, pp. 268-276, 1976.

[25] E. Broyer and C. W. Macosko, "Curing and Heat Transfer in Polyurethane Reaction Modeling," *Polymer Engineering and Science,* vol. 18, pp. 382-387, April 1978.

[26] B. R. Gebart, "Critical Parameters for Heat Transfer and Chemical Reactions in Thermosetting Materials," *Journal of Applied Polymer Science,* vol. 51, pp. 153-168, 1994.

[27] M. R. KAMAL and P. G. LAFLEUR, "Heat Transfer in Injection Molding of Crystallizable polymers," *Polymer Engineering and Science,* vol. 24, pp. 692-697, JUNE 1984.

[28] L. J. Lee and C. W. Macosko, "Heat Transfer in Polymer Reaction Modeling," *International Journal of Heat and Mass Transfer,* vol. 23, pp. 1479-1492, 1980.

[29] A. C. Loos and G. S. Springer, "Curing of Epoxy Matrix Composites," *Journal of Composite Materials,* vol. 17, March 1983.

[30] J. H. Oh, "Prediction of Temperature Distribution During Curing Thick Thermoset Composite Laminates," *Materials Science Forum,* vol. 544-545, pp. 427-430, 2007.

[31] J. H. OH and D. G. LEE, "Cure Cycle for Thick Glass/Epoxy Composite Laminates," *Journal of Composite Materials,* vol. 36, pp. 19-45, 2002.

[32] C. L. Tucker, "Heat Transfer and Reaction Issues in Liquid Composite Molding," *Polymer Composites,* vol. 17, February 1996.

[33] P. Carlone, D. Aleksendric, V. Cirovic, and G. S. Palazzo, "Modelling of Thermoset matrix composite curing process," *Key Engineering Materials,* vol. 611-612, pp. 1667-1674, 2014.

[34] R. S. Dave and A. C. Loos, *Processing of Composites*: Hanser Publishers, 2000.

[35] Z. S. Guo, S. Du, and B. Zhang, "Temperature field of thick thermoset composite laminates during cure process," *Composite Science and Technology,* vol. 65, pp. 517-523, 2005.

[36] A. Yousefi and P. G. Lafleur, "Kinetic Studies of Thermoset Cure Reactions: A Review," *Polymer Composites,* vol. 18, April 1997.

[37] M. J. Vold, "Differential Thermal Analysis," *Analytical Chemistry,* vol. 21, June 1949.

[38] A. Cheung, Y. Yu, and K. Pochiraju, "Three-dimensional finite element simulation of curing of polymer composites," *Finite Element in Analysis and Design,* vol. 40, pp. 895-912, 2004.

[39] A. Shojaei, S. R. Ghaffarian, and S. M. H. Karimian, "Three-dimensional process cycle simulation of composite parts manufactured by resin transfer molding," *Composite Structures,* vol. 65, pp. 381-390, 2004.

2

Literature Review on Thick Thermoset Composites

2.1 Introduction

During the manufacturing of a thermoset composite, polymerization of the resin system is the most important phenomenon in which the molecules are bonded to each other forming a 3D network [1]. As this is an exothermic reaction, it generates a large amount of heat. It is also accompanied with physical changes such as the volumetric cure shrinkage which generates residual stresses in the composites. This may result in potential defects such as dimensional inaccuracy, delamination and failures of the composite structures. Consequently, this curing reaction is a combination of thermal and chemical processes which requires a thermo-chemical model study. In order to handle this work, a fully understanding of the background is required. A general introduction about the theories of cure kinetics and heat transfer is presented first in this chapter.

2.2 Theory of cure kinetics

According to the theory of Lim and Lee (2000), the thermo-chemical model can be described as a heat transfer model coupled with cure kinetics (see Equation 1.3). It is known that the term of internal heat source generates the heat and causes the temperature overshoot in the composites. Since the parameters ρ_r, v_r and H_r are constants, only the term of $\frac{d\alpha}{dt}$ is a variable which is a function of degree of cure and temperature. As the most important parameter in this thermal-chemical model, it is determined by the cure kinetic models.

2.2.1 Cure kinetic models

For different resin systems, the reaction mechanisms are different. Researchers such as Kissinger, Springer, Yousefi, Dave and Loos have studied on this topic using different resins [2-5]. In the family of thermoset resins, several specialty resins are widely used for composite applications, such as unsaturated polyesters, epoxies, vinyl esters, phenolics, polyimides and related polymers [6]. Among these thermosets, epoxy products have relatively good thermal stability and mechanical properties used as high-performance composites. Some of the resins can cure at room temperature, while generally it needs to be heated up to activate the curing reaction. For example, usually polyester thermosets are cured at 82 ℃ and some epoxy resins are cured at 120 ℃ [6]. In this thesis, an epoxy-amine resin system is used as a matrix for the glassfiber reinforced composites.

In the Kissinger's research, the cure kinetic was expressed as ' n^{th} order reaction' where the reaction rate started from the peak value [5]. However, some other epoxy mixed with the initiator component can start the reaction from zero or a very low rate even at the room temperature which are called as the 'autocatalytic reaction' or 'n^{th} order + autocatalytic reaction', respectively. A conclusion of the epoxy-based cure kinetic models is presented in Table 2.1.

Table 2.1 Cure kinetic models for epoxy resin systems [3]

Models	Equations
1. n^{th} order reaction	$\frac{d\alpha}{dt} = k(1-\alpha)^n$
2. Autocatalytic reaction	$\frac{d\alpha}{dt} = k\alpha^m(1-\alpha)^n$
3. n^{th} order + autocatalytic reaction	$\frac{d\alpha}{dt} = (k_1 + k_2\,\alpha^m)(1-\alpha)^n$
Arrhenius dependent rate constant	$k_i(T) = A_i\, e^{-\frac{E_{ai}}{RT}}$

In Table 2.1, the parameters of k, k_1, and k_2 are the reaction rate constants which are defined by Arrhenius equation. A_i and E_{a_i} are the pre-exponential factor and activation energy of the i^{th}order; R is the universal gas constant, $R \approx 8.314$ J/

$(\mathrm{mol}\cdot\mathrm{K})$; m and n are the reaction orders. Figure 2.1 shows the different features of these three cure kinetic models.

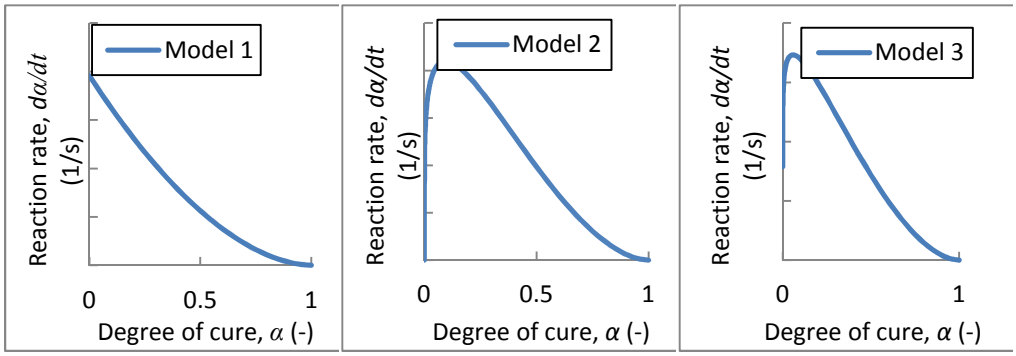

Figure 2.1 Sketch of cure kinetic models for epoxy resins.

As shown in Figure 2.1, the reaction rate in Model 1 starts from its peak value and decreases with the degree of cure. In Model 2, the reaction rate begins from zero, then increasing to its peak value. While in Model 3 it has an initial rate k_1 where $k_1 > 0$. Model 3 is an extension of Model 2 which has two additional fitting parameters. For the epoxy-amine resin system, it is an autocatalytic reaction and its initial reaction rate $k_1 > 0$. Thus, Model 3 known as the Kamal-Sourour equation can be used as its cure kinetic model.

The cure kinetic parameters can be determined from the experimental results by differential thermal analysis technologies such as Differential Scanning Calorimetry measurements (DSC) [5, 7]. It can be used to measure the characteristic properties of polymers, liquid crystals and drugs, etc. With the DSC curves of the heat flux, the degree of cure and reaction rate can be calculated versus temperature and time. Note that the cure data obtained from isothermal and dynamic measurements are different in most cases [2, 8]. This difference is caused by the existing cure kinetic models rather than the experimental techniques. In this thesis, the isothermal measurement procedure is chosen and the data result is used for the estimation of the cure kinetic parameters. More details will be discussed in the Chapter 3.

2.2.2 Diffusion limitation effects

With increasing the degree of cure, the glass transition temperature in the resin increases and the movement of the reactants slows down. Especially at the end of the reaction, the curing process is controlled by the reactants movement rather than the chemical reaction. This diffusion phenomenon is shown in Figure 2.2.

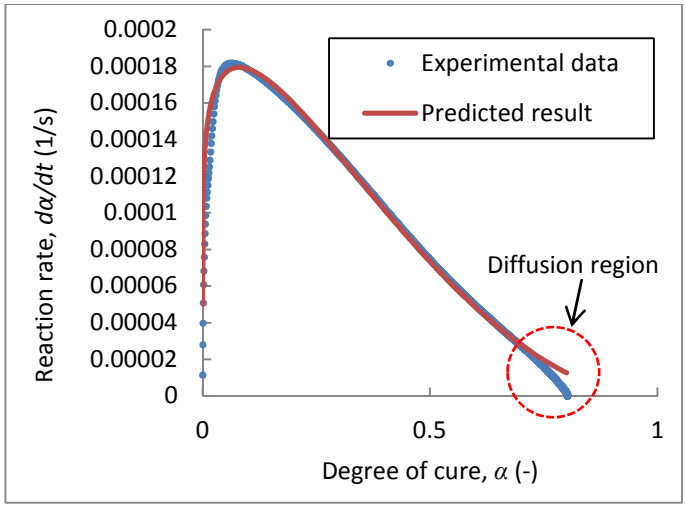

Figure 2.2 Diffusion limitation effect in the curing reaction.

As shown in Figure 2.2 that at the end of the reaction the predicted curve shows the reaction is still going on. However, the experimental result shows that the reaction has stopped at a certain conversion because of the diffusion limitation. These maximum cure values can be measured by curing a sample at a constant temperature until the degree of cure stopped changing and then determine the conversion level by measuring the remaining heat of reaction with a standard dynamic DSC scan [3, 8].

Several modifications of the cure kinetic models are proposed in the literatures to incorporate these maximum cure effects. Lam and Kenny proposed to introduce an α_{max} as the final degree of cure instead of the value of 1 [9, 10]. Refer to the Model 3 in Table 2.1, the cure kinetic equation can be written as:

$$\frac{d\alpha}{dt} = (k_1 + k_2\,\alpha^m)(\alpha_{max} - \alpha)^n \qquad (2.1)$$

where α_{max} is the maximum degree of cure according to the experimental results. Note that this parameter depends on the curing temperature.

Based on the Model 3, Khanna and Chanda developed a diffusion factor which is multiplied with normal reaction rate equations [11]. The diffusion factor is written as:

$$f_d(\alpha) = \frac{1}{1 + \exp\,[C(\alpha - \alpha_{max})]} \qquad (2.2)$$

where C is a constant. For $\alpha \ll \alpha_{max}$, the effect of $f_d(\alpha)$ can be neglected. As α approaches α_{max}, this diffusion factor will decrease the predicted values to approach the experimental results.

2.3 Theory of heat transfer

The basic thermo-chemical model (see Equation 1.3) is based on the heat transfer theory. Heat transfer is defined as a movement of energy due to a temperature difference. It is characterized by the mechanisms of heat conduction, convection and radiation [12, 13].

2.3.1 Conduction heat

During the manufacturing of the composites, the heat conduction takes place during the whole curing process and the heat flux is proportional to the temperature gradient in the composite. The heat conduction equation is known as Fourier's law. A 1D heat conduction model with internal heat source is shown in Figure 2.3.

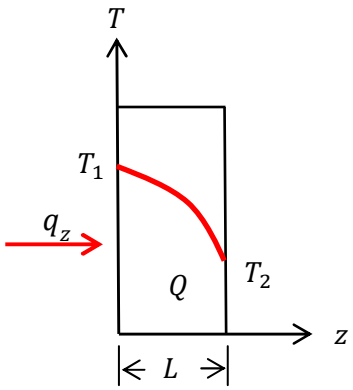

Figure 2.3 Schematic of a 1D heat conduction model with internal heat source.

In Figure 2.3, L is the thickness of the composite, q_z is the heat flux which is the heat transfer rate in the z-direction per unit area perpendicular to the temperature gradient direction. The definition of the heat flux is:

$$q_z = \frac{\Phi}{A} = -k_{zz}\frac{\partial T}{\partial z} \tag{2.3}$$

where Φ is the heat transfer rate, A is the conductive area and k_{zz} is the thermal conductivity in the z-direction.

According to Equation 1.3, it is known that the changes in the total energy of the system during a curing process is equal to the total energy difference between the entering and leaving the system and pluses the energy generated by the internal heat source. The energy balance can be expressed as $\Delta E = E_{in} - E_{out} + Q$, where in the rate form (in the unit of W/m^3) that the total energy changes $\Delta E = \rho_c C_{p_c}\frac{\partial T}{\partial t}$, conduction heat $E_c = E_{in} - E_{out} = \frac{\partial}{\partial z}(k_{zz}\frac{\partial T}{\partial z})$ and internal heat source $Q = \rho_r v_r \Delta H_r \frac{d\alpha}{dt}$. Thus, for a 1D transient heat conduction equation with internal heat source in a plane wall, the equation becomes:

$$k_{zz}\frac{\partial^2 T}{\partial z^2} + \frac{Q}{\rho_c C_{p_c}} = \frac{1}{D}\frac{\partial T}{\partial t} \tag{2.4}$$

where $D = \frac{k_{zz}}{\rho_c C_{p_c}}$ is the thermal diffusivity of the composite.

For a unit element of the composite where the size is $\Delta z = 1\ mm$, we assume that the temperature gradient $\Delta T = 1$ ℃, thermal conductivity of a GF/Epoxy composite $k_{zz} = 0.54\ W/(mK)$ (see Chapter 3), then we can calculate the conduction heat in this unit element that $E_c = 5.4 \times 10^5\ W/m^3$.

In many thermal engineering problems, there is no internal heat source or this term is assumed constant, but here it is a function of reaction rate and varies in a complex way with time and position. Thus, it needs to be studied in this thesis.

2.3.2 Convection and radiation boundary conditions

Heat convection here refers to the heat transfer from the composite surfaces to the external. The heat convection equation is known as Newton's law of cooling. For example, at the right surface of the wall ($z = L$) in Figure 2.3, the convection boundary condition can be expressed as [14, 15]:

$$q_{conv} = h_c|T_\infty - T_2| \tag{2.5}$$

where q_{conv} is the rate of convection in W/m^2, h_c is the heat transfer coefficient in $W/(m^2 \cdot K)$, T_∞ is the external temperature of surroundings. For example, if the right surface has a nature convection, $h_c = 45\ W/(m^2 K)$, at room temperature $T_\infty = 20$ ℃, wall temperature $T_2 = 70$ ℃, then the rate of convection is 2250 W/m^2.

The composite also emits the heat by the radiation though this effect is at a relatively low level at our curing temperature range. The heat radiation equation is known as Stefan-Boltzmann law. The radiation boundary conditions can be expressed as:

$$q_r = \varepsilon\sigma\left|{T_2}^4 - {T_\infty}^4\right| \tag{2.6}$$

where q_r is the rate of radiation in W/m^2, ε is the surface emissivity in the range $0 \leq \varepsilon \leq 1$ and σ is the Stefan-Boltzmann constant, $\sigma = 5.67 \times 10^{-8}\mathrm{W/(m^2 \cdot K^4)}$. For a composite surface, the value of ε can choose 0.8, the temperatures are the same as mentioned above in K, then the rate of radiation is about 294 W/m^2.

Commercial software also offers a package called Generalized Boundary Condition (GBC) which is a generalized formulation of the above boundary conditions [16, 17].

2.4 Heat transfer studies in thick thermoset composites

Recently researchers did a lot of studies on the manufacturing of thick thermoset composites and estimated the temperature distribution during cure. For example, Twardowski made a 5 cm thick graphite/epoxy laminate using a hot press mold [18]. The experimental results show that the initial degree of cure did not play an important role in the entire curing process; however a temperature overshoot about 20 ℃ in the center of the laminate was created even for high thermal conductivity graphite reinforced composites. In order to produce high quality thick composites, Michaud found that the curing temperature must be much lower than the recommended temperature for a thin product through an experimental method [19]. He found that the maximum temperature overshoot can be up to 60 ℃ for a certain cure cycle in a 2.54 cm thick glassfiber epoxy-based composite [20]. Olofsson studied the wet filament winding process for glass/epoxy composite cylinder mandrels [21]. Temperature profiles were calculated and measured for different pipes thicknesses. The experimental results show that at the same cure temperature of 80 ℃ for both a 14.6 mm and a 50.4 mm thick pipes, the measured peak temperatures are 86 ℃ and 111 ℃, respectively. These results indicate that the recommended curing temperature previously for a thin pipe is too high for a thick pipe because of the large exothermic peak temperature is created. Kim also studied the temperature overshoot problem in thick graphite/epoxy laminates using a continuous curing method [16, 22]. In this method the fresh prepreg layers were continuously laid down on a heating mold at a steady speed. The inner surface was heated up to an initial curing temperature to build-up a cure-front propagated through the thickness. The experimental results show that the continuous curing method can greatly prevent the inherent temperature overshoot and reduce the curing time by controlling the material accretion rate, temperature boundary conditions and cure-front speed.

Several researchers studied epoxy-based composites cured in an autoclave. Ciriscioli studied graphite/epoxy laminates with thicknesses about 35 mm [23]. In order to test and verify the Loos-Springer cure model, they created their own cure model and it indicates that a temperature overshoot of more than 200 ℃ in a 200 plies laminate may occur if using the cure cycle recommended by the manufacturer. The results show that the maximum temperature inside the composite depends on not only the curing temperature and heating rate, but also its thickness.

2.4.1 Analytical solutions and scaling analysis

Based on the heat transfer equations, analytical solutions for the temperature distribution in thick thermoset composites were proposed by Broyer (1976, 1978), Li (2001), Tucker (1996), Gebart (1994) and Second (2011) and others. In the heat transfer systems, dimensionless numbers are created to get a brief view of the thermal performance in the composites. For example, Damkohler number Da can be used to describe as a ratio between the heat conduction and reaction. Whereas Biot number Bi represents as a ratio of convection heat on the surface and conduction heat inside. It can be expressed as:

$$Bi = \frac{h_c l}{k} \tag{2.7}$$

where l is the characteristic length of the material and k is the thermal conductivity. This ratio also identifies the response speed of the temperature changes on the surface and inside.

The Fourier number is another dimensionless number that used to present the transient heat conduction problems. The expression can be written as:

$$Fo = \frac{D\tau}{l^2} \tag{2.8}$$

where τ is the characteristic time in second. This number shows the ratio of heat diffusive rate and the storage rate in the material.

By using a dimensionless equation, Broyer studied a 1D transient heat transfer calculations to predict the curing performance in a reaction injection molding [24].

The cure kinetics are represented by an n^{th} order equation. In this molding, a constant temperature boundary condition is applied at the both sides of the laminate and it may represent the maximum temperature rise possible during cure through the thickness as many actual molding. Moreover, he introduced a dimensionless reaction rate $\hat{k}$ which changes with the cure kinetics and the laminate thickness. At the critical reaction rate of $\hat{k} = 1$ that 75% of the laminate reaches the gel point, then the critical thickness for a curing composite is given as:

$$L_c = 2\sqrt{\frac{D}{A\exp(-\frac{E_a}{RT_c})}} \tag{2.9}$$

where T_c is the applied curing temperature.

Second defined a theoretical critical thickness to distinct between the thin and thick composites using a similar scaling analysis [25]. The cure reaction is represented by an autocatalytic equation. In this 1D heat equation, a surface temperature at the both sides of the composite follows a ramp and hold temperature profile. A modified Damkohler number Da^*, where $Da^* = Da \cdot f(\alpha)_{max}$, is introduced to evaluate if the heat generated during cure is significant or not. At $Da^* = 1$, it is used to define the critical thickness L_c and it is given as:

$$L_c = \sqrt{\frac{D}{A\exp\left(-\frac{E_a}{RT_c}\right)f(\alpha)_{max}}} \tag{2.10}$$

where $f(\alpha)_{max} = (\frac{m}{m+n})^m(\frac{n}{m+n})^n$ is a maximum of the autocatalytic cure kinetic equation at $\alpha = \frac{m}{m+n}$.

For a woven glass fiber prepreg composite, Second calculated the critical thickness and it is about 14.4 mm. Compared with the Equation 2.9, Equation 2.10 has an added factor $f(\alpha)_{max}$ which means this heat transfer equation is evaluated at the time when the reaction rate reaches its maximum.

2.4.2 Numerical studies of the thermos-chemical model

In certain cases, analytical methods enable to solve the problems which have steady-state, simple geometries and/or boundary conditions. However, in many cases such problems are transient, multidimensional and with complex boundary conditions such that exact solutions cannot be found and numerical methods are then carried out to find approximate solutions [24, 26, 27]. Furthermore, in contrast to an analytical solution which provides the temperatures at any point in a medium, a numerical solution only evaluates the temperatures at discrete points. Thus, the first step in a numerical analysis is to mesh the geometry to build up a nodal network. The results obtained for a fine grid normally provide a more accurate solution than a coarse grid but is also more time-consuming.

A numerical approach to obtain a solution for the curing of a thick thermoset composite may appear simple at first sight, but is far from standard and cannot be solved directly with the usual commercial finite element software like ANSYS or Abaqus not even in the 1D model. The reason is that the internal heat source term Q (in Equation 1.3) is not a constant but is position and time dependent and is largely affected by the temperature itself which can be expressed as a function of $Q = f(z, t, T)$. Moreover, in order to capture the acceleration effect correctly, special precaution is needed.

As the dominant approach to numerical solutions of partial differential equations (PDEs), Finite Difference method (FDM) or Finite Element method (FEM) are widely used to evaluate the heat transfer problems [12]. FDM is a method based on the application of a Taylor's expansion to approximate the differential equations. FEM is established on the subdivision of a whole domain into finite non-overlapping and continuous elements and uses its simplest form of the linear functions to approximate the exact solution in each element.

Based on the governing equation of the thermo-chemical model, it has to build up its discretization equation by using the Taylor series expansion method [15, 28]. The first order term $\frac{dT}{dt}$ can be expanded by a forward difference, backward difference and central difference method and for the second order term $\frac{\partial^2 T}{\partial z^2}$, the

central difference expansion is commonly used. In addition, the heat balance method is also used to establish the discretization based on the energy balance.

As mentioned before, White and Kim focused on a continuous curing process for thick thermoset composites [16, 22, 29]. They proposed a numerical 1D transient heat transfer model which was solved by an Alternating Direction Explicit (ADE) FDM method with generalized boundary conditions. ADE method is used to solve the heat transfer equations where the temperature distribution is obtained by taking an average of both the forward and backward temperature approximation [17, 30].

In the ADE method, at the grid point $z = z_i$, and time $t = t_j$, for $i = 1,2, \dots, I$, $j = 1,2, \dots, J$, the temperature is written as T_i^j. For the forward temperature approximation, $u_i^j = T_i^j$. Similarly, for the backward temperature approximation, $v_i^j = T_i^j$. The ADE temperature T_i^{j+1} at time $t = t_{j+1}$ is given as

$$T_i^{j+1} = \frac{u_i^{j+1} + v_i^{j+1}}{2} \tag{2.11}$$

The degree of cure at time $t = t_{j+1}$ can be integrated as

$$\alpha_i^{j+1} = \alpha_i^j + (\frac{d\alpha}{dt})_i^{j+1} \Delta t \tag{2.12}$$

In Equation 2.12, the time step size need to be selected properly. Yi mentioned that the numerical results shows that degree of cure is very sensitive to the time step size [31].

Furthermore, in order to support the stability of the FDM method, several constrains need to be established to reach the convergence state. For the stability of the internal nodes in a 1D heat transfer equation, it is required that it satisfies $\frac{D\Delta t}{(\Delta z)^2} \leq \frac{1}{2}$ which gives the limitation of the time step Δt for a given Δz. For the convection boundary conditions, the requirement is $\frac{D\Delta t}{\Delta z^2} \leq \frac{1}{2(1+Bi)}$ where Bi is the Biot number (see Equation 2.7) [14, 28].

2.5 Cure cycle optimization

As mentioned in Section 1.3, there are many kinds of defects, such as shape deformation, delamination, microcracks and residual stresses during manufacturing the composites. All of these defects may be caused by a too high curing temperature during the manufacturing. Thus, an optimized cure cycle for manufacturing the composites has to be designed to complete the curing without a high temperature overshoot.

Several strategies are used for cure cycle optimization. One is called the online-control system, in which it constructs a processing plan according to the information of temperature sensors. However, noisy or missing signals could result in poor control ability. Pillai developed a modified online-control system to optimize the curing process with model-based optimization technique [32]. It is coupled with a simulation tool of TGCURE (Bogetti 1991) for solving the heat transfer equation. According to Bogetti, for a thick laminate, a cure gradient is unavoidable and it is desired that the laminate is cured inside-out to minimize the residual stress. In this case, the degree of cure throughout the composite (at the surface and center) must be less than its value at the gel point as $\alpha < \alpha_{gel}$. It means that the resin at the center is still able to move outwards.

The other cure cycle optimization strategy is called the simulation-based method which is very popular recently [32-36]. In this strategy, temperature controlling is the most useful tool. Loos (1982) used a parametric study to determine the cure cycle by controlling the maximum temperature inside the composite within the shortest curing time. Oh (2002) introduced a cooling and reheating cure cycle to prevent the temperature overshoot in a glassfiber/epoxy composite. With this technique, a temperature overshoot that is more than 35 ℃ is presented in a 20 mm thick composite as shown by both of the numerical and experimental results.

Using Multi-Stage Curing technique(MSC), Teoh improved the dimensional accuracy of the composites during the manufacturing [37]. In the MSC process, the first preform is placed on the mold and cured. After that, a new set of preforms are placed above the previous laminate until the desired total number of the plies is achieved. A 16 mm thick hollow C-shaped composite was made for

the measuring of its spring-in angles. The experimental results show that the spring-in angles decrease from 2.5 degree to 0.5 degree. However, the curing time increases from 1 to 4 units.

Artificial Intelligence algorithms (AI) such as the Genetic Algorithm (GA), Evolution Strategy (ES) and Meta-Heuristic Method (MHM) are also used to optimize the cure cycles [38-41]. Chang used the GA method for reducing the curing time and temperature overshoot for a autoclave process [38]. As it mimics the process of the natural selection, the GA method is designed to find the best cure cycle solutions based on the coded objective function and its constraints. The objective function is defined by the total curing time and the temperature with the constraints of the maximum temperature and the heating rate during the cure. For a 10 cm thick composite, this method can obtain an optimized cure cycle within 300 generations with a uniform temperature distribution between the surface and the center.

Reference

[1] D. J. Walton and J. P. Lorimer, *Polymers*: Oxford Science Publications, 2000.

[2] A. Yousefi and P. G. Lafleur, "Kinetic Studies of Thermoset Cure Reactions: A Review," *Polymer Composites,* vol. 18, April 1997.

[3] R. S. Dave and A. C. Loos, *Processing of Composites*: Hanser Publishers, 2000.

[4] G. S. Springer and S. W. Tsai, "Thermal Conductivities of Unidirectional Materials," *Composite Materials,* vol. 1, 1967.

[5] H. E. Kissinger, "Reaction Kinetics in Differential Thermal Analysis," *Analytical Chemistry,* pp. 1702-1706, 1959.

[6] A. B. Strong, *Fundamentals of Composites Manufacturing - Materials, Methods, and Applications*: Society of Manufacturing Engineers, 2008.

[7] M. J. Vold, "Differential Thermal Analysis," *Analytical Chemistry,* vol. 21, June 1949.

[8] L. Sun, "Thermal rheological analysis of cure process of epoxy prepreg," PhD, Chemical engineering, Louisiana State University, 2002.

[9] P. W. K. Lam, "The Characterization of Thermoset Cure Behavior by Differential Scanning calorimetry. Part 1: Isothermal and dynamic study," *Polymer Composites,* vol. 8, pp. 427-436, December 1987.

[10] J. M. Kenny, "Determination of Autocatalytic kinetic Model Parameters Describing Thermoset Cure," *Journal of Applied Polymer Science,* vol. 51, pp. 761-764, 1994.

[11] U. Khanna and M. Chanda, "A Kinetic Scheme for Anhydride Curing of Diglycidyl Ester With Tertiary Amine as Catalyst," *Journal of Applied Polymer Science,* vol. 50, 1993.

[12] F. P. Incropera and D. P. Dewitt, *Fundamentals of Heat and Mass Transfer*: John Wiley & Sons, 2007.

[13] J. H. L. IV and J. H. L. V, *A heat transfer textbook* 4th ed.: Phlogiston Press, 2011.

[14] A. F. Mills, *Heat Transfer*: CRC Press, 1992.

[15] S. M. Yang and W. Q. Tao, *Heat Transfer*, 4th ed.: Higher Education Press, 2012.

[16] C. KIM, H. TENG, C. L. TUCKER, and S. R. WHITE, "The Continuous Curing Process for Thermoset Polymer Composites. Part 1: Modeling and Demonstration," *Journal of Composite Materials,* vol. 29, pp. 1222-1253, 1995.

[17] T. A. Bogetti and J. John W. Gillespie, "Two-Dimensional Cure Simulation of Thick Thermosetting Composites," *Journal of Composite Materials,* vol. 25, March 1991.

[18] T. E. TWARDOWSKI, S. E. LIN, and P. H. GEIL, "Curing in Thick Composite Laminates: Experiment and Simulation," *Journal of Composite Materials,* vol. 27, pp. 216-250, 1993.

[19] D. J. Michaud, A. N. Beris, and P. S. Dhurjati, "Curing Behavior of Thick-Sectioned RTM Composites," *Journal of Composite Materials,* vol. 32, pp. 1273-1296, 1998.

[20] D. J. MICHAUD, A. N. BERIS, and P. S. DHURJATI, "Thick-Sectioned RTM Composite Manufacturing: Part 1: In Situ Cure Model Parameter Identification and Sensing," *Journal of Composite Materials,* vol. 36, pp. 1175-1200, 2002.

[21] K. S. OLOFSSON, "Temperature prediction in thick composite laminates at low cure temperature," *Applied Composite Materials,* vol. 4, pp. 1-11, 1997.

[22] C. KIM and S. R. WHITE, "The Continuous Curing Process for Thermoset Polymer Composites. Part 2: Experimental Results for a Graphite/Epoxy Laminate," *Journal of Composite Materials,* vol. 30, pp. 627-647, 1996.

[23] P. R. Ciriscioli, Q. Wang, and G. S. Springer, "Autoclave Curing - Comparison of Model and Test Results," *Journal of Composite Materials,* vol. 26, pp. 90-102, 1992.

[24] E. Broyer and C. W. Macosko, "Heat Transfer and Curing in Polymer Reaction Modeling," *AIChE Journal,* vol. 22, pp. 268-276, 1976.

[25] T. W. Second, S. C. Mantell, and K. A. Stelson, "Scaling Analysis and a Critical Thickness Criterion for Thermosetting Composites," *Journal of Manufacturing Science and Engineering,* vol. 133, February 2011.

[26] E. Broyer and C. W. Macosko, "Curing and Heat Transfer in Polyurethane Reaction Modeling," *Polymer Engineering and Science,* vol. 18, pp. 382-387, April 1978.

[27] Z. S. Guo, S. Du, and B. Zhang, "Temperature field of thick thermoset composite laminates during cure process," *Composite Science and Technology,* vol. 65, pp. 517-523, 2005.

[28] F. P. Incropera and D. P. Dewitt, *Fundamentals of Heat and Mass Transfer*: JOHN WILEY & SONS, 2011.

[29] S. R. WHITE and C. KIM, "A Simultaneous Lay-Up and in situ Cure Process for Thick Composites," *Journal of Reinforced Plastics and Composites,* vol. 12, pp. 520-535, May 1993.

[30] S. Leung and S. Osher, "An Alternating Direction Explicit (ADE) Scheme for Time-Dependent Evolution Equations," 2005.

[31] S. Yi, H. H. Hilton, and M. F. Ahmad, "A Finite Element approach for Cure Simulation of Thermosetting Matrix Composites," *Computers & Structures,* vol. 64, pp. 383-388, 1997.

[32] V. PILLAI, A. N. BERIS, and P. DHURJATI, "Intelligent Curing of Thick Composites Using a Knowledge-Based system," *Journal of Composite Materials,* vol. 31, pp. 22-51, 1997.

[33] A. C. Loos and G. S. Springer, "Curing of Epoxy Matrix Composites," *Journal of Composite Materials,* vol. 17, March 1983.

[34] J. H. OH and D. G. LEE, "Cure Cycle for Thick Glass/Epoxy Composite Laminates," *Journal of Composite Materials,* vol. 36, pp. 19-45, 2002.

[35] N. RAI and R. PITCHUMANI, "Optimal Cure Cycles for the Fabrication of Thermosetting-Matrix Composites," *Polymer Composites,* vol. 18, pp. 566-581, 1997.

[36] J. S. KIM and D. G. LEE, "Development of an Autoclave Cure Cycle with Cooling and reheating Steps for Thick Thermoset Composite Laminates," *Journal of Composite Materials,* vol. 31, pp. 2264-2282, 1997.

[37] K. J. Teoh and K.-T. Hsiao, "Improved dimensional infidelity of curve-shaped VARTM composite laminates using a multi-stage curing technique - Experiments and modeling," *Composite : Part A - Applied Science and Manufacturing,* vol. 42, pp. 762-771, 2011.

[38] M.-H. CHANG, C.-L. CHEN, and W.-B. YOUNG, "Optimal Design of the cure Cycle for Consolidation of Thick Composite Laminates," *Polymer Composites,* vol. 17, pp. 743-750, 1996.

[39] P. Carlone and G. S. Palazzo, "Composite laminates cure cycle optimisation by meta-heuristic algorithms," *International Journal of Materials and Product Technology,* vol. 46, pp. 106-123, 2013.

[40] N. Pantelelis, T. Vrouvakis, and K. Spentzas, "Cure cycle design for composite materials using computer simulation and optimisation tools," *Forschung im Ingenieurwesen,* vol. 67, pp. 254-262, 2003.

[41] D. J. Michaud, A. N. Beris, and P. S. Dhurjati, "Thick-Sectioned RTM Composite Manufacturing, Part 2. Robust Cure Cycle Optimization and Control," *Journal of Composite Materials,* vol. 36, pp. 1201-1231, 2002.

3

Determination of Material Properties

3.1 Introduction

The purpose of this chapter is to determine the parameters in the governing equations of heat transfer and cure kinetics. In these governing equations, the material properties of the GF/Epoxy composite and the resin system, such as density, heat capacity, thermal conductivity and cure kinetic parameters, are required for the evaluation of the thermal analysis during cure.

During the curing process, the temperature of the composite varies from room temperature to the curing temperature, and then climbs up to the peak temperature. It is known that the material properties changes with temperature as well as the degree of cure. Thus, it is important to find that how large these effects are. For instance, the density of the epoxy resin changes during cure which was measured by Saraswat using a PVT (Pressure-Volume-Temperature) apparatus [1]. The results show that for an epoxy resin, the total volumetric shrinkage during cure is about 3.5%. In general, the cure shrinkage of epoxy resins are approximately 3∼5% [2].

Thermal conductivity of the composites also changes with temperature. Furthermore, most of the composites are anisotropic, resulting in unequal thermal conductivities along the in-plane and through-thickness directions. Sweeting found that for a cured carbon/epoxy plain weave composite, in the temperature range from 20 to 180 ℃, the in-plane thermal conductivity increases from 2 to 3 $W/(m \cdot K)$, while the through-thickness thermal conductivity changes from 0.5 to 0.7 $W/(m \cdot K)$ [3]. Mutnuri studied an E-glass/vinyl ester composite and his results show that the thermal conductivity through the thickness is 0.32 $W/(m \cdot K)$ at 60 ℃ and 0.35 $W/(m \cdot K)$ at 80 ℃ [4]. In addition to the

temperature, the degree of cure of the resin also affects the thermal conductivity. For the RTM 6 epoxy resin, Skordos and Partridge found that the thermal conductivity changes from 0.051 to 0.075 $W/(m \cdot K)$ during cure at the curing temperature 70 ℃ [5].

Undoubtedly, as a thermal property, the heat capacity also varies as a function of degree of cure and temperature. Turi studied the heat capacity for polystyrene and the results show that the heat capacity increases with the temperature and has a jump at the T_g [6]. Balvers (2007) studied the changes in heat capacity curves during cure for an RTM epoxy resin (see Figure 3.1). The results show that for epoxy resins, the heat capacity increases stepwise during the glass transition and the main effect of cure is that this glass transition is shifted to higher temperatures. Before and after the T_g the heat capacity increases linearly with temperature.

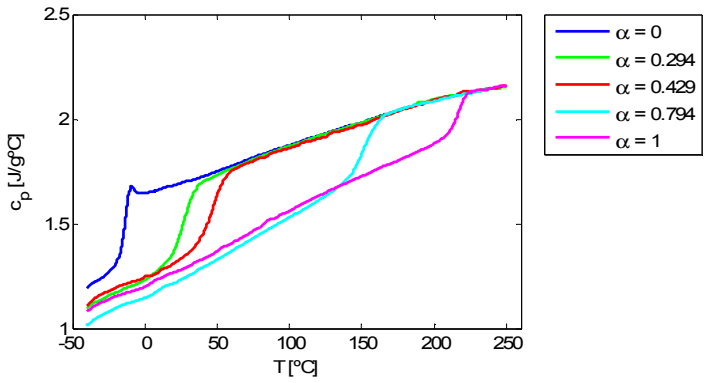

Figure 3.1 Measured heat capacity curves for an RTM epoxy resin (Balvers 2007)

3.2 Material properties of the selected epoxy resin system and GF/Epoxy composite

In this study, the Airstone™ infusion resin system (DOW®) – 780E epoxy resin and 785H hardener is used. This resin system is recommended for large-scale, continuous fiber-reinforced composites which need long infusion times. It has been widely applied for the manufacture of structural composites in the wind

energy industry such as wind turbine blades, turbine nose cones, generator nacelles and fairings.

Due to the low prices and high performance, E-glass fibers are widely utilized in the industry as the reinforcement in combination with epoxy resin matrix. The E-glass we used here is the E-glass Fabric 1200 g/m^2 (0°/+45°/-45°). It is a longitudinal tri-axial (nonwoven) layered fabric that contains rovings in longitudinal direction (0°) and in the double bias direction (±45°) (see Figure 3.2). The aerial weight of this fabric is 1200 g/m^2.

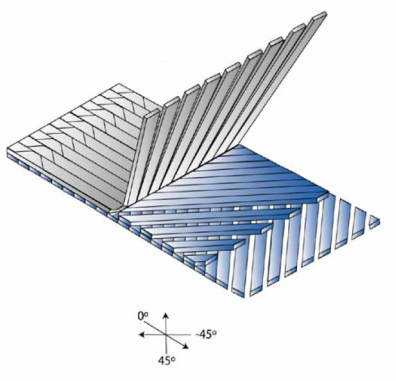

Figure 3.2 Sketch of the E-glass Fabric 1200 g/m^2 (0°/+45°/-45°).

In general, the density of E-glass fiber is about 2.58 g/cm^3, the thermal conductivity is 1.3 $W/(m \cdot K)$ at room temperature and the heat capacity values can be 810 $J/(kg \cdot K)$ at 23 ℃ and 1030 $J/(kg \cdot K)$ at 200 ℃ [7].

According to the heat transfer equation (Equation 1.3), the parameters needed for the modeling and calculations are listed in Table 3.1.

Table 3.1 Parameters used in the heat transfer equation

Parameters	**Description**
ρ_r, ρ_c	Density of the resin and composite, respectively.
k_{xx}, k_{yy}, k_{zz}	Thermal conductivities of the composite in the x, y and z directions, where xy is defined as in-plane and z is the direction through the thickness.

C_{p_c}	Heat capacity of the composite.
v_r	Resin volume fraction in the composite.
H_r	Total heat generation by the resin during cure.
A, E_a, m, n	Cure kinetic parameters

3.2.1 Determination of Density

3.2.1.1 Density Calculations of epoxy resin system and GF/Epoxy composite

The density is a very fundamental property of a material. From the experiments, we already know that the density of polymers is close to that of water. A lot of studies were carried out on different polymers. For the aromatic amine-epoxy resin system, it changes between 1.15 to 1.21 g/cm^3 from uncured to cured state [2]. The densities of E-glass and S-glass are 2.58 and 2.46 g/cm^3, respectively. For an S-glass fiber unidirectional epoxy composite, its density is between 1.96-2.02 g/cm^3 with fiber volume 57-63% [7].

In the Airstone™ Infusion resin system, the epoxy and hardener components are mixed at a certain ratio (see Table 3.2). Note that these density values of uncured epoxy and hardener components are measured at 25 ℃ (ASTM D-4052). Table 3.2 shows these material properties.

Table 3.2 Material properties of uncured epoxy and hardener components (Airstone™ infusion resin system (DOW®) – 780E epoxy resin and 785H hardener)

Property	Epoxy	Hardener
Density (g/cm^3)	1.15	0.95
Parts by weight	100	31

In this epoxy/hardener resin system, the rule of mixtures can be applied for the calculation of the density and it is given as:

$$\rho_r = v_e\rho_e + v_h\rho_h \tag{3.1}$$

where v_e, v_h are the epoxy resin volume fraction and hardener volume fraction, respectively. Here $v_e = 0.72$, $v_h = 0.28$. The subscripts e and h represent epoxy resin and hardener, respectively. According to the Equation 3.1, the density of the mixed uncured resin is $\rho_r^{uncured} = 1.1\ g/cm^3$.

For GF/Epoxy composites, the density also can be calculated using the rule of mixtures if the resin volume fraction is known. The expression is written as:

$$\rho_c = v_r\rho_r + v_f\rho_f \tag{3.2}$$

where v_r is the resin volume fraction, $v_r = 0.444$ (see Table 3.7), ρ_r is the density of uncured epoxy resin determined by Equation 3.1. Whereas ρ_f is the density of E-glass fiber, $\rho_f = 2.58\ g/cm^3$ as mentioned above. Thus, the density of the uncured GF/Epoxy composite can be calculated and it is $\rho_c^{uncured} = 1.92\ g/cm^3$.

In the next section, the density values of the fully cured epoxy resin system and GF/Epoxy composites are determined and compared with the above predictions in order to find the cure shrinkage of the epoxy resin and GF/Epoxy composite.

3.2.1.2 Density measurements of epoxy resin and GF/Epoxy composite

The density of the fully cured epoxy resin and GF/Epoxy composite can be determined by using the density determination kit (Mettler Toledo® Balance) which is suitable for solids and liquids as shown in Figure 3.3.

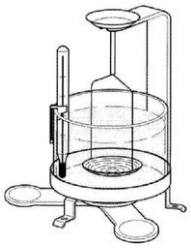

Figure 3.3 Density determination kit (Mettler Toledo® Balance).

The density determination kit is based on the Archimedes' principle. Hereby the sample is immersed in deionized water and the weights before and after the immersion are recorded as m_A and m_B, respectively. Before the measurements,

the sample needs to be dried in a vacuum drying oven for more than 8 hours. In addition, at least 6 samples are required to obtain reliable results.

The density can be calculated by Equation 3.3:

$$\rho = \frac{m_A}{m_A - m_B}(\rho_{water} - \rho_{air}) + \rho_{air} \qquad (3.3)$$

where ρ is the density of the sample, ρ_{water} is the density of the deionized water, ρ_{air} is the air density. m_A is the mass in the air before immersion, m_B is the mass in the water after immerse.

The density of deionized water at 22.2 ℃ is 0.99775 g/cm^3 and the air density is 0.0012 g/cm^3. Here both the fully cured epoxy resin and GF/Epoxy composite are measured at room temperature by this set-up. The experimental results are presented in Table 3.3.

Table 3.3 Experimental values of the density of the fully cured epoxy resin and GF/Epoxy composite

Density	**Experimental values** (g/cm^3)
ρ_r^{cured}	1.1600 ± 0.0004
ρ_c^{cured}	1.98 ± 0.01

Here the density was an average value obtained from six samples for the resin and composite, respectively. During the measurements, the systematic deviations can occur, for example, the sample contains voids or if small air bubbles attach to the samples. Note that the density of the cured composite is 1.98 g/cm^3 which is very close to the density of S-glass/epoxy composite which is between 1.96-2.02 g/cm^3. Here the density of the E-glass is a slightly higher than the S-glass, though its fiber volume $v_f = 0.556$ which is lower than the value 57-63% in the S-glass fiber unidirectional epoxy composite as mentioned above.

3.2.1.3 Volumetric cure shrinkage

By comparing the results for both of the material properties before and after curing, the cure shrinkage can be determined from the increases of the density. Khoun (2010) measured the volumetric cure shrinkage of an epoxy resin for a RTM process by using the modified rheology and gravimetric methods. The results show that the volumetric cure shrinkage at gelation ($\alpha_{gel} = 0.7$) is about 5.39% which is not influenced by the curing temperature [8]. Nawab found that the cure shrinkage of an epoxy vinylester resin is approximately 7.1% by using PVT-α measurements [9].

According to the definition of cure shrinkage [1], the volumetric cure shrinkage can be calculated as:

$$\varepsilon_{cure} = 1 - \frac{\rho_{uncured}}{\rho_{cured}} \tag{3.4}$$

As mentioned above, the predicted density for both the uncured epoxy resin and uncured GF/Epoxy composite are 1.10 g/cm^3 and 1.92 g/cm^3, respectively. Thus, the volumetric cure shrinkages for the neat epoxy resin and GF/Epoxy composite are approximately 5.2% and 3.0 %, respectively. Note that the 5.2% shrinkage of the neat resin is relatively large compared to the above mentioned typical cure shrinkage of 3-5%.

Normally the volumetric cure shrinkage of resin carrying fibers can be calculated by using $\varepsilon_c = \varepsilon_r - v_f H$, where H is a hindrance factor which can be found experimentally and is found equal to 0.03 [9]. From this equation, it indicates that the fibers can hinder the shrinkage of the resin in the composite during cure. In our case, the above equation predicts a composite shrinkage of $\varepsilon_c \approx 3.5\%$ which is slightly larger than the measured 3.0%. This difference could be caused by the fact that for different epoxy systems, a different hindrance factor is needed.

3.2.2 Thermal conductivity

Thermal conductivity is a transport property of a material for the conduction of heat which is evaluated primarily in terms of Fourier's law. Materials of high

thermal conductivity can transfer the heat at a higher rate than those of low thermal conductivity. In general, polymers have lower thermal conductivity than metals. Table 3.4 shows the thermal conductivity ranges of different material groups (C-THERM TECHNOLOGIES™).

Table 3.4 Literature values of thermal conductivities of different material groups[1]

Material groups	k **Range** $(W/(m \cdot K))$
Liquids & powders	0 – 0.6
Foams	0.04 – 0.09
Polymers	0.25 – 1.1
Ceramics	1.1 – 29
Metals	6 – 110

For continuous glass fibers, such as the high strength C-glass, E-glass and S-2 glass, the thermal conductivities are 1.1, 1.3 and 1.45 $W/(m \cdot K)$ near room temperature, respectively [7]. For cured epoxy resins, the thermal conductivity is in a range of 0.17 to 0.35 $W/(m \cdot K)$ [10]. In a fiber reinforced composite, due to the anisotropic properties of the material, the thermal conductivity parallel and transverse directions to the fiber are different. This parameter can be measured experimentally or calculated using the rule of mixtures (See the details in Table 3.5 and Section 3.2.2.3).

3.2.2.1 Thermal conductivity modeling

Thermal conductivity is a temperature-dependent property but only varies slightly in a limited temperature range. In addition, the character of inhomogeneous materials is another notable influence that may result in anisotropic property along the different fiber orientations. As mentioned before, tri-axial E-glass fabric is used for manufacturing the composites in this thesis. The composite made by

[1] http://www.axelproducts.com/downloads/TCi_Principles_of_Operation.pdf

this kind of reinforcement definitely will have the anisotropic thermal conductivity. A simple structural model of a composite shows the anisotropy of thermal conductivity in Figure 3.4.

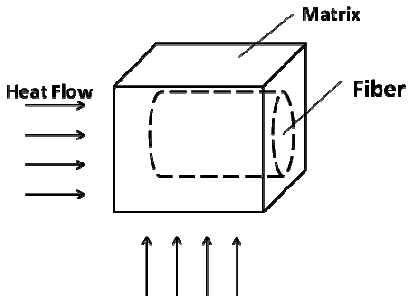

Figure 3.4 Anisotropy of thermal conductivity of a composite.

Theoretically, the thermal conductivity of a composite relates to its geometrical disposition of fibers and matrix. Using the heat transfer model of Fourier's law of heat conductivity, the thermal conductivity of a composite can be simulated for various kinds of geometries. For an evenly distributed homogeneous fiber-resin composite, the thermal conductivity model can be simulated as shown in Figure 3.5.

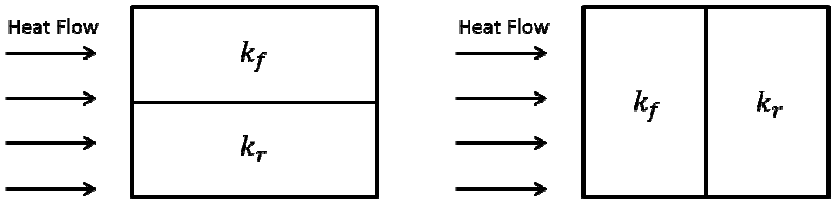

(a) (b)

Figure 3.5 (a) thermal conductivity model for heat flow parallel to the fiber orientation $k_{\parallel}$; (b) thermal conductivity model for heat flow perpendicular or transverse to the fiber orientation $k_{\perp}$.

Here k_f and k_r are the thermal conductivities of the fiber and resin, respectively. Considering the heat flows through this composite along different fiber directions, it will result in different thermal gradients due to the anisotropy of the composite.

The thermal conductivity models for the parallel and perpendicular (or transverse) directions can be expressed as

$$k_{\parallel} = v_f k_f + (1 - v_f) k_r \qquad (3.4\text{ a})$$

$$k_{\perp} = \frac{1}{\frac{v_f}{k_f} + \frac{1 - v_f}{k_r}} \qquad (3.4\text{ b})$$

Many other thermal conductivity models have been developed for different composite materials. For unidirectional fibers (UD) composites, the thermal conductivity model was studied by Springer and Tsai by using the thermal modelling [11]. Afterwards, many other researchers studied this topic and found the expressions for different types of composites. Some parts of these work are listed in Table 3.5 as shown below.

The thermal conductivity of the E-glass fiber used here is 1.3 $W/(m \cdot K)$ (AGY®) and the cured epoxy resin is 0.27 $W/(m \cdot K)$ as measured experimentally (see Table 3.6). The fiber volume fraction for GF/Epoxy composites is approximately 0.556 ($v_r = 0.444$). With these values, the thermal conductivities of the materials can be evaluated by using the models presented in Table 3.5 [12, 13].

Table 3.5 Thermal conductivity models and their predicted values of GF/Epoxy composite

Parallel direction (along the fibers)		$k_{\parallel}$ $(W/(m \cdot K))$
Filament-matrix composite model by Springer and Tsai [11]	$k_{\parallel} = v_f k_f + (1 - v_f) k_r$	0.84
Perpendicular direction (transverse to the fibers)		$k_{\perp}$ $(W/(m \cdot K))$
Filament-matrix composite model by Springer and Tsai [11]	$k_{\perp} = \frac{1}{\frac{v_f}{k_f} + \frac{1 - v_f}{k_r}}$	0.48

Square array filaments by Springer and Tsai [11]	$\frac{k_\perp}{k_r} = \left(1 - 2\sqrt{\frac{v_f}{\pi}}\right) + \frac{1}{B}(\pi - \frac{4}{\sqrt{1 - \frac{B^2 v_f}{\pi}}} tan^{-1} \frac{\sqrt{1 - \frac{B^2 v_f}{\pi}}}{1 + \sqrt{\frac{B^2 v_f}{\pi}}})$ $B = 2(\frac{k_r}{k_f} - 1)$	0.40
Sanford [14]	$\frac{k_\perp}{k_r} = \frac{1 - B_1 B_2 v_f}{1 - B_1 v_f}$ $B_1 = \frac{\frac{k_f}{k_r} - 1}{\frac{k_f}{k_r} + B_2}, B_2 = \frac{1}{4 - 3(1 - v_f)}$	0.39
Tsai [15]	$\frac{k_\perp}{k_r} = 1 + \frac{3v_f(k_f - k_r)}{(1 - v_f)(k_f - k_r) + 3k_r}$	0.64
Cylindrical assembly by Christensen [16]	$\frac{k_\perp}{k_r} = \frac{k_f + k_r + (k_f - k_r)(1 - v_f)}{k_f + k_r - (k_f - k_r)(1 - v_f)}$	0.49

Table 3.5 shows that the values of $k_\perp$ is in the range of 0.39 to 0.64 $W/(m \cdot K)$. It agrees with the results for the polymer matrix fabric (carbon, glass) composites in the range of 0.2 to 4 $W/(m \cdot K)$ [6]. However, $k_\perp$ is much lower compared to $k_\parallel$ which means the heat is dispersed faster along the fibers than in the resin matrix due to the relatively high thermal conductivity of the fibers.

Note that in the above models, $k_\parallel$ and $k_\perp$ are always considered as the in-plane thermal conductivities as k_{xx} and k_{yy} in a 3D geometry. However, the thermal conductivity through the thickness k_{zz} is more interesting because it is related to the temperature gradients through the thickness and thus, has a direct effect on the magnitude of the temperature overshoot during cure, which is the main focus of the present work. As a first estimation, the thermal conductivity model for the perpendicular direction (Springer and Tsai model) can be used to evaluate k_{zz} and it is $0.48\ W/(m \cdot K)$.

3.2.2.2 Thermal conductivity measurements

For the measurement of thermal conductivity, there are two classes of methods: steady-state methods and non-steady-state (or transient) methods. The most famous steady-state method is based on Fourier's law of heat conduction where the sample is placed between a hot and cold plate with a constant heat flux to maintain this steady state. However, in this method it would take a long time even for a thin composite to reach the steady state. For the transient methods, one is called Laser Flash Analysis Method (LFA) which is developed by Parker [17]. The process is that an energy pulse heats a plane-parallel sample on the bottom side, while a detector on top detects the time-dependent temperature rise which is used to calculate the thermal conductivity. Another method is known as the Transient Plane Source Method (TPS) that a flat-thin film type sensor is placed between two halves of the sample. During the measurement, the heat is generated and dissipated into the sample from both sides of the sensor and the temperature versus time signal is recorded by a detector.

In this thesis, a TCi Thermal Conductivity Analyzer instrument (C-THERM TCi™) is used for the determination of the thermal conductivity. The TCi system and set-up are shown in Figure 3.6.

(a) (b)

Figure 3.6 (a) Thermal Conductivity Analyzer instrument (C-THERM TCi™); (b) Schematic diagram of TCi set-up.

It is based on the Modified Transient Plane Source Method (MTPS). It uses a one-sided interfacial heat reflectance sensor which is designed to supply a momentary, constant heat source to the sample. During the measurement, a known current is applied to the sensor's heating element and providing a small amount of heat which results in a temperature rise at the interface between the sensor and sample. Meanwhile an induced voltage change is created in the sensor due to the temperature rise. Eventually thermal conductivity as well as other thermal properties can be calculated in this system.

In this measurement, samples should be loaded upon the sensor with distilled water as thermal conductive medium. A flat smooth surface of the sample is recommended which is not only to improve the condition of the contact surfaces, but also to avoid damaging the soft and sensitive element of the sensor. The minimum size of the sample should be at least 17 mm diameter in order to cover the whole surface. Moreover, a minimum of 0.5 mm thickness is required depending on thermal conductivity of the materials. The system has broad testing capabilities from 0 to 220 $W/(m \cdot K)$ and with an heating/cooling oven it is possible to measure in a temperature range from -50 to 200 ℃.

The thermal diffusivity is a property that indicates the ability of heat to diffuse through a material. The higher the thermal diffusivity of a material, the higher the rate of temperature propagation. The thermal diffusivity is defined as:

$$D = \frac{k}{\rho c_p} \tag{3.5}$$

and has the unit of m^2/s.

3.2.2.3 Experimental results of thermal conductivity

In this part, the cured neat epoxy resin and cured GF/Epoxy composite samples are prepared for the measurements. The dimension of the composite sample is $90 \times 70 \times 40\ mm$ and the epoxy resin sample is $60 \times 60 \times 15\ mm$. Considering the anisotropic properties of GF/Epoxy composite, all of the three directions are measured. Here the length direction of the composite is along the $0°$ fiber orientation and the through-thickness direction is considered as the height.

However, the cured epoxy sample can be considered as an isotropic material and is measured only in one direction. All of the measurements are operated at room temperature using fully cured samples. The results are shown in Table 3.6.

Table 3.6 Experimental values of thermal properties of cured epoxy resin and GF/Epoxy composite measured by C-THERM TCi

Property	**GF/Epoxy composite**			**Epoxy resin**
	$x-direction$	$y-direction$	$z-direction$	
Diffusivity $(\times 10^{-7} m^2/s)$	4.59	4.31	3.52	2.00
Thermal conductivity $(W/(m \cdot K)$	0.75	0.69	0.54	0.27

Table 3.6 shows that the thermal conductivity k_{xx} is higher than y and z directions which agrees with the trend as presented in Table 3.5. Because the continuous fibers can transfer heat much faster than the epoxy resin matrix due to its high thermal conductivity. Furthermore, the heat flow needs to pass through more resin matrix in the z direction in this multi-layered unidirectional fiber reinforced laminate which also makes the heat propagate at a relatively slow speed. Because the thermal conductivity predictions in Table 3.5 are based on the filament-matrix model, or square/cylindrical array filaments models, none of their fiber-matrix structure is strictly the same as our longitudinal tri-axial (nonwoven) layered fabric. Thus, these experimental results can be considered more reliable.

3.2.3 Heat capacity

The heat capacity is defined as the quantity of heat required to raise the temperature of a unit of mass of a substance by a single degree. Generally a DSC apparatus can be used to measure the heat capacity. It is normally used for homogeneous materials, like liquids or powders as well as the selected epoxy resin. However, for glassfiber reinforced composites, it is difficult to cut a proper small sample because of the fiber layers. Other factors, such as rough surface and

uneven portions taken from the matrix and fiber could result in significant deviation of a DSC measurement.

To determine the heat capacity of a composite, usually the rule of mixtures can be used and the expression is written as:

$$C_{p_c} = m_r C_{p_r} + m_f C_{p_f} \tag{3.6}$$

where C_{p_c}, C_{p_r} and C_{p_f} represent the heat capacity of composite, resin and fiber, respectively. m_r, m_f are the mass fraction of resin and fiber, $m_r = 0.26$ and $m_f = 0.74$ (see Table 3.7).

For the E-glass fiber, the heat capacity $C_{p_f} = 810\, J/(kg \cdot K)$ (High Strength Glass Fibers, AGY®). The heat capacity of the epoxy resin can be calculated by using Equation 3.7. With the experimental data from Table 3.6, we get $C_{p_r} = 1164\, J/(kg \cdot K)$. Using Equation 3.6, it results in a heat capacity for the GF/epoxy composite, $c_{p_c} = 902\, J/(kg \cdot K)$.

By using the data of the TCi measurements, we also can calculate the specific heat capacity. In Table 3.6 the thermal conductivity and diffusivity are determined. Thus, if the density is known, the heat capacity can be calculated as:

$$C_p = \frac{k}{\rho D} \tag{3.7}$$

According to the previous experimental results, the density of cured epoxy resin is 1.16 g/cm^3 and cured GF/Epoxy composite is 1.98 g/cm^3. From the data in Table 3.6 we see that the heat capacity of the composite at three directions are different. This would result in three different values for the heat capacity of the composite and they are 825, 809 and 775 $J/(kg \cdot K)$ in the x, y and z directions, respectively. But the heat capacity has to be a scalar quantity, so it is processed by taking the average value, resulting in $C_{p_c} = 803\, J/(kg \cdot K)$. This is about 11% lower than that from the rule of mixtures approach above. For the epoxy resin, it gets $C_{p_r} = 1164\, J/(kg \cdot K)$ as mentioned above. It is still in the range of 1046 to 1256 $J/(kg \cdot K)$ for the cured epoxy resin (Application Guide, Watlow®).

3.2.4 Resin and fiber volume fractions

For the fiber reinforced composites, the resin volume fraction is a very important factor for the determination of thermal properties. In this thesis, the vacuum infusion process is used for manufacturing the GF/Epoxy composites. During the process, the resin volume fraction changes slightly because of different vacuum pressures. Here a vacuum pressure at 200 $mbar$ is applied in the vacuum bag. It makes the resin flow smoothly along the fibers and ensures that it can reach the high fiber volume fraction needed to improve the mechanical properties of the composite.

According to the Standard Test Methods for constituent content of composite materials (ASTM D3171-06), the method is to physically remove the matrix by dissolving or burning off, leaving the reinforcement material essentially unaffected and thus allowing calculation of reinforcement and matrix content (by weight or volume). Before the testing, all of the six samples are dried in a dry oven for six hours at 80 ℃. Here, a furnace at 400 ℃ is used to remove the epoxy resin matrix from the glass fiber reinforcement. The final mass of the samples after combustion is obtained by taking the mass of the crucibles with fibers minus the crucible mass as $M_f = M_{c+f} - M_c$. Before the testing, the crucible should be cleaned by heating to 500 ℃ or more in the furnace and cooled in a desiccator to room temperature before weighing. The resin of the samples is removed by heating at 400 ℃ for 4 hours. After that it is cooled down to the room temperature within the furnace before taking it out.

The weight fraction of resin can be calculated by Equation 3.8 as:

$$m_r = \frac{M_i - M_f}{M_i} \tag{3.8}$$

And the resin volume fraction can be calculated by Equation 3.9 as:

$$v_r = \frac{M_i - M_f}{M_i}\frac{\rho_c}{\rho_r} \tag{3.9}$$

where M_i is the initial mass of the samples, M_f is the final mass of the samples after combustion. It is already known that $\rho_c = 1.98\ g/cm^3$, $\rho_r = 1.16\ g/cm^3$

(see Table 3.3). With the measurements of M_i and M_f, we can calculate the resin weight and volume fraction. The results are shown in Table 3.7.

Table 3.7 Experimental values of resin weight and volume fraction of GF/Epoxy composites

Samples	$M_i\ (g)$	$M_f\ (g)$	v_r	m_r
S1	4.67	3.47	0.439	0.257
S2	4.53	3.35	0.445	0.260
S3	4.52	3.34	0.444	0.260
S4	4.92	3.65	0.442	0.259
S5	4.81	3.55	0.445	0.261
S6	4.47	3.30	0.447	0.262
Average			0.444 ± 0.003	0.260 ± 0.002

According to the results from Table 3.7, the average value of resin volume fraction is
$v_r = 0.444$ and the resin weight fraction is $m_r = 0.260$. For the S-2 glassfiber unidirectional epoxy composite (AGY®), its resin volume fraction is about $0.37 \sim 0.43$ which is close to our result.

3.3 Cure kinetics of epoxy resin system

3.3.1 Introduction to cure kinetic models

As described in Chapter 2, cure kinetic models are applied to predict the curing behavior of thermoset resins. In general, curing reaction of epoxy-amine systems show complex kinetics and have been considered as autocatalytic reactions. Furthermore, since according to the experimental results the initial reaction rate of this resin is slightly above zero, it is more proper to use the n^{th} order + autocatalytic reaction model (see Table 2.1).

In general , both isothermal and dynamic scanning method can be used for the thermoset resin systems [18]. However, because the Airstone Infusion Resin is a slow reaction resin, it requires to cure at 70 ℃ for at least four hours and an extra four hours for the post-cure process at the same temperature. Considering the

long isothermal curing process, isothermal scanning of DSC measurement is more suitable to characteristic this resin system.

Various fitting methods have been developed to determine the kinetic parameters. The most common method is using a multi-linear regression such as the Kissinger and Ozawa methods [18-21]. However, these methods only can figure out the parameters at one single temperature point at each time, but not the full temperature range during cure. It can be called a local fitting method. In the work of this thesis, a global fitting method is created to determine the kinetic parameters at a group of different curing temperatures simultaneously.

3.3.2 Experimental preparation

To perform the DSC measurements properly, the following procedure was applied:

- All samples were prepared in the same manner. This includes that all samples are taken from the same mixture, and using samples of roughly the same weight. A sample weight of $10\sim15\ mg$ is preferred.
- The recommended curing temperature for the Airstone Infusion Resin is 70 ℃. In order to cover the whole temperature profile in a curing composite, a more broad temperature range from 60 to 110 ℃ is chosen with an interval of 10 ℃.
- For an isothermal cure, the sample is heated from the initial temperature to the curing temperature at a constant heating rate. The heating rate is chosen depending on the thermal sensitivity of the resin system [22]. The heating rate of 20 $℃/min$ is implemented here.
- After reaching the curing temperature, it needs to hold on for enough time that makes sure the sample is fully cured. Furthermore, due to the long curing time for each DSC measurement, the untested samples in the waiting line were stored in the fridge to avoid curing in advance.

3.3.3 Results and discussions

During the measurements, the DSC instrument records the change of heat flow passing through a pan with resin and another empty pan as a reference for calibrating the furnace. Totally seven experiments were performed at the

temperatures of 60, 70, 80, 90 100 and 110 ℃. Because all of the samples were stored in the fridge below 0 ℃, they firstly were equilibrated at 0 ℃ for 1 minute and then heated up to the curing temperature at the heating rate of 20 ℃/min. The DSC results of heat flow versus time at different isothermal cure temperatures are shown in Figure 3.7.

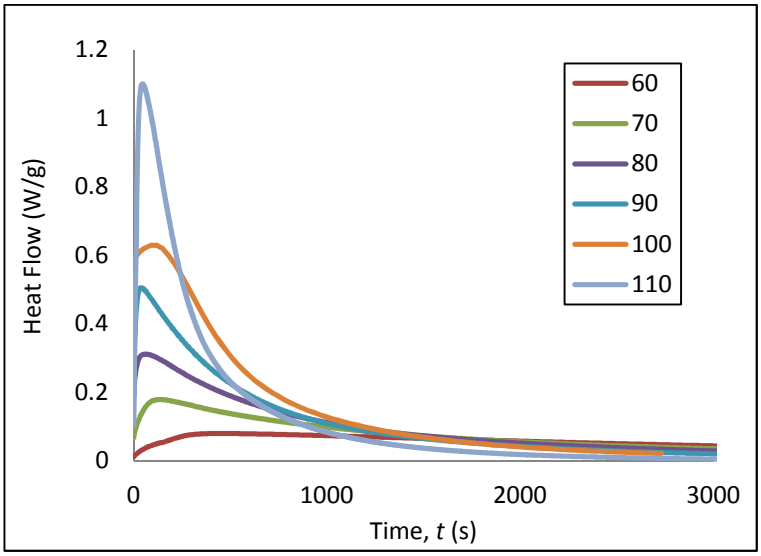

Figure 3.7 DSC results of heat flows of isothermal cure reaction at 60, 70, 80, 90, 100 and 110 ℃, respectively. The time scale here is only shown until 3000 seconds, although the actual recordings continued until 21000 seconds.

Figure 3.7 shows that the reaction peaks increased with the curing temperatures and the cure reaction at high temperatures are completed sooner than those at the low temperatures. By integrating the heat flow with time, the total heat of reaction can be calculated for each isothermal cure. However, for the isothermal cure reactions at lower temperatures, it is difficult to reach the fully cured state even for a very long curing time. Therefore, a dynamic curing process at heating rate of $10\sim20$ ℃/min were carried out to measure the total heat of reaction when $\alpha = 1$. The results are shown in Table 3.8.

Table 3.8 Determination of total heat of reaction by dynamic curing process at different heating rates

Heating rate (°C/min)	Total heat of reaction (J/g)
10	435.4
14	442.4
20	440.9
Average	440 ± 4

As a result, the total reaction heat is $H_r = 440\ J/g$. Because the total heat of reaction is a constant for a particular resin, the final degree of cure of the isothermal cure can be calculated as:

$$\alpha_{max} = \frac{H^*}{H_r} \tag{3.10}$$

where α_{max} is the maximum or final degree of cure of the isothermal cure. H^* is the heat generated by the reaction per unit mass of the resin. The resin is considered to be uncured at $\alpha = 0$ and fully cured at $\alpha = 1$. Table 3.9 shows the final degree of cure at different curing temperatures.

Isocure temp. (°C)	Total heat of reaction (J/g)	Final degree of cure [-]
60	340	0.77
70	348	0.79
80	372	0.85
90	384	0.87
100	415	0.94
110	424	0.96

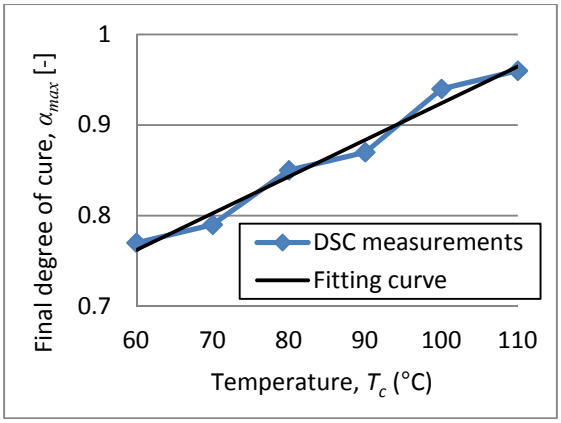

Figure 3.8 Left: Table of the total heat generation at different isothermal cure temperatures and the final degree of cure; Right: Curve of the final degree of cure at different isothermal cure temperatures with its fitting curve.

A linear fitting curve of α_{max} was found and it is expressed as

$$\alpha_{max} = \begin{cases} 0.0041T_c + 0.5185, & 60℃ \leq T_c \leq 117\ ℃ \\ 1, & T_c > 117\ ℃ \end{cases} \quad (3.11)$$

In Equation 3.11, α_{max} is a function of the curing temperature in unit of ℃. When T_c exceeds 117℃, it can be considered as fully cured.

For the isothermal cure process, the final degree of cure at 60 ℃ is only 0.77 and increases to 0.96 at 110 ℃. It shows that the final degree of cure is increasing with the curing temperature. However, it is not significant to reach the fully cured state by an isothermal curing process. Thus, the post-cure temperature is better to be above 117 ℃.

Since the measured heat flow curves are proportional to the reaction rate, we can use the total heat of reaction to obtain the reaction rate. The expression is written as:

$$\frac{d\alpha}{dt} = \frac{1}{H_r}\frac{dH_t}{dt} \quad (3.12)$$

where dH_t is the heat at a specific time.

As mentioned above, the reaction rate can be calculated directly from the measured heat flow data according to Equation 3.12. For the modeling of the cure kinetics, it is useful to make a plot of the reaction rate versus degree of cure. The results are shown in Figure 3.9.

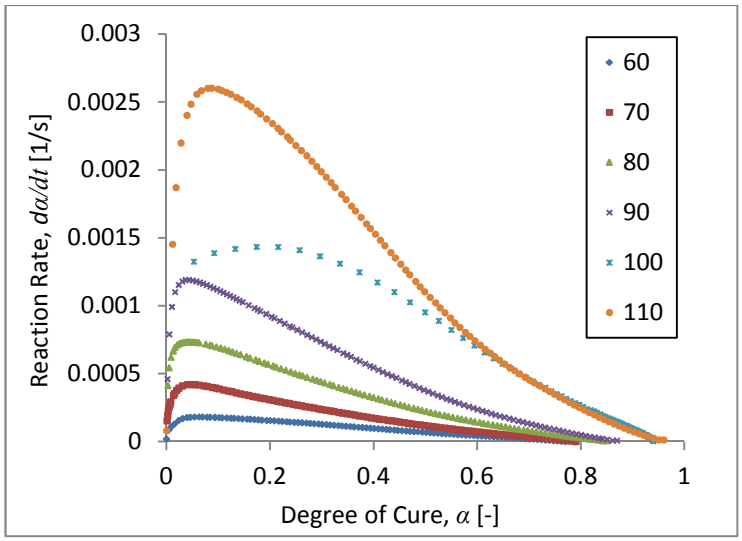

Figure 3.9 Reaction rate versus degree of cure at different isothermal cure temperatures.

Subsequently integrate Equation 3.12 to obtain the curve of desired degree of cure versus time. The results are shown in Figure 3.10.

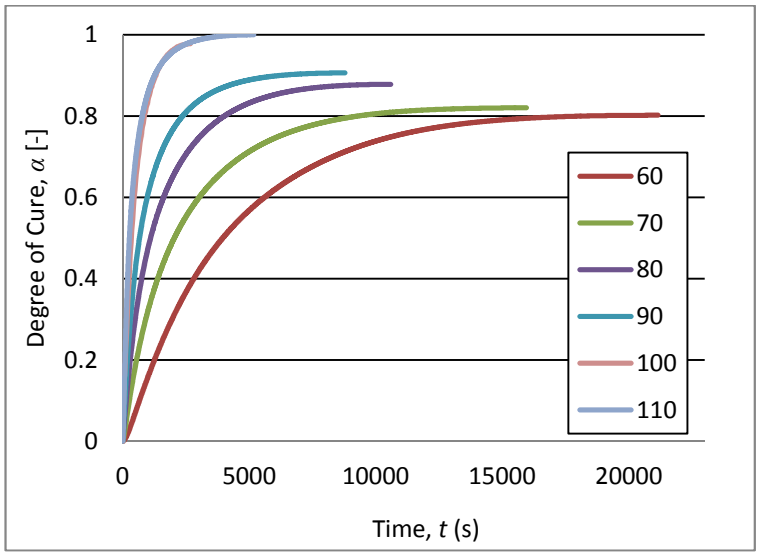

Figure 3.10 Degree of cure at different isothermal cure temperatures versus time.

Figure 3.10 shows that at curing temperature 60 ℃, it takes about 6 hours to reach the final conversion. However, at curing temperature 110 ℃, it is shortened to 5000 seconds. Note that in Figure 3.10 the 100 and 110 ℃ curves overlap because of experimental scatter. It shows that the curing time becomes shorter when increasing the curing temperature. When the temperature rises to a certain level, such as 100 or 110 ℃, this time change could be very small.

3.3.3.1 Normalized degree of cure

It is found above that the maximum experimental degree of cure at different temperatures does not always reach $\alpha = 1$ which is caused by the diffusion limitation effect [13]. A simple method to improve the expression of cure kinetic models is to normalize the degree of cure. It can be modified in the form of:

$$\hat{\alpha} = \frac{\alpha}{\alpha_{max}} \tag{3.13}$$

where $\hat{\alpha}$ is the normalized degree of cure. In this way, the maximum degree of cure is automatically normalized to 1. Note that there are many other methods which can incorporate the diffusion limitation effect (see Chapter 2).

According to the data of the reaction rate versus degree of cure, the results of normalized degree of cure curves are shown in Figure 3.11.

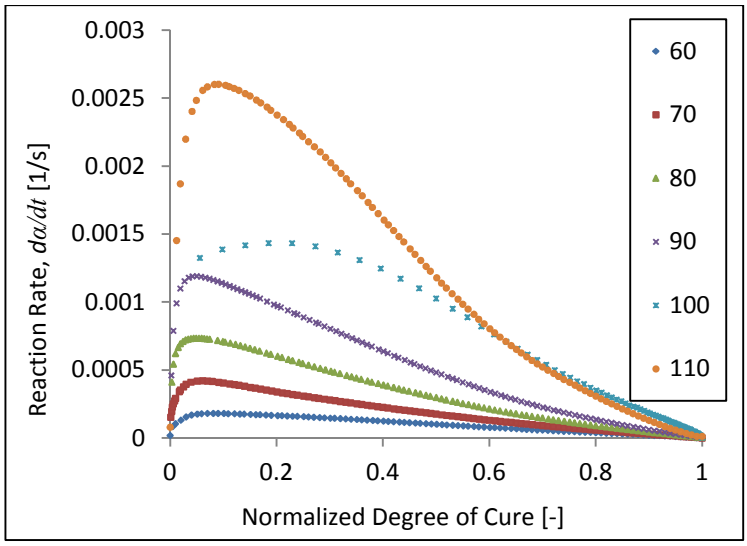

Figure 3.11 Reaction rate versus normalized degree of cure at different isothermal cure temperatures.

3.3.3.2 Global fitting method for the estimation of cure kinetic parameters

Here the intention is to determine the cure kinetic parameters. For the epoxy-amine resin system, the n^{th} order + autocatalytic cure kinetic model is chosen to represent the reaction rate (cure kinetic Model 3 in Table 2.1). In this model, the reaction rate $\frac{d\alpha}{dt}$ is a function of the degree of cure α and temperature T, with six cure kinetic parameters A_1, E_{a_1}, A_2, E_{a_2}, m and n. Here the software Mathematica 8 with the Quasi-Newton fitting strategy is used to find a globally optimal fit based on the experimental data. The fitting results are shown in Table 3.9.

Table 3.9 Global optimal fitting values of cure kinetic parameters

Parameter	A_1 $(1/s)$	E_{a_1} (J/mol)	A_2 $(1/s)$	E_{a_2} (J/mol)	m	n

Value	0.0010	13000	32000	50000	0.19	1.8

The fitting curves compared with the experimental data are shown in Figure 3.12.

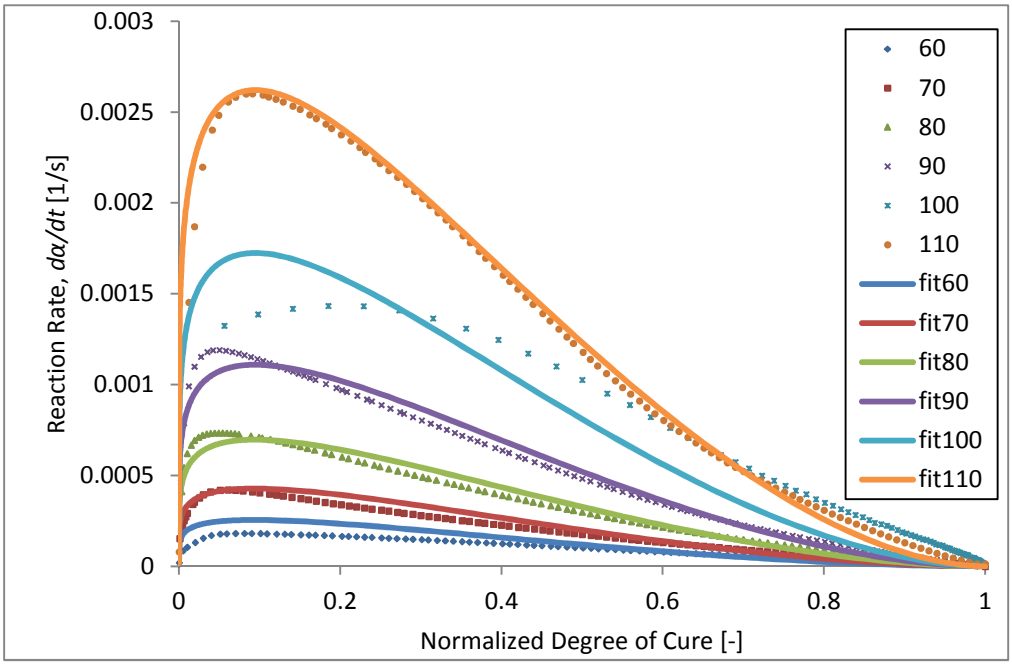

Figure 3.12 Global optimal fitting of the cure kinetic model (Model 3) at different isothermal cure temperatures. The solid lines are the fitting curves and the markers are the experimental data.

Figure 3.12 shows that it has a good agreement between the fitting curves and the experiments. Only at the curing temperature 100°C, it has a notable deviation. It may be cause by experimental scatter as mentioned before. At the end of the cure, the experimental results are slightly higher than the fitting curves which indicates that the diffusion limitation effect still exists but becomes very weak.

In Figure 3.12 the fitting curve is based on the n^{th} order + autocatalytic cure kinetic model (Model 3). In addition, the fitting based on Model 2 as the first reaction rate $k_1 = 0$, are also carried out the see the influence of the first reaction rate. The results are shown in Figure 3.13 below.

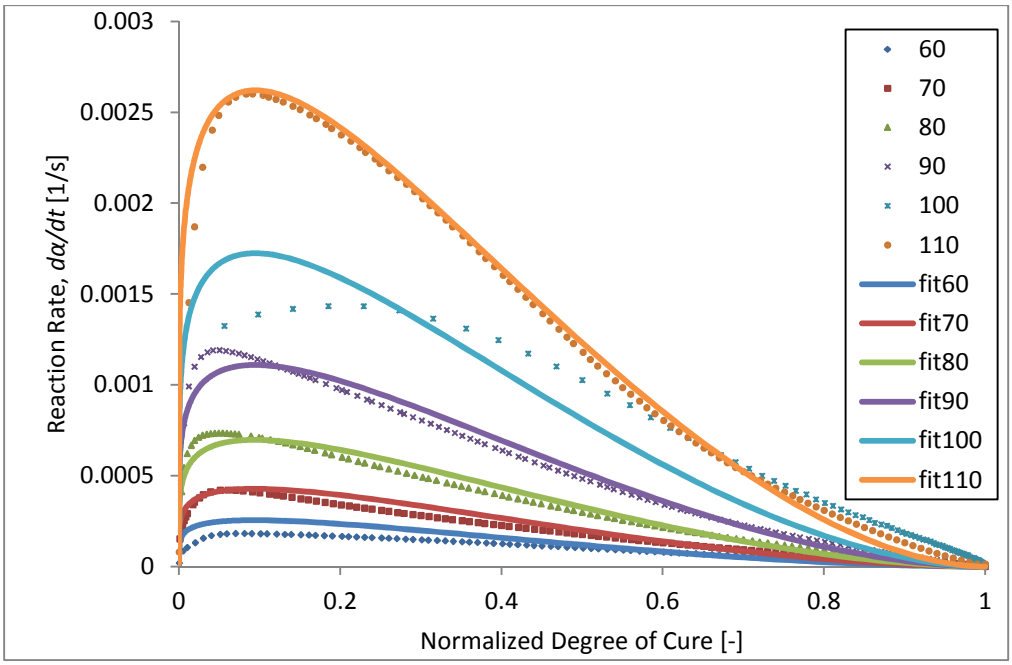

Figure 3.13 Global optimal fitting of the cure kinetic model (Model 2) at different isothermal cure temperatures. The solid lines are the fitting curves and the markers are the experimental data.

From the Figure 3.13 we see that the fitting curves for the cure kinetic Model 2 and 3 are almost the same though the reaction rate of Model 2 should be a little bit lower than the value of Model 3 theoretically. This is because that the values of k_1 is much smaller than k_2 as shown in Figure 3.14. The ratio of k_2/k_1 varies from 51 to 289 when the temperature is increasing from 60 ℃ to 110 ℃. Thus, in the actual modeling, the difference between Model 2 and Model 3 are very small.

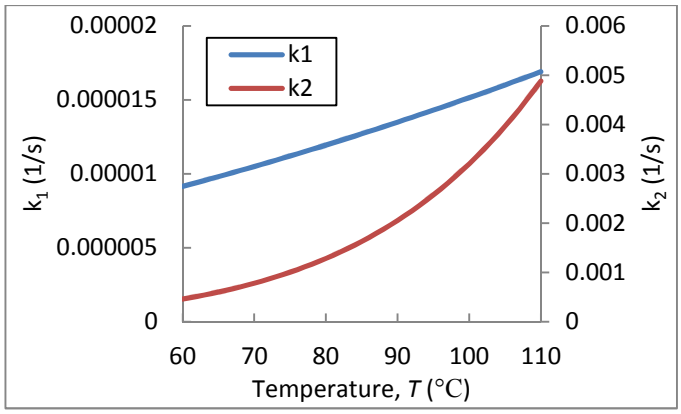

Figure 3.14 Reaction rate k_1 and k_2 versus temperature.

3.4 Conclusions

For the determination of the density, the rule of mixtures is used to predict the uncured epoxy resin and GF/Epoxy composite and density determination kit (Mettler) measurements are carried out for the cured ones. For the uncured epoxy resin, the density is calculated as 1.10 g/cm^3 and for the uncured composite, it is 1.92 g/cm^3. The experimental results of cured epoxy resin and GF/Epoxy composite are 1.16 g/cm^3 and 1.98 g/cm^3, respectively. Because of the cure shrinkage, the cured materials are slightly heavier than the uncured. The volumetric cure shrinkage of epoxy resin is 5.2% and it is only 3% in the GF/Epoxy composite due to the fibers hindering.

Based on the previous thermal conductivity models, the thermal conductivity of GF/Epoxy composite is evaluated at both parallel and perpendicular directions. In Table 3.5 we can see that $k_{\parallel} = 0.84\ W/(m \cdot K)$ and $k_{\perp}$ is in a range from 0.39 to 0.64 $W/(m \cdot K)$. Using the thermal conductivity analyzer instrument TCi, the thermal conductivities of epoxy resin and GF/Epoxy composite are measured at room temperature. For the epoxy resin, the thermal conductivity is 0.27 $W/(m \cdot K)$. As an anisotropic material, the thermal conductivities of GF/Epoxy composite are different at x, y and z directions which are 0.75, 0.69 and 0.54 $W/(m \cdot K)$, respectively. These experimental results agree well with the predicted values.

Using the rule of mixtures, we calculated the heat capacity of GF/Epoxy composite to be 902 $J/(kg \cdot K)$. Using the diffusivity, the heat capacity was estimated as $803\ J/(kg \cdot K)$ which is somewhat lower. For the epoxy resin, it is $1164\ J/(kg \cdot K)$.

When using the rule of mixtures, the volume fraction and weight fraction of resin or fiber are always needed which can be determined by a burning test. For the GF/Epoxy composite, the resin volume fraction and weight fraction are 0.444 and 0.260, respectively. This result agrees with the typical resin volume fraction of 0.5 for a composite manufactured by the vacuum infusion process.

For this epoxy-amine resin, the n^{th} order + autocatalytic cure kinetic model is used and DSC measurements are carried out to determine the kinetic parameters. Here isothermal DSC method was used to determine the heat flow during cure at 60, 70, 80, 90, 100 and 110 ℃. It is found that it is hard to reach the fully cure at the isothermal curing temperatures. It is measured that the degree of cure is 0.77 when it is cured at 60 ℃ and it increases to 0.96 when it is cure at 110 ℃. The dynamic DSC method is used to determine the total heat of reaction during cure which is 440 J/g measured at different heating rates. In order to count the diffusion limitation effect, a normalized degree of cure is used for the experimental data process. With the normalized degree of cure, reaction rate at different curing temperatures, the global fitting method is built up to find a solution of the kinetic parameters. Compared to the normal fitting methods, this global fitting method can search for the solution in the whole temperature range instead of finding the fitting curves at each specific temperature, so it can give a more comprehensive and robust result.

Reference

[1] M. K. Saraswat, K. M. B. Jansen, and L. J. Ernst, "Cure Shrinkage and Bulk Modulus determination for Moulding Compounds," presented at the ESTC Conference, Dresden, 2006.

[2] G. Lubin, *Handbook of compositess*. New York: Van nostrand reinhold company, 1982.

[3] R. D. Sweeting and X. L. Liu, "Measurement of thermal conductivity for fibre-reinforced composites," *Composites : Part A - Applied Science and Manufacturing,* vol. 35, pp. 933-938, 2004.

[4] B. Mutnuri, R. Liang, and H. GangaRao, "Thermal conductivity characterization of FRP composites: Experimental," presented at the ANTEC 2006, Charlotte, NC, 2004.

[5] A. A. Skordos and I. K. Partridge, "Inverse heat transfer for optimization and on-line thermal properties estimation in composites curing," *Inverse Problems in Science and Engineering,* vol. 12, pp. 157-172, 2004.

[6] A. Turi, *Thermal characterization of polymeric materials*, 2nd ed. ed.: Academic Press, 1997.

[7] AGY. (2006). *High strength glass fibers*. Available: http://www.agy.com/wp-content/uploads/2014/03/High_Strength_Glass_Fibers-Technical.pdf

[8] L. Khoun and P. Hubert, "Cure Shrinkage Characterization of an Epoxy Resin System by Two in Situ Measurement Methods," *Polymer Composites,* 2010.

[9] Y. Nawab, X. Tardif, N. Boyard, V. Sobotka, P. Casari, and F. Jacquemin, "Determination and modelling of the cure shrinkage of epoxy vinylester resin and associated composites by considering thermal gradients," *Composite Science and Technology,* vol. 73, pp. 81-87, 2012.

[10] Watlow. (1997). *Application guide - physical properties of solids, liquids and gases*. Available: https://www.watlow.com/common/catalogs/files/appguide.pdf

[11] G. S. Springer and S. W. Tsai, "Thermal Conductivities of Unidirectional Materials," *Composite Materials,* vol. 1, 1967.

[12] R. C. Progelhof, J. L. Throne, and R. R. Ruetsch, "Methods for Predicting the Thermal Conductivity of Composite Systems: A Review," *polymer engineering and science,* vol. 16, 1976.

[13] R. S. Dave and A. C. Loos, *Processing of Composites*: Hanser Publishers, 2000.

[14] W. M. Sanford, "Cure Behavior of Thermosetting Resin Composites," PhD, University of Delaware, 1987.

[15] J. C. Halpin, *Primer on Composite Materials Analysis*: CRC Press, 1984.

[16] R. M. Christensen, *Mechanics of composite materials*. New York: Wiley Interscience, 1979.

[17] W. J. Parker, R. J. Jenkins, C. P. Butler, and G. L. Abbott, "Flash Method of Determining Thermal Diffusivity, Heat Capacity, and Thermal Conductivity," *Journal of Applied Physics,* vol. 32, 1961.

[18] L. Sun, "Thermal rheological analysis of cure process of epoxy prepreg," PhD, Chemical engineering, Louisiana State University, 2002.

[19] H. E. Kissinger, "Reaction Kinetics in Differential Thermal Analysis," *Analytical Chemistry,* pp. 1702-1706, 1959.

[20] C. S. Chern and G. W. Poehlein, "A Kinetic For Curing Reactions of Epoxides with Amines," *Polymer Engineering and Science,* vol. 27, June 1987.

[21] L. Chiao and R. E. Lyon, "A Fundamental Approach to Resin Cure Kinetics," *Journal of Composite Materials,* vol. 24, pp. 739-752, 1990.

[22] P. I. Karkanas and I. K. Partridge, "Cure Modeling and Monitoring of Epoxy/Amine Resin Systems. 1. Cure Kinetics Modeling," *Journal of Applied Polymer Science,* vol. 77, pp. 1419-1431, 2000.

4

Analytical Approximation of Core Temperature

4.1 Introduction

In the past decades several studies on analytical solutions have been published for thermo-chemical behavior in composites during cure. Because the parameters such as curing temperature, cure kinetics, are so important for the curing process, dimensionless groups correlating to these parameters were introduced for the evaluation of these thermo-chemical models. Also because the temperature profile during cure is not constant, it rises when the curing reaction goes on until reaching its peak value, then it goes down while the reactants are finished, so this nonlinear profile needs to be evaluated by a tool like dimensionless groups.

In addition, researchers also show interests in providing a definition for a thick composite. Previously the definition of a thin or thick composite mainly depended on its geometry. However, in a thermo-chemical model, it has to include the thermal effect. For a thin laminate, the heat generated during cure can be conducted to the surroundings in a short time. Even for a low thermal conductivity composite material, the core temperature will not increase too much in thin laminates [1]. However, the situation in a thick laminate is quite different. Because of the low thermal conductivity, the reaction heat generated in the core is trapped inside the laminate. As a result, the core temperature will rise. Since the reaction rate increases with temperature, even more heat is produced, leading to a large temperature overshoot in the core. Some unexpected defects, such as deformation, overheating or thermal residual stresses may occur by this temperature overshoot.

One way to deal with this problem is to determine a critical thickness for the curing composites. This critical thickness was first mentioned by Broyer who developed a critical half thickness for adiabatic curing systems [2]. Balvers introduced a numerical method to predict the maximum achievable thickness according to the material degradation temperature for thick-wall composites [3]. Also Second introduced dimensionless groups including a modified Damkohler number and finally defined a critical thickness to distinct the composite parts between thin and thick [4]. In this thesis, we will develop analytical solutions to predict the core temperature as well as temperature distribution through the thickness, and use it to define a new critical thickness which includes cure kinetic parameters as well as thermal and processing parameters.

4.2 Governing equations

In this chapter, a scaling analysis using dimensionless numbers is proposed to evaluate the curing process of the epoxy-based composites. Before introducing the thermo-chemical model, some assumptions have to be made for simplifying the modeling processes and calculations.

During this composite manufacturing process, epoxy resin flows through fibers following with curing reaction. The thermal equilibrium between the resin and fibers can be expressed by Equation 4.1 (see also Chapter 1).

$$\underbrace{\rho_c C_{p_c} \frac{\partial T}{\partial t}}_{\text{Transient}} + \underbrace{\rho_r c_{p_r} \left(\vec{V} \cdot \nabla T\right)}_{\text{Convection}} = \underbrace{\nabla (k_c \cdot \nabla T)}_{\text{Conduction}} + \underbrace{\rho_r v_r H_r \frac{d\alpha}{dt}}_{\text{Heat generation}} \quad (4.1)$$

where ρ, C_p, k, are the density, heat capacity and thermal conductivity, respectively; V is the velocity of the resin flow; v_r is the resin volume fraction, and H_r is the total heat generated during cure. The subscripts c and r denote composite and resin, respectively. Equation 4.1 shows that the overall energy equation consists of a transient, a convection, a conduction and a heat generation term. The convection term is due to the motion of the epoxy resin. Because this

model is focusing on the curing stage, the resin flow velocity is considered as zero, thus the convection heat term is neglected.

The following assumptions are made:

1. The resin filling phase is neglected and at time $t = 0$, the mold is occupied by uncured resin at temperature T_c;
2. One dimensional heat transfer model through the thickness;
3. Constant thermal-physical properties;
4. Autocatalytic cure kinetic model;
5. Wall temperatures are constant as T_c.

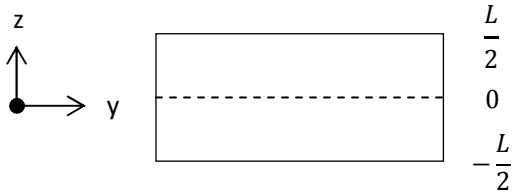

Figure 4.1 1D heat transfer model of a cross-section view. z-direction is through the thickness of the composite (thickness is L).

Note that the wall temperature of the composite is kept at T_c for both sides, so the temperature curve is symmetrical in the thickness direction. In Figure 4.1 the boundary conditions are $T(t = 0) = T_c$, $T\left(z = \pm\frac{L}{2}, t\right) = T_c$.

After applying the above assumptions, the thermo-chemical model can be written as:

$$\rho_c C_{p_c} \frac{\partial T}{\partial t} = k_{zz} \frac{\partial^2 T}{\partial z^2} + \rho_r v_r H_r \frac{d\alpha}{dt} \qquad (4.2)$$

where the second term on the left side of this equation is the internal heat source generated by the curing reaction. The thermal-physical properties, such as ρ_c, C_{p_c}, k_{zz}, ρ_r, v_r and H_r are all constant (see Chapter 3). The reaction rate is considered to be an autocatalytic cure kinetic model (Model 2 in Table 2.1) which can be written as:

$$\frac{d\alpha}{dt} = A \cdot \exp\left(-\frac{E_a}{RT}\right) \alpha^m (1-\alpha)^n \tag{4.3}$$

Note that this is a simplification of the more general n^{th} order + autocatalytic model that was used for the material characterization in Chapter 3. However, Equation 4.3 produces a kinetic fit which does not deviate much from the cure kinetic Model 3 according to the corresponding graphs in Figure 3.12 and 3.13. Thus, it is assumed to be able to model the cure kinetics in a sufficiently accurate way.

In this study one of the aims is to determine the maximum temperature during cure. The core temperatures starts at T_c and then rises due to the curing reaction until it reaches its maximum. When the maximum temperature is approached, the heat generation term is balanced by the heat conduction to the mold walls and the transient term on the left side of the equation can also be neglected. Then Equation 4.3 becomes:

$$k_{zz}\frac{\partial^2 T}{\partial z^2} + \rho_r v_r H_r \frac{d\alpha}{dt} = 0 \tag{4.4}$$

By this assumption the core temperature will be slightly over estimated. Furthermore, by analyzing Equation 4.3, we find the reaction rate $\frac{d\alpha}{dt}$ is at its peak value at:

$$\alpha_p = \frac{m}{m+n} \tag{4.5}$$

Combining Equation 4.3 - 4.5, the thermo-chemical model in this steady state can be expressed as:

$$\frac{\partial^2 T}{\partial z^2} + \frac{1}{k_{zz}}\rho_r v_r H_r A \exp\left(-\frac{E_a}{RT}\right) \cdot f(\alpha)_{max} = 0 \tag{4.6}$$

where $f(\alpha)_{max}$ is a constant (see Equation 2.10).

Since we assume the reaction rate is at its peak value, it again overestimates the peak temperature. This equation is a second-order partial differential equation for the temperature with an exponential temperature term and it is difficult to solve

it analytically in this way. The following paragraphs will introduce how to find approximate solutions for this problem.

4.3 Non-dimensionalization process

To solve Equation 4.6, dimensionless numbers of characteristic temperature and characteristic thickness were introduced in the definition of:

$$\hat{T} = \frac{T}{T_c} \qquad \hat{z} = \frac{z}{L} \tag{4.7}$$

where $\hat{T}$ is the dimensionless temperature, T_c is the curing temperature in Kelvin which is applied by the wall of the heating mold; $\hat{z}$ is the dimensionless thickness, L is the total thickness of the composite.

After inserting this into Equation 4.6, we obtain:

$$\frac{\partial^2 \hat{T}}{\partial \hat{z}^2} + N_a \cdot \exp\left(\frac{-c}{\hat{T}}\right) = 0, \qquad \hat{T}\left(\hat{z} = \pm\frac{1}{2}\right) = 1 \tag{4.8}$$

where N_a is a dimensionless number and c is a constant. Their expressions are:

$$N_a = \frac{L^2}{k_{zz} T_c} \rho_r v_r H_r A f(\alpha)_{max} \tag{4.9 a}$$

$$c = \frac{E_a}{R T_c} \tag{4.9 b}$$

The dimensionless number N_a depends on the parameters of the material properties k_{zz}, ρ_r, v_r, cure kinetic parameters H_r, A, m, n, and process parameters L, T_c.

In Equation 4.8, the term of $\hat{T}$ is a part of an exponential function, which makes it difficult to solve. Therefore, we write $T = T_c + \Delta T$, such that $\hat{T}$ becomes $\hat{T} = \frac{T_c + \Delta T}{T_c} = 1 + \Delta\hat{T}$, where ΔT is the temperature difference. Note that since T_c is in Kelvin, the temperature difference ΔT is always relatively small such that $\Delta\hat{T}$ is typically 0.1 or less. Thus, the term of $\frac{1}{\hat{T}}$ can be expanded as $\frac{1}{\hat{T}} = \frac{1}{1+\Delta\hat{T}} = 1 - \Delta\hat{T} + O(\Delta\hat{T}^2)$. Here the error in this approximation is no more than $\Delta\hat{T}^2$. Finally,

the exponential function in Equation 4.8 can be expressed as $\exp\left(\frac{-c}{\hat{T}}\right) \approx \exp\left[-c\left(1-\Delta\hat{T}\right)\right]$.

Taking the above approximations into Equation 4.8, it becomes:

$$\frac{\partial^2\hat{T}}{\partial\hat{z}^2} + N_b \cdot \exp\left(c\,\Delta\hat{T}\right) = 0, \qquad \Delta\hat{T}\left(\hat{z} = \pm\frac{1}{2}\right) = 0 \tag{4.10}$$

where N_b is expressed as $N_b = N_a \cdot \exp(-c)$.

Let $\theta = c \cdot \Delta\hat{T}$, and rewriting the Equation 4.10 then it gives

$$\boxed{\frac{\partial^2\theta}{\partial\hat{z}^2} + N_c \cdot \mathrm{e}^{\theta} = 0, \qquad \theta\left(\hat{z} = \pm\frac{1}{2}\right) = 0} \tag{4.11}$$

where N_c is expressed as $N_c = c \cdot N_b = \mathrm{c} \cdot e^{-c} \cdot N_a$.

$$N_c = \frac{L^2 c}{e^c k_{zz} T_c}\rho_r v_r H_r A f(\alpha)_{max} \tag{4.12}$$

As shown in Equation 4.12, in a curing composite, the dimensionless number N_c is related to the composite thickness, curing temperature, cure kinetic parameters and material properties.

Equation 4.11 is a nonlinear differential equation which is known as the Bratu's equation. In 1914 Bratu solved a second order Ordinary Differential Equation (ODE) which was used to analyze the temperature distribution in a 1D combustion model. Now this equation has been applied in solid fuel thermal combustion problems, chemical reaction theory, radiative heat transfer and nanotechnology, as well as the expansion of universe [5]. According to Bratu's theory [6], once it satisfies the two-point boundary condition as $\theta\left(-\frac{1}{2}\right) = \theta\left(\frac{1}{2}\right) = 0$, the exact solution is given as:

$$\theta(\hat{z}) = 2\ln\left[\frac{\cosh\left(\frac{\varphi}{4}\right)}{\cosh\left(\frac{\varphi}{2}\hat{z}\right)}\right] \tag{4.13}$$

where φ satisfies:

$$\varphi = \sqrt{2N_c}\cosh\left(\frac{\varphi}{4}\right) \tag{4.14}$$

Equation 4.14 is a transcendental function. Unlike algebraic equations, such equations often do not have closed form solutions. Many researchers studied and found different types of solutions, such as Boyd who used Chebyshev polynomials method to solve the 1D Bratu's equation, and Karkowski introduced four kinds of numerical methods in one, two and three dimensions [7-13].

This transcendental equation has two roots φ_1 and φ_2 ($\varphi_1 < \varphi_2$) of which φ_2 is discarded because that means that for increasing N_c, the dimensionless temperature $\theta(\hat{z})$ would decrease which is not realistic in our situation. Thus, we only consider the first root φ_1.

In order to find an approximate expression for $\varphi(N_c)$, we first evaluated Equation 4.14 numerically and plotted the results as the triangle markers in Figure 4.2. The solution thus appeared to be a monotonically increasing function of N_c with an asymptote near 3.5. From the study of Bratu's equation, we find that this asymptote is given as $N_{cc} = 3.5138$ [8, 14-19].

$$\varphi(N_c) = a_1\left[\frac{\pi}{2} + \arcsin\left(\frac{2}{a_2}N_c - 1\right)\right] \tag{4.15}$$

With the boundary condition $\varphi(0) = 0$ and $\varphi(N_{cc}) = \varphi_c$, then we can get $a_1 = \frac{\varphi_c}{\pi}$, $a_2 = N_{cc}$. Here φ_c is the critical value of φ being $\varphi_c = 4.7987$. The error between the exact solution and this approximation was evaluated by R-squared method, $R^2 = 0.9952$. Using this closed form approximation, it reduces the computation of Bratu's equation to an algebraic equation which is more efficient for solving the problem.

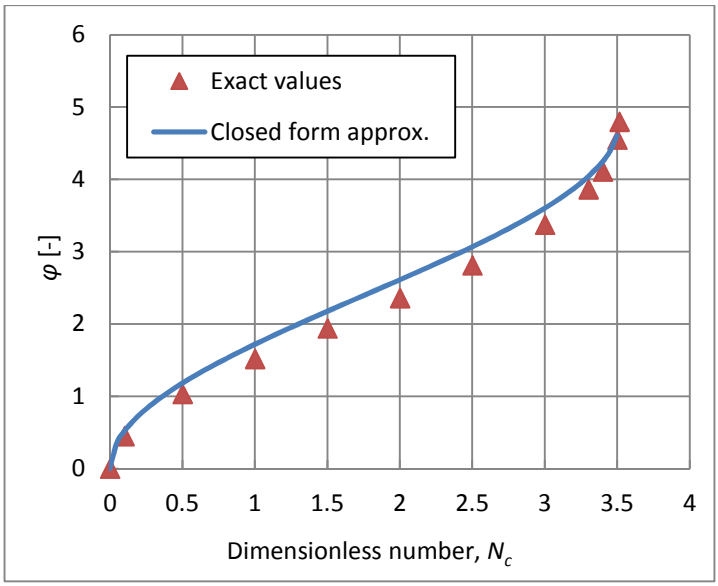

Figure 4.2 Exact and closed form approximation of the transcendental equation $\varphi(N_c)$.

Figure 4.2 shows that the closed form approximation is slightly higher than the exact values but they are strictly equivalent at the start and end points.

With these results, the dimensionless temperature $\theta(\hat{z})$ can be calculated by using Equation 4.13 and 4.15, and the results are shown in Figure 4.3.

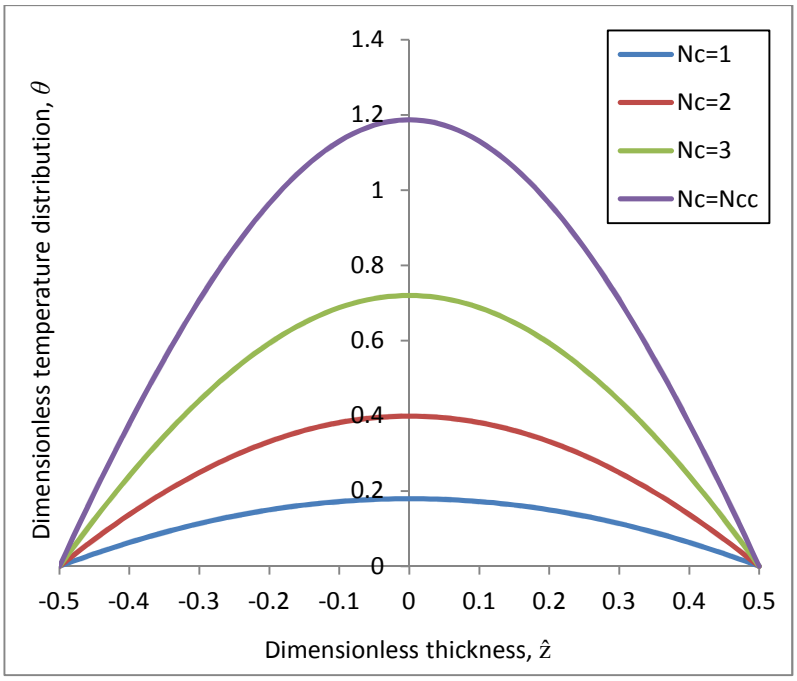

Figure 4.3 Predicted dimensionless temperature distribution $\theta(\hat{z})$ at $N_c = 1, 2, 3, N_{cc}$.

As shown in Figure 4.3 the predicted dimensionless temperature $\theta(\hat{z})$ increases with the dimensionless number N_c. For the different values of N_c, this means that different curing temperatures or laminate thicknesses are used for the manufacturing and results in different temperature distributions through the thickness.

Furthermore, the maximum dimensionless temperature for a thick curing composite has also been studied. Inserting $\hat{z} = 0$ into Equation 4.13, the expression of θ_{max} is given as:

$$\theta_{max} = 2ln\left[cosh\left(\frac{\varphi}{4}\right)\right] \tag{4.16}$$

Since $\varphi(N_c)$ depends on the dimensionless number N_c, the maximum dimensionless temperature only varies with N_c as shown in Figure 4.4.

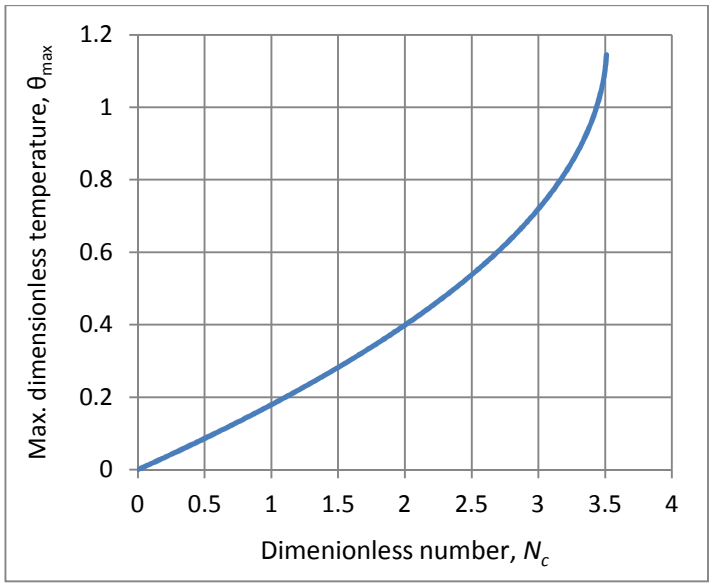

Figure 4.4 Analytical solution of maximum dimensionless temperature θ_{max} vs. dimensionless number N_c.

As shown in Figure 4.4 that the maximum dimensionless temperature θ_{max} increases with the dimensionless number N_c. When it is close to the critical value of N_c, the value of θ_{max} increases asymptotically. It indicates that if the boundary conditions like curing temperature or laminate thickness increase, the curing reaction speed will accelerate and generate much more heat, leading to a very high temperature overshoot in the core of a curing composite.

Note that Figure 4.3 and 4.4 are dimensionless graphs and were calculated without using specific material or process data. It means that the $cosh$ shape of the temperature profile and the asymptote behavior near the critical limit will also be observed in all practical situations.

4.4 Determination of critical thickness

According to the Equation 4.12 the dimensionless number N_c depends quadratically on the thickness L. Since the critical dimensionless number N_{cc} has been found, the critical thickness L_c can be calculated as:

$$L_c = \sqrt{\frac{e^c N_{cc}\, k_{zz} T_c}{c\rho_r v_r H_r A f(\alpha)_{max}}} \qquad (4.17)$$

Equation 4.17 shows that the critical thickness L_c is related to the curing temperature T_c. Moreover, it is inversely proportional to the cure kinetic terms $H_r A f(\alpha)_{max}$, which means that if the cure reaction speed accelerates, the value of the critical thickness has to decrease.

We can compare this with the expression of Second (2011) mentioned earlier in Chapter2, $L_c^{Second} = \sqrt{\frac{e^c k_{zz}}{\rho_c C_{p_c} A f(\alpha)_{max}}}$. These two equations differ by the factors of the dimensionless number N_{cc} , the curing temperature T_c, the resin's material properties of ρ_r, v_r and the total heat generation H_r.

If we use the material properties of a typical epoxy resin mentioned in Chapter 3, we can find the relation between the critical thickness L_c and curing temperature T_c as shown in Figure 4.5.

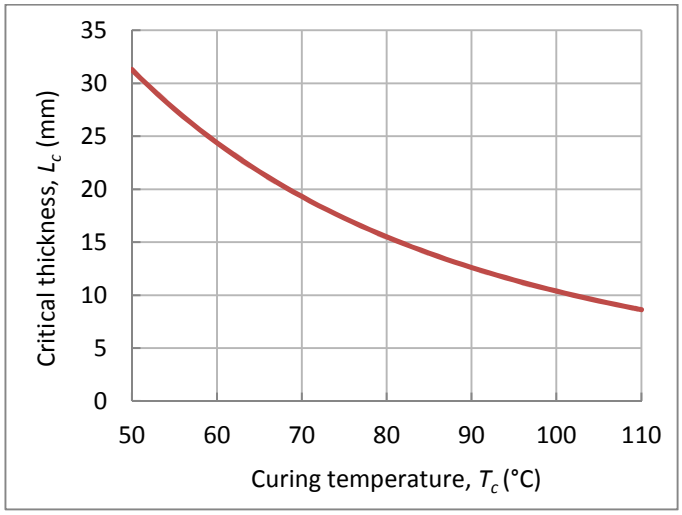

Figure 4.5 Analytical critical thickness L_c vs. curing temperature T_c from 50 to 110 °C.

As shown in Figure 4.5 the critical thickness is decreasing with the curing temperatures. It means when the applied curing temperature increases, the

acceptable critical thickness of the laminate has to decrease to avoid extreme temperature overshoot in the composite. For example, if a laminate is cured at 50 ℃, the maximum thickness is allowed up to 31 mm. However, if it cured at 110 ℃, then the maximum thickness reduces to 8.6 mm.

Besides the critical thickness, θ_{max} also can be expressed in the form of $\theta_{max}(L)$ based on Equation 4.16. The results are shown in Figure 4.6.

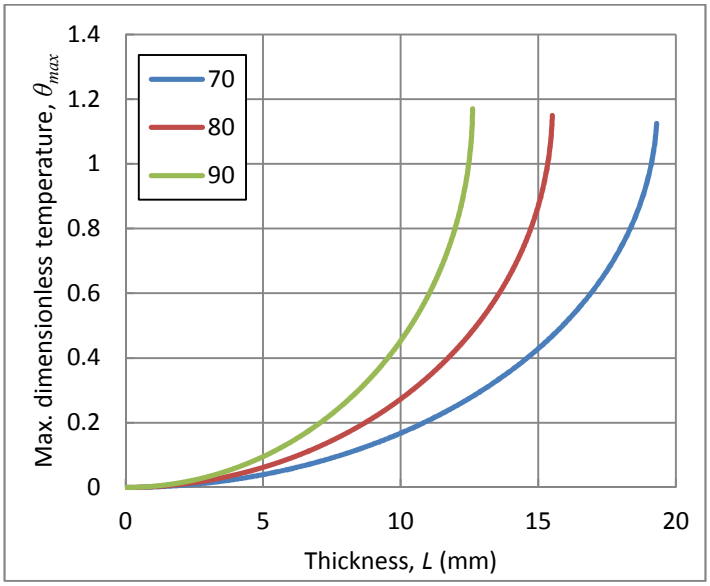

Figure 4.6 Analytical maximum dimensionless temperature θ_{max} vs. thickness L at curing temperature 70, 80 and 90 ℃, respectively.

Note that at different curing temperatures, the maximum dimensionless temperature θ_{max} has its own critical thickness. It also shows that the values of the critical thickness is inversely proportional to the curing temperature. For example, if set the upper limitation as $\theta_{max} = 1$, the critical thicknesses at curing temperature 70, 80 and 90 ℃ are 19.1 mm, 15.3 mm, 12.5 mm, respectively. It means at the same θ_{max} level, the allowable thickness for a curing composite has to be thinner while increasing the curing temperature. More practical examples of the use of these equations are presented in Chapter 6.

4.5 Core temperature

The main purpose of this study is to predict the maximum temperature in the core of a curing composite. According to the definition of the maximum temperature difference ΔT_{max}, the expression can be written as:

$$\Delta T_{max} = \frac{T_c}{c}\theta_{max} \tag{4.18}$$

In the Equation 4.18, since $\frac{T_c}{c}$ is the scale factor for θ_{max}, the figures of ΔT_{max} and θ_{max} are similar. With this equation, we can predict the maximum temperature overshoot in a curing composite for a certain thickness and curing temperature.

In Section 4.3, we made an assumption for $\frac{1}{\hat{T}}$ with an error $O(\Delta\hat{T}^2)$. Now we can calculate the maximum value of $\Delta\hat{T}$ that is about 0.0677, so that $O(\Delta\hat{T}^2) \approx 0.0046$. Thus, the approximation for $\frac{1}{\hat{T}}$ is quite acceptable.

Here the analytical solutions are verified by the numerical method that the laminate thickness is within its critical thickness as shows in Figure 4.7. The details about the numerical process will be described in chapter 5.

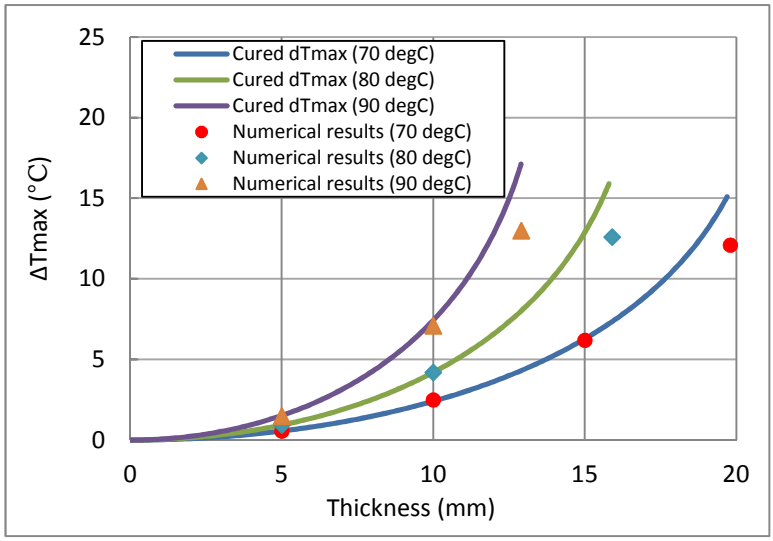

Figure 4.7 Analytical and numerical results of ΔT_{max} versus thickness at curing temperature 70, 80 and 90 ℃, respectively.

As shows in Figure 4.7 that the analytical results agree well with the numerical values. Only when approaching the critical thickness, the analytical solutions become slightly higher than the numerical results which is caused by the approximation process in the analytical model. At 70 ℃, the analytical ΔT_{max} is 15.1 ℃ and the numerical result is 12.1 ℃, the deviation between them is 3 ℃. At 80 ℃ and 90 ℃, the deviations are 3.3 ℃ and 4.1 ℃, respectively. But it is still acceptable compared to their curing temperatures.

4.6 Conclusions

For the thermo-chemical phenomenon in a curing composite, a 1D heat transfer model was established to calculate and simulate the temperature profiles through the thickness. In this study it was focusing on the case of the maximum temperature during the curing reaction. Some assumptions and simplifications were made for the calculations of a dimensionless number N_c which depends on the curing temperature T_c, thickness L, cure kinetic parameters and its material properties. It is an important factor as a ratio of conduction heat and reaction heat. A critical dimensionless number N_{cc} was found which indicates that a steady-state thermo-chemical model can be accomplished only below this value. Using the critical dimensionless number N_{cc} we can calculate the critical thickness L_c at different curing temperatures. The results show that it is decreasing with the curing temperature T_c which means if the laminate is cured at a higher temperature, the thickness has to be thinner to avoid the temperature overshoot. Moreover, based on the well-known Bratu's equation, a new analytical approximation was found which matches its exact values well.

Furthermore, a direct closed form expression for the dimensionless temperature $\theta(\hat{z})$ was obtained which can be used to evaluate the temperature profiles through the thickness. Similarly, the maximum dimensionless temperature θ_{max} and the maximum temperature difference ΔT_{max} can be calculated to predict the temperature overshoot in the core of a curing composite.

In order to find out how appropriate our series of simplifications is, numerical simulation was studied to compare with these analytical solutions. The results show that the predicted maximum temperature difference agrees well with its numerical results within the critical thickness. Only when approaching the critical thickness, the analytical values are slightly higher than the numerical ones which is caused by the approximation process. The deviations between them are less than 4.1 ℃. This part of work will be the topic of the Chapter 5.

Reference

[1] T. A. Bogetti and J. John W. Gillespie, "Two-Dimensional Cure Simulation of Thick Thermosetting Composites," *Journal of Composite Materials,* vol. 25, March 1991.

[2] E. Broyer and C. W. Macosko, "Heat Transfer and Curing in Polymer Reaction Modeling," *AIChE Journal,* vol. 22, pp. 268-276, 1976.

[3] J. M. Balvers, H. E. N. Bersee, A. Beukers, and K. M. B. Jansen, "Determination of Cure Dependent Properties for Curing Simulation of Thick-Walled Composites," presented at the AIAA conference Chicago, US, 2008.

[4] T. W. Second, S. C. Mantell, and K. A. Stelson, "Scaling Analysis and a Critical Thickness Criterion for Thermosetting Composites," *Journal of Manufacturing Science and Engineering,* vol. 133, February 2011.

[5] L. Jin, "Application of Modified Variational Iteration Method to the Bratu-Type Problems," *INTERNATIONAL JOURNAL OF CONTEMPORARY MATHEMATICAL SCIENCES,* vol. 5, pp. 153-158, 2010.

[6] H. T. Davis, *Introduction to Nonlinear Differential and Integral Equations*: Dover Publications, 1962.

[7] M. Zarebnia and Z. Sarvari, "New Approach for Numerical Solution of the One-Dimensional Bratu Equation," *Thai Journal of Mathematics,* vol. 11, 2013.

[8] J. P. Boyd, "An Analytical and Numerical Study of the Two-Dimensional Bratu Equation," *Journal of Scientific Computing,* vol. 1, 1986.

[9] J. P. Boyd, "Chebyshev polynomial expansions for simultaneous approximation of two branches of a function with application to the one-dimensional Bratu equation," *Applied Mathematics and Computation,* vol. 143, pp. 189–200, 2003.

[10] N. Cohen and J. V. T. Benavides, "Exact solutions of Bratu and Liouville equations," presented at the National Congress of Applied Mathematics and Computer (CNMAC), 2010.

[11] J. Jacobsen and K. Schmitt, "The Liouville-Bratu-Gelfand Problemfor Radial Operators," *Journal of Differential Equations,* vol. 184, pp. 283–298, 2002.

[12] J. Karkowski, "Numerical experiments with the Bratu equation in one, two and three dimensions," *Computational and Applied Mathematics,* vol. 32, pp. 231–244, 2013.

[13] M. I. Syam and A. Hamdan, "An efficient method for solving Bratu equations," *Applied Mathematics and Computation,* vol. 176, pp. 704–713, 2006.

[14] J. P. Boyd, "Chebyshev polynomial expansions for simultaneous approximation of two branches of a function with application to the one-dimensional Bratu equation," *Applied Mathematics and Computation,* vol. 143, pp. 189-200, 2003.

[15] N. Cohen and J. V. T. Benavides, "Exact solutions of Bratu and Liouville equations," presented at the CNMAC 2010, 2010.

[16] J. Jacobsen and K. Schmitt, "The Liouville-Bratu-Gelfand problem for radial operators," *Journal of Differential Equations,* vol. 184, pp. 283-298, 2002.

[17] J. Karkowski, "Numerical experiments with the Bratu equation in one, two and three dimensions," *Computational and Applied Mathematics,* vol. 32, pp. 231-244, 2013.

[18] M. I. Syam and A. Hamdan, "An efficient method for solving Bratu equation," *Applied Mathematics and Computation,* vol. 176, pp. 704-713, 2006.

[19] M. Zarebnia and Z. Sarvari, "New approach for numerical solution of the one-dimensional Bratu equation," *Thai Journal of Mathematics,* vol. 11, pp. 611-621, 2013.

5

Numerical Study of Temperature Distributions in Thick Thermoset Composites

5.1 Introduction

In this chapter, a numerical method is developed to simulate the thermo-chemical behavior in a curing GF/Epoxy composite. In Chapter 4, we found an analytical solution for predicting the temperatures through the thickness of a composite during cure. Here a numerical solution is used to verify the analytical solution numerically. Furthermore, the degree of cure in the composites during cure also can be obtained which could be very important for the mechanical properties of the composites.

Generally an analytical study can solve a physical or chemical problem which has a simple geometry or boundary conditions. However, most of the practical engineering processes are multi-physical problems which may have a complex geometry and/or boundary conditions. In the last decades, with the development of computer science, the numerical methods, such as Finite Difference Method (FDM), Finite Element Method (FEM) were developed for 1D, 2D and 3D heat transfer problems [1-8]. For example, Kim and White studied an 1D transient heat transfer problem for a continuous curing process in a thick thermoset composite [9]. Bogetti and Gillespie built a 2D model to predict the temperature and degree of cure in thick glass/polyester and Graphite/epoxy composites [5]. The results show that the 2D model is efficient to work at arbitrary cross-section of a composite, while the 1D model is significantly influenced by the part geometry and the anisotropic material properties. Using a 3D transient heat transfer FEM

analysis, Oh simulated the curing process in thick glass/epoxy composites [10]. The results show that the laminate thickness has a dominant influence on the temperature distribution in the core compared with the laminate size (length and width). Moreover, a 3D model provides more accurate predictions than a 1D model.

The general process of the numerical analysis of a heat transfer problem is to find an approximate solutions of the algebraic equations of the temperature field based on a finite amount of discrete points on the physical body in the time and space coordinates. The workflow of this process is represented in Figure 5.1.

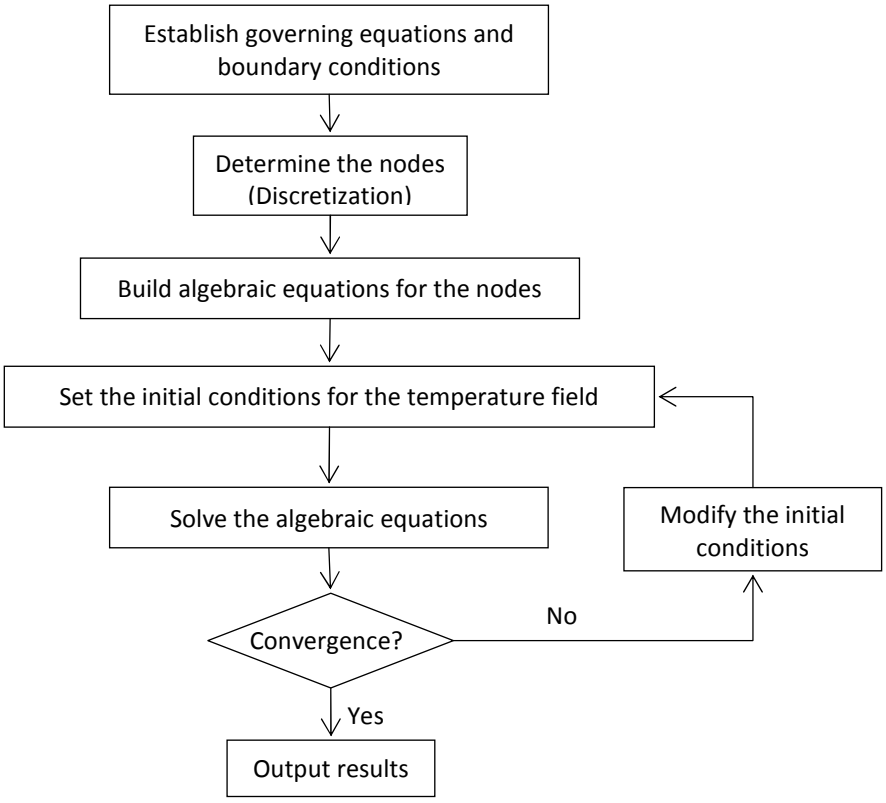

Figure 5.1 Workflow of numerical solution process.

5.2 Numerical processes

According to the workflow of the numerical solution, the first step is to establish the governing equation for the thermo-chemical model. This governing equation is based on the heat transfer equation which has an internal heat source. It is used to evaluate the temperature distribution as well as the degree of cure. As mentioned before, the size of the composite almost has no influence on the temperature in the thickness direction in the center of a composite during cure. Here we build a 3D heat transfer model for the simulation instead of 1D model.

5.2.1 Governing Equation

For a 3D transient heat transfer problem, the geometry of the part is subdivided into a number of small regions which can be solved by numerical techniques such as FEM later. For an arbitrary finite element in the part, the heat flux passes through it and separates into x, y and z directions as shown in Figure 5.2.

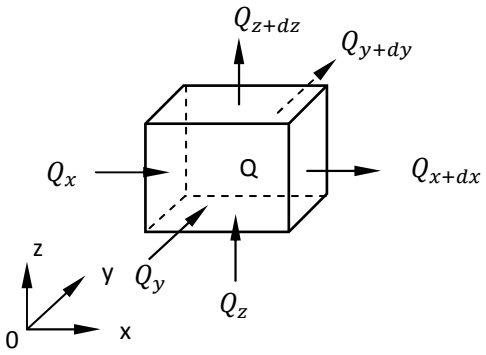

Figure 5.2 3D heat transfer analysis in a finite element of a part.

In order to get the mathematical formulation of this thermo-chemical model, it has to obey the law of conservation of energy and the Fourier's law of heat conduction, then this governing equation becomes the partial differential equation (PDE) of heat conduction. According to Equation 1.1, the governing equation can be written as:

$$\frac{\partial T}{\partial t} = D\left(\frac{\partial^2 T}{\partial x^2} + \frac{\partial^2 T}{\partial y^2} + \frac{\partial^2 T}{\partial z^2}\right) + \frac{Q}{\rho_c C_{p_c}} \tag{5.1}$$

where D is the thermal diffusivity. In a 3D model, the temperature variation is expressed as $T(x, y, z, t)$. Q is the internal heat per unit volume W/m^3 generated by the curing reaction.

5.2.2 Initial values and boundary conditions

In a 3D model, the dimension of geometry is defined by length × width × height. Here the height is treated as its thickness. As mentioned before, Oh found that the temperature in the middle is not influenced by the size of the composites when the length varies from 200 mm to 1000 mm. Thus, here we choose a $200mm \times 200\ mm$ square laminate with a 40 mm thickness as the geometry of the composite.

Refer to the analytical solution in Chapter 4, the initial temperature of the composite is the same as the curing temperature. Thus, at time $t = 0$, the initial temperature of the composite is:

$$T(x, y, z, 0) = T_c \tag{5.2}$$

The experimental set-up is designed such that the laminate is placed between a heating mold which has a constant surface temperature T_s, where $T_s = T_c$. Practically, because of the thermal resistance, the initial temperature cannot distribute evenly through the thickness if it is heated from the outside surfaces. However, the experimental measurements show that the initial temperature gradient in a 40 mm thick glassfiber laminate is less than 1℃ in the steady state. Therefore, we assume that the initial temperature in the laminate is even.

Here the temperature T_s is applied to the top and bottom surfaces of the laminate and the vertical walls are all thermal insulated as shown in Figure 5.3.

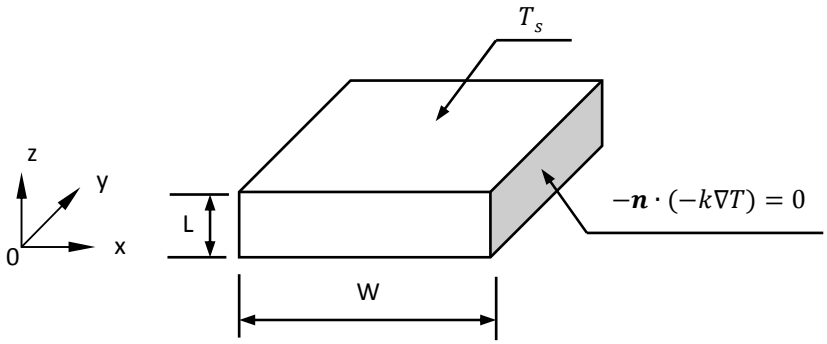

Figure 5.3 Geometry of a laminate and its boundary conditions.

On a thermal insulate wall, there is no heat flux passing through from one side to another side. This boundary condition is also suitable for the situation where the laminate has an infinite size of length and width.

The boundary conditions can be written as

$$T(x,y,0)=T(x,y,L)=T_s \tag{5.3}$$

For the thermal insulation walls, it has

$$\begin{aligned} -k\frac{\partial T}{\partial x}\Big|_{\substack{x=0\\x=W}}&=0\\ -k\frac{\partial T}{\partial y}\Big|_{\substack{y=0\\y=W}}&=0 \end{aligned} \tag{5.4}$$

In this case, because of the thermal insulation and heating mold, there is neither convection nor radiation on the side surfaces of the laminate. This heat transfer model then becomes a heat conduction problem with constant surface temperature and an internal heat source generated by the curing reaction.

In Chapter 3, all required material properties were determined by a set of dedicated experiments. In addition, proper material values have to been chosen for the modeling process. The results are shown in Table 5.1.

Table 5.1 Material properties and initial values for the heat transfer modeling

Name	Value	Unit	Description
W	200	mm	Length and the width of the laminate.
L	40	mm	Thickness of the laminate.
T_c	70	℃	Curing temperature.
T_{ini}	T_c	℃	Initial temperature for the laminate.
ρ_c	1.98	g/cm^3	Density of the composite
C_{p_c}	902	$J/(kg \cdot K)$	Heat capacity of the composite
k_c	$\{0.75, 0.69, 0.54\}$	$W/(m \cdot K)$	Thermal conductivity of the composite in the x, y and z directions, respectively.
ρ_r	1.16	g/cm^3	Density of the resin.
v_r	0.444	$[-]$	Resin volume fraction.

The cure kinetic parameters for this modeling are taken from Table 3.9. Here the experimentally determined densities of the cured resin and composite are chosen. For the heat capacity of the composite, the value determined by the rule of mixtures is used as described in Chapter 3. The thermal conductivity of the composite is determined by the TCi measurements in the x, y and z directions, respectively. Although the material properties are varying with the temperature and degree of cure, constant room temperature values are used in this model.

5.2.3 Coefficient form PDE for the heat transfer model

Here the Heat Transfer Module of COMSOL Multiphysics 4.4 with MATLAB is used to evaluate the temperature distribution and degree of cure. In this heat transfer module, the temperature T is the only default global variable. However, in order to calculate the internal heat source, the degree of cure should be also a global variable which is coupled with the temperature during the entire simulation. Therefore, a heat transfer model with two dependent variables (T, α) has to be built up.

According to Equation 1.2, the internal heat source term can be defined as:

$$Q = \rho_r v_r H_r d(\alpha, t) \tag{5.5}$$

where $d(\alpha, t)$ is the reaction rate $\frac{d\alpha}{dt}$. It is a differential operator that is a differentiation of the degree of cure α with respect to time t.

According to the cure kinetic model 3 in Table 2.1, the reaction rate can be written as:

$$d(\alpha, t) = [k_1(T) + k_2(T) \cdot \alpha^m] \cdot (1 - \alpha)^n \tag{5.6}$$

where k_1 and k_2 are the Arrhenius dependent rate constant as a function of the temperature. Thus, the internal heat source Q becomes a function of temperature and degree of cure.

Using the coefficient form PDE, the second dependent variable α can be added to the heat transfer model. To solve the degree of cure, a general form of the coefficient form PDE is used and expressed as:

$$e_a \frac{\partial^2 \alpha}{\partial t^2} + d_a \frac{d\alpha}{dt} + \nabla \cdot (-c\nabla\alpha - \mu\alpha + \gamma) + \beta \cdot \nabla\alpha + f_a\alpha = f \tag{5.7}$$

According to Equation 5.6, the second derivative of the degree of cure is not used here, thus we set $e_a = 0$ and $d_a = 1$ and $f = d(\alpha, t)$. Other parameters on the left side of the equation are all set as zero. In this operation, the reaction rate $d(\alpha, t)$ is calculated in both time and space and the degree of cure is also obtained simultaneously.

5.3 Results and discussions

In practice, it needs time to preheat the dry fibers to the required initial temperature as well as the resin infusion process. In this simulation, we assume that the fiber preheating and resin infusion are both prepared at time $t = 0$. Then the curing reaction starts and generates heat as an internal heat source. The total curing time is more than 4 hours, here we only study the specific time sections which may contain the most important information during these periods.

As shown in Figure 5.3, the temperature T_s is applied on the whole top and bottom surfaces with thermally insulated vertical walls. As a result, the temperature gradient only exists in the z-direction and the temperature on the xy-plane is uniform even if it is an anisotropic material. Thus, the study is focused on the temperature distribution, degree of cure and reaction heat through the thickness.

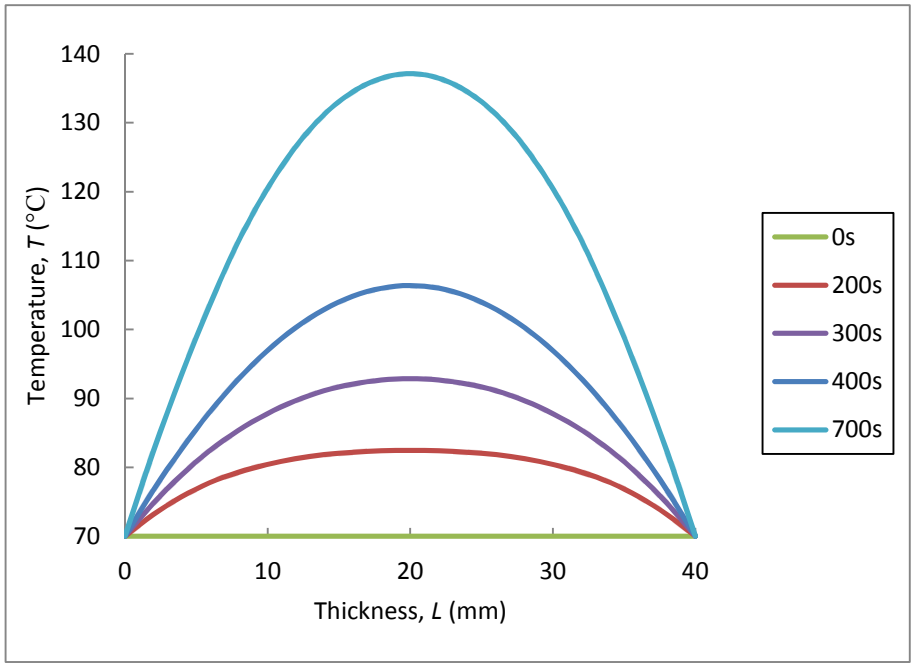

Figure 5.4 Temperature distribution during cure through the thickness of the composite at time 0, 200, 300, 400 and 700 s (Here it only shows the temperature increase stage, $T_c = 70$ ℃).

Figure 5.4 shows that because of the curing reaction heat, the temperature of the composite is rising quickly. The temperature reaches its maximum value at 700 s. After that it decreases to its initial temperature again until the material is fully cured. In the middle point of the thickness, it is the highest position of the temperature during cure. The temperature evaluation at this middle point is shown below.

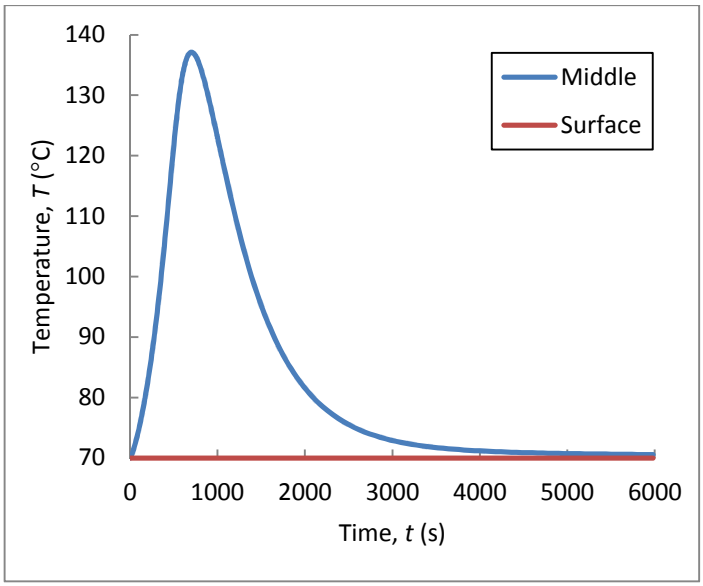

Figure 5.5 Temperature vs. time at the middle point and the surface through the thickness of the composite during cure ($T_c = 70$ ℃, $L = 40$ mm).

From Figure 5.5 we can see that the temperature increases from 70 ℃ to its peak temperature 137.1 ℃ at time $t = 700$ s. After that the temperature decreases until it returns back to the initial temperature. During this period, the heat generated by the curing reaction provides the power of the temperature changes in the composite.

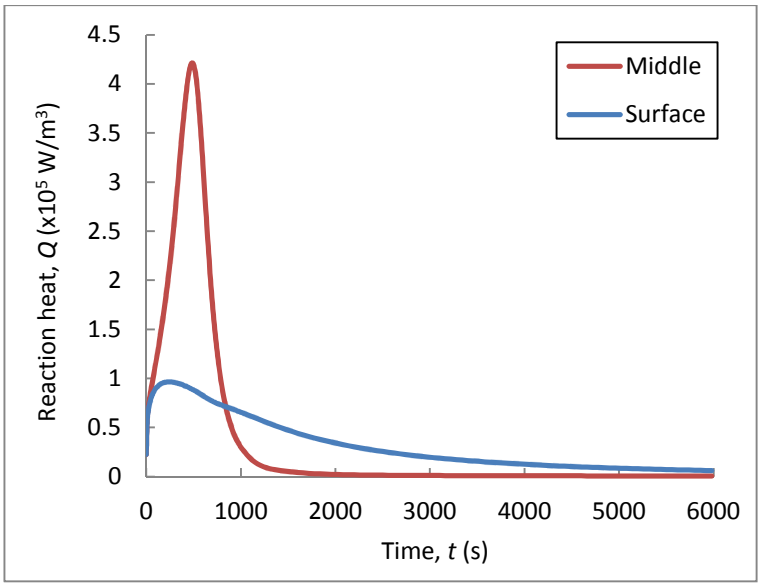

Figure 5.6 Reaction heat in the middle and surface of the composite during cure ($T_c = 70$ ℃, $L = 40\ mm$).

The reaction heat curves are different and vary from the middle to the surface in the composite during cure. Figure 5.6 shows that the middle and surface points reach their peak values at time $t = 490\ s$ and $t = 240\ s$, respectively. For the middle point, the peak values of the reaction heat is $4.21 \times 10^5 W/m^3$ and at the surface, it is $9.65 \times 10^4 W/m^3$. As known from Figure 5.5 at time $t = 700\ s$, it reaches the peak temperature in the middle and the reaction heat at this moment is $1.76 \times 10^5 W/m^3$. It means that before time $t = 700\ s$, the heat generated by the curing reaction is higher than the heat conducted from the middle point to its surroundings. In this situation, the middle point is heated up continuously until it reaches its peak temperature. However, after time $t = 700\ s$, the reaction heat is not enough to balance the heat conducted to its surroundings and then the temperature goes down. For the points at the surface, because of the constant temperature load, the reaction rate is limited at a lower level compared to the middle point. In this situation, its reaction heat is lower and stopped earlier compared to the middle point.

Because of the temperature gradient, it also creates a degree of cure gradient in the composite through the thickness. Here we only study the first 6000 s of the curing reaction though the total curing time is 4 hours. Figure 5.6 shows the degree of cure distribution in a composite during cure.

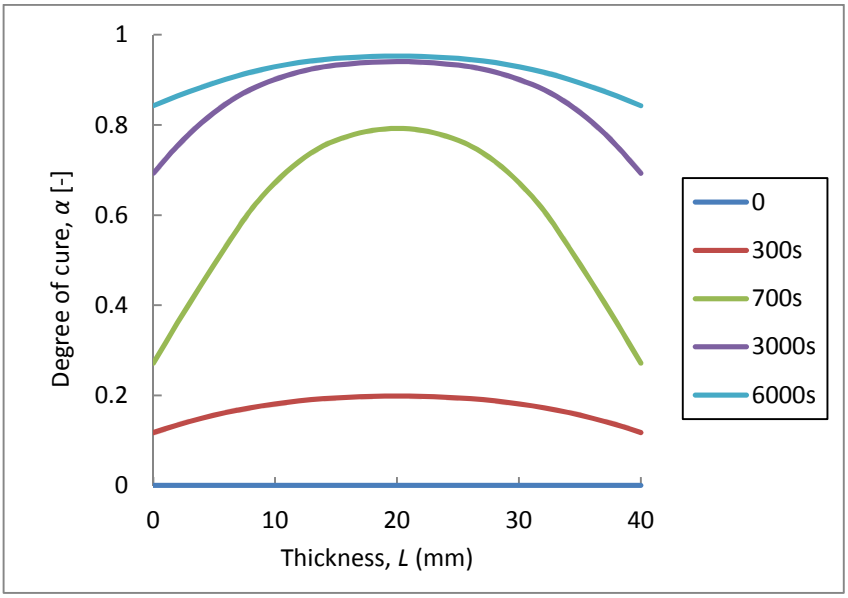

Figure 5.6 Degree of cure distribution through the thickness at time 0, 300, 700, 3000 and 6000 s during cure ($T_c = 70$ ℃, $L = 40$ mm).

From Figure 5.6 we can see that the degree of cure increases to approach the fully cured state. In the first 700 s, the degree of cure increases from 0 to 0.79 in the middle of the composite. Because the temperature at the edge is lower than the middle, the degree of cure there is only about 0.27. Thus, the degree of cure gradient between these two point is 0.52 which is extremely high. Furthermore, in the first 3000 s, the degree of cure increases to 0.94 and the remaining approximate 0.01 takes a similar time 3000 s. The degree of cure changes with time are shown in Figure 5.7.

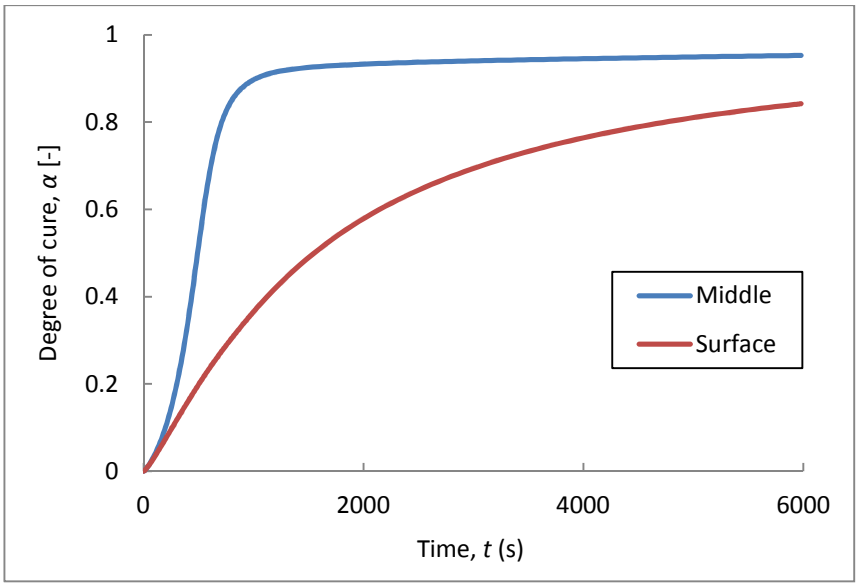

Figure 5.7 Degree of cure in the middle and surface through the thickness during cure ($T_c = 70$ ℃, $L = 40\ mm$).

Figure 5.7 shows that the degrees of cure distributions are different in the middle and surface of the composite during cure. In the first 1000 s, the resin is cured quickly and it reaches $\alpha = 0.9$ in the middle point. After that it takes a long time to approach the fully cured state. At time $t = 6000\ s$, the degree of cure in the middle reaches 0.95, but at the surface it is only 0.84. For the isothermal curing at 70 ℃ in Table 3.9, the final degree of cure of a pure resin is 0.79 in the DSC measurements. Compared these two groups of results we found that the reaction heat in a thick composite can increase its degree of cure.

5.4 Conclusions

In this chapter, a 3D heat transfer model is established to simulate the temperature and degree of cure distribution in the composite. As a thermo-chemical model, the governing equation is based on the heat transfer equation with an internal heat source. Here a laminate with dimensions of $200 \times 200 \times 40\ mm$ is simulated with the material properties determined in Chapter 3. The top and bottom surfaces are heated at a constant temperature 70 ℃ and the

other surfaces are thermally insulated. In this situation, the temperature gradient only exists in the z-direction. Thus, the study is focusing on the temperature distribution through the thickness in the middle of the central section. Once the curing reaction starts, the temperature in the composite increases quickly. It reaches its peak temperature 137.1 ℃ within 700s at the middle point. After that, because the reaction heat is less than the heat conducted from the middle to the surfaces, the temperature at the middle point starts to decrease. In this 40 mm thick composite, the degree of cure at the middle point reaches approximately 0.9 at 1000 s, but it is only 0.37 at the surface. Because of the temperature gradient through the thickness, the final degrees of cure at 6000 s at the middle and surface points are 0.95 and 0.84, respectively. It means that the gradient of the degree of cure distribution through the thickness can be significantly large at the end of the cure that may occur the residual stresses.

Reference

[1] S. M. Yang and W. Q. Tao, *Heat Transfer*, 4th ed.: Higher Education Press, 2012.

[2] E. Broyer and C. W. Macosko, "Heat Transfer and Curing in Polymer Reaction Modeling," *AIChE Journal,* vol. 22, pp. 268-276, 1976.

[3] E. Broyer and C. W. Macosko, "Curing and Heat Transfer in Polyurethane Reaction Modeling," *Polymer Engineering and Science,* vol. 18, pp. 382-387, April 1978.

[4] Z. S. Guo, S. Du, and B. Zhang, "Temperature field of thick thermoset composite laminates during cure process," *Composite Science and Technology,* vol. 65, pp. 517-523, 2005.

[5] T. A. Bogetti and J. John W. Gillespie, "Two-Dimensional Cure Simulation of Thick Thermosetting Composites," *Journal of Composite Materials,* vol. 25, March 1991.

[6] A. Cheung, Y. Yu, and K. Pochiraju, "Three-dimensional finite element simulation of curing of polymer composites," *Finite Element in Analysis and Design,* vol. 40, pp. 895-912, 2004.

[7] A. Shojaei, S. R. Ghaffarian, and S. M. H. Karimian, "Three-dimensional process cycle simulation of composite parts manufactured by resin transfer molding," *Composite Structures,* vol. 65, pp. 381-390, 2004.

[8] L. J. Lee and C. W. Macosko, "Heat Transfer in Polymer Reaction Modeling," *International Journal of Heat and Mass Transfer,* vol. 23, pp. 1479-1492, 1980.

[9] C. KIM, H. TENG, C. L. TUCKER, and S. R. WHITE, "The Continuous Curing Process for Thermoset Polymer Composites. Part 1: Modeling and Demonstration," *Journal of Composite Materials,* vol. 29, pp. 1222-1253, 1995.

[10] J. H. Oh, "Prediction of Temperature Distribution During Curing Thick Thermoset Composite Laminates," *Materials Science Forum,* vol. 544-545, pp. 427-430, 2007.

[11] F. P. Incropera and D. P. Dewitt, *Fundamentals of Heat and Mass Transfer*: JOHN WILEY & SONS, 2011.

6

Experimental Validation

6.1 Introduction

In the previous chapters, the analytical and numerical solutions have been introduced to predict the temperature distribution in the curing composites. In this chapter experiments are carried out to validate the results of those solutions. According to the thermo-chemical model, the key parameters for manufacturing a thick composite are the thickness and curing temperatures. Thus, these two parameters are considered as the variables used for the design of the experiments.

6.2 Set standard curing temperature and standard thickness

In order to have a comprehensive view of the temperature changes in a curing composite, different thickness composites are selected for the experiments which also be cured at selected different temperatures. Before determining the test range of the thickness and the curing temperature, the standard thickness and standard curing temperature have to be set.

Here the standard thickness is selected to be close to the critical thickness, so that it can generate significant heat to be measured during the experiments. According to Equation 4.17, the critical thickness L_c is 19.4 mm when the laminate is cured at 70 ℃. Besides, the thickness of one lay of the Glass Fabric 1200 is 0.8 mm when it is placed in the vacuum bag under the pressure. Finally, the laminates with 20, 30, 40 and 50 layers are used for the experiments and their final thicknesses are 16, 24, 32 and 40 mm, respectively. Here the 40 layers laminate is chosen as the standard thickness.

For the Airstone epoxy resin system, the recommended curing temperature is 70 ℃. At this temperature, the resin can be cured within 4 hours. From the experimental measurements, the temperature overshoot already becomes significant high when the composite is cured at 90 ℃ (see the results in Section 6.4). Thus, the temperatures of 70, 80 and 90 ℃ are selected as the curing temperatures for the experiments and 70 ℃ is set as the standard curing temperature.

In addition, other factors such as boundary conditions, the properties of heating mold and experimental procedure, will be discussed in this chapter.

6.3 Experimental set-up

The GF/Epoxy composites were manufactured for these experiments as mentioned in Chapter 3. Airstone® infusion Epoxy resin system and AGY® Tri-axial Glass Fabric 1200 were used as the resin matrix and the reinforced material, respectively.

6.3.1 Vacuum infusion process

The vacuum infusion process (VIP) is applied here for manufacturing the composites. VIP is a technique that uses vacuum pressure to introduce the resin into the laminate in a mold. The pressure is applied by the atmosphere against an evacuated system (vacuum pump). Normally vacuum pump is placed at the location where the resin is to fill last [1]. Compared with resin transfer molding (RTM), VIP is a single-sided open mold or termed vacuum-assisted resin transfer molding (VARTM). It only has an excellent surface finish on the mold side. However, it can improve the fiber-resin ratio to obtain a fiber volume fraction about 45-55% [2]. The vacuum infusion set-up is shown in Figure 6.1.

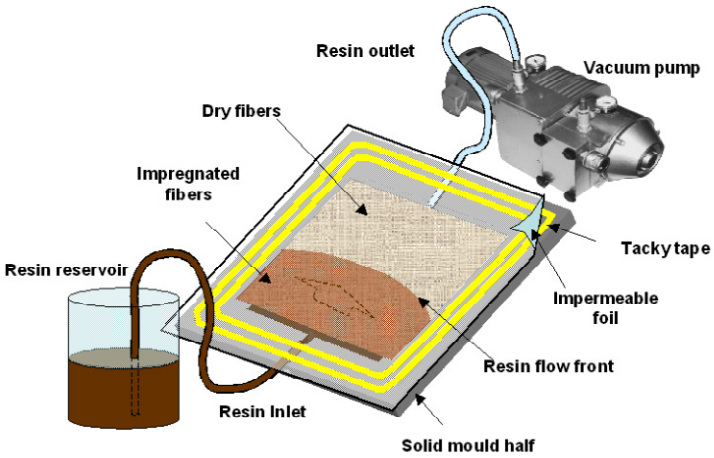

Figure 6.1 Vacuum infusion process set-up.

During the infusion and curing process, the vacuum pressure is set at 200 $mbar$ and it is keeping constant during the whole process. As shown in Figure 6.1, a solid half mold (here it is a flat aluminum plate) is used for placing the glass fiber laminate, vacuum bag, inlet and outlet tubes and tacky tape, etc. Note that, as described in Chapter 4, the heat source is applied from both sides of the laminate. Thus, in order to heat it up symmetrically, another half mold is placed on the top of it inside the vacuum bag as shown in Figure 6.2. In addition, three thermocouples are placed inside the laminate through the thickness as shown in Figure 6.4. The experimental VIP set-up is shown in Figure 6.2.

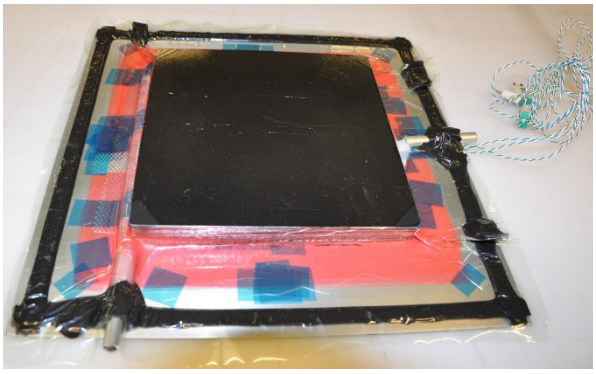

(a)

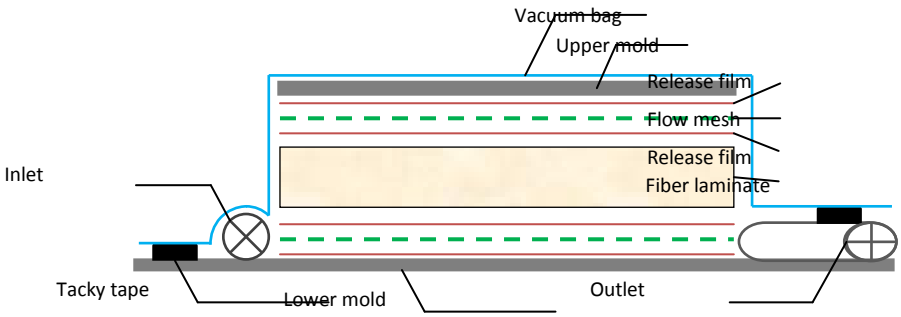

(b)

Figure 6.2 Experimental VIP set-up. (a) The laminate with VIP set-up; (b) Schematic cross-section view of VIP set-up.

The heating system is a temperature-controlled water heating mold. The mold is made by an aluminum plate and the thermal conductivity is about 237 $W/(m \cdot K)$. The inlet and outlet tubes are on the bottom and top of the mold, respectively. When the heating water passing through the tunnels that distributed evenly inside the mold, the temperature difference on the mold surface is very small (less than 1 ℃ in these experiments). The structure of this heating system and the vacuum infusion set-up are shown in Figure 6.3.

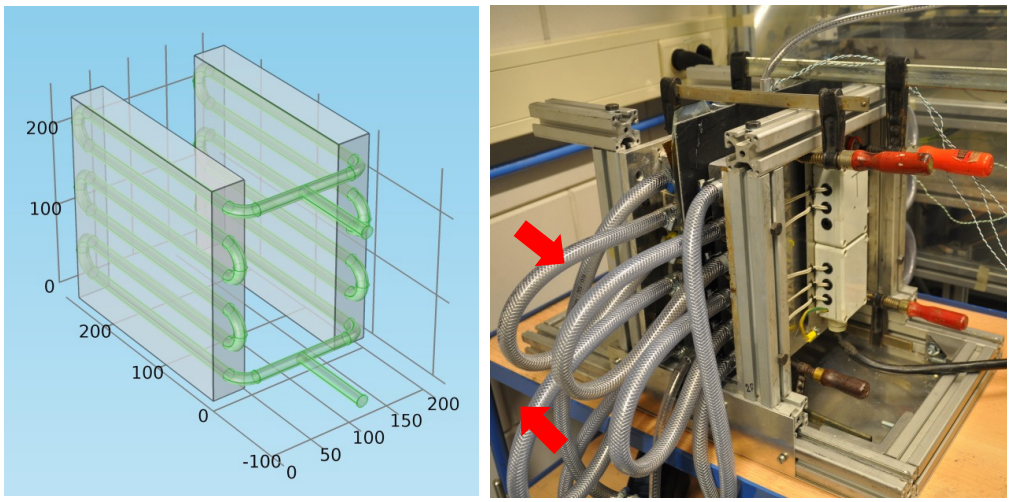

(a) (b)

Figure 6.3 Structure of the heating system. (a) 3D model of the heating system; (b) Experimental heating system with VIP set-up.

As shown in Figure 6.3 that the VIP set-up is fixed between the mold. The whole set-up is placed vertically which will let the resin flow from the bottom of the laminate to the top. This set-up helps the resin impregnating the dry fibers in one direction to avoid creating the voids. Moreover, this heating mold is opened at the edge of the part. However, these experiments only investigate the temperatures in the center of the laminate through the thickness, a proper size (big length-to-thickness ratio) of the laminate can significantly weaken the heat dispersion by the edge. A glass fiber mat is also used as the thermal isolation material to prevent the heat loss. The dimension of the laminate is 200 mm × 200 mm, the solid half mold used in the VIP set-up is 300 mm × 300 mm (2 mm thick), the heating mold is 250 mm × 250 mm. The heating mold is fixed on a mold framework and the VIP set-up is clipped between the heating molds.

6.3.2 Thermocouples

For the temperature measurement, the K-type thermocouples are used to measure the temperature values. Keithley® (Tektronix Company), a multi-channel measurement system, is used for the data collection and process. Here three thermocouples are placed at the bottom, middle and top positions of the laminate, respectively. The scheme of the thermocouples placement in the glass fiber laminate is shown in Figure 6.4.

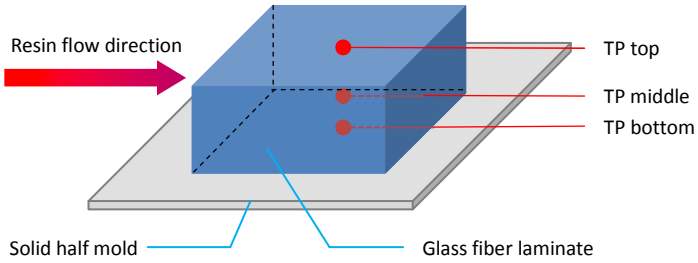

Figure 6.4 Scheme of the thermocouples (TP) placement in the glassfiber laminate.

Note that the thermocouples on the top and bottom are placed between glass fibers and release films referred to Figure 6.2. They are placed in the same direction with the resin flow to avoid creating voids during the infusion.

6.4 Experimental procedure

6.4.1 Resin mixture and degas

Airstone® infusion Epoxy resin system consists of two components: epoxy resin and hardener. They need to be mixed evenly by the ratio 100 : 31 by weight at room temperature. After that the mixture will be degassed in a vacuum vessel to remove the air bubbles which is created during the mixture. Normally the resin mixture and degas will totally take more than 10 minutes depending on the amount of resin. Here we assume that at room temperature this procedure does not influence the exothermic behavior in the following curing reaction.

6.4.2 Preheating process

Before the infusion, the glass fiber laminate and resin need to be preheated. Because the curing temperature is at less 70 ℃, if the glass fiber laminate is heated up from the room temperature, it will take a long time due to its low thermal conductivity. The curing reaction may be finished before the whole laminate reaches the curing temperature. Thus, in these experiments, all of the glass fiber laminates are firstly heated up to the curing temperature. For the epoxy resin, it is heated up to 40 ℃ to decrease the viscosity which makes it flow smoothly. At the beginning of the infusion, the resin can be heated up quickly when it passes through the hot glass fibers and before the resin front reaches the places where the thermocouples are placed, the resin has already been heated up to the same temperature as the glass fibers. Thus, it is considered that the glass fiber laminate and resin have the same temperature after infusion.

6.4.3 Resin infusion process

The vacuum pressure in the vacuum bag is 200 $mbar$ during the whole process. Once the thermocouples are connected to the Keithley, then turn on the inlet and let the resin flow into the glass fiber laminate. Because the whole set-up is placed vertically, so the resin front rises up continually until it reaches the outlet on the top. The resin infusion time can be different for different thick laminates which is also influenced by the curing temperature. In this study totally six GF/Epoxy composite are manufactured for the experiments. The detailed information about the infusion time at different thickness and different curing temperatures is shown in Figure 6.5.

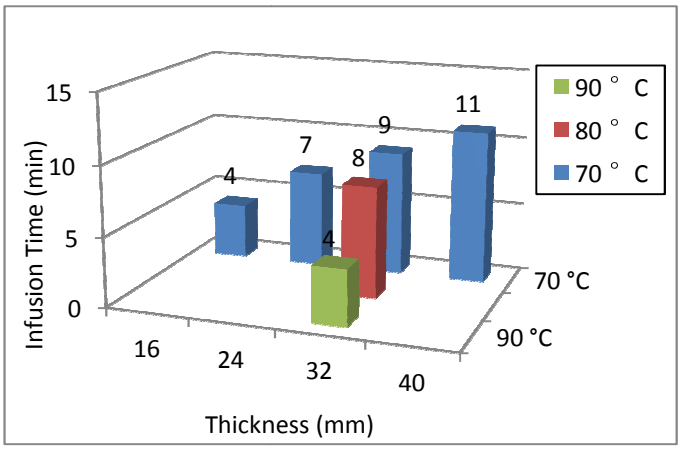

Figure 6.5 Experimental results of the resin infusion time at curing temperature 70, 80 and 90 ℃ using different thick laminates (16, 24, 32 and 40 mm).

As shown in Figure 6.5 that when increasing the thickness, it takes more time for the infusion process. However, at a higher curing temperature, the viscosity of the resin is decreased and it takes less time for the infusion. Many other factors such as the diameter of the inlet tube, the fiber orientations, whether or not including the flow mesh, may influence the infusion time. For the typical reaction injection molding, the infusion time generally lasts for several seconds to minutes which is significant short compared to the curing time [3]. However, for a 40 mm thick

composite, the infusion time as 11 $minutes$ is significant long and the heat generated during this time cannot be ignored anymore.

6.4.4 Experimental measurements

The measurement is started when the resin is infused into the laminate and ended when the resin is fully cured. Figure 6.6 shows the temperature distributions in a 32 mm thick laminate cured at 70 ℃. The temperature profiles are recorded during cure at the bottom, middle and top positions of the laminate.

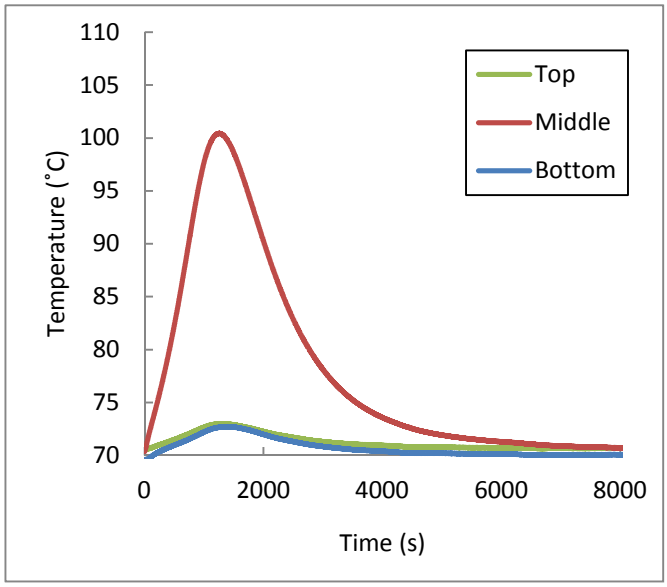

Figure 6.6 Temperature distributions in a 32 mm thick GF/Epoxy composite cured at 70 ℃.

As shown in Figure 6.6 that the temperature in the middle of the composite rises rapidly and creates a temperature peak at 100.4 ℃ which has a 30.4 ℃ temperature overshoot compared to the curing temperature. The main exothermic reaction lasts about one hour before it cools down. It also shows that at the bottom and top surfaces, the temperatures increase slightly under the peak region. This is because during the curing process, the temperature in the core becomes higher than the surfaces, then the heat is transferred from the core to

the surfaces during this period and this feedback heat is too much to be removed by the heating mold immediately.

6.5 Results and discussions

6.5.1 Experimental results

In this experiment, two groups of measurements were carried out as mentioned in Figure 6.5. The first group is based on the standard curing temperature which is using 16, 24, 32 and 40 mm thick laminates cured at 70 ℃, respectively. The second group is based on the standard thickness which is cured at 70, 80 and 90 ℃ using the 32 mm thick laminates, respectively. The results are shown in Figure 6.7.

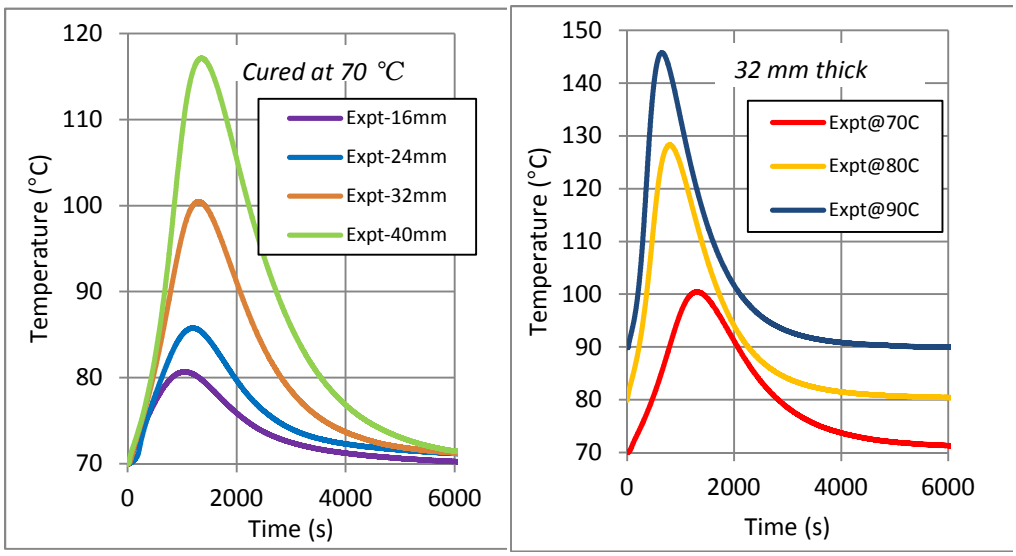

(a) (b)

Figure 6.7 Experimental results of the temperature profiles in the middle of the GF/Epoxy composites during cure. (a) 16, 24, 32 and 40 mm thick laminates cured at 70 ℃, respectively; (b) 32 mm thick laminates cured at 70, 80 and 90 ℃, respectively.

Figure 6.7(a) shows that at the curing temperature 70 ℃, the peak temperatures are 80.7, 85.8, 100.4 and 117.1 ℃ measured in the 16, 24, 32 and 40 mm thick

laminates, respectively. It shows that the peak temperatures are getting higher when increasing the thickness. In Figure 6.7(b), using the 32 mm thick laminates, the peak temperatures are 100.4, 128.3 and 145.8 ℃ cured at 70, 80 and 90 ℃, respectively. It is clear that the peak temperature also increases with the curing temperature.

Here the peak temperature is defined as the maximum temperatures T_{max}, and the maximum temperature differences ΔT_{max} is defined as the temperature different between the maximum temperature T_{max} and its related curing temperature T_c. The results of the maximum temperature differences ΔT_{max} are shown in Figure 6.8.

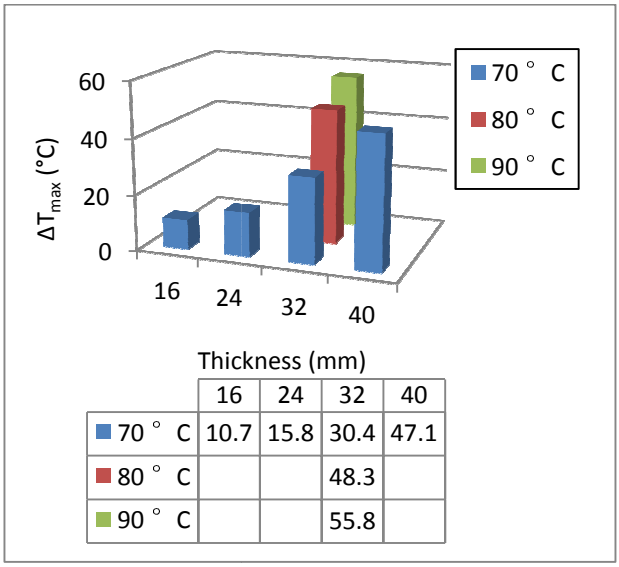

	16	24	32	40
70 ° C	10.7	15.8	30.4	47.1
80 ° C			48.3	
90 ° C			55.8	

Figure 6.8 Experimental results of ΔT_{max} at curing temperatures 70, 80 and 90 ℃ and thicknesses 16, 24, 32 and 40 mm.

Figure 6.8 shows that the maximum temperature difference ΔT_{max} also increases with the thickness and curing temperature. At the standard curing temperature 70 ℃, the maximum temperature difference ΔT_{max} in a 40 mm thick composite is 47.1 ℃ which is 67% higher than its curing temperature. Meanwhile at the standard thickness 32 mm, when the composite is cured at 90 ℃, ΔT_{max} becomes 55.8 ℃ which is 62% higher than its curing temperature. More details about ΔT_{max} are shown in Figure 6.9.

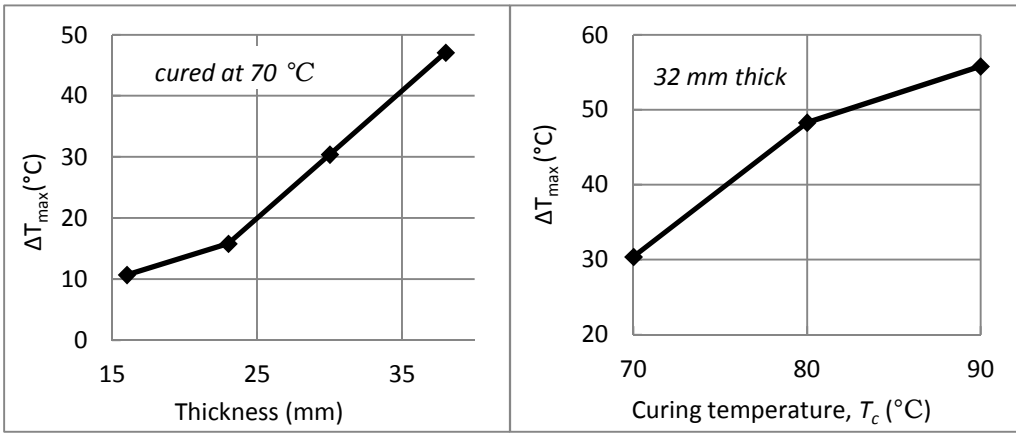

(a) (b)

Figure 6.9 Experimental results of the maximum temperature different ΔT_{max}. (a) ΔT_{max} in the 16, 24, 32 and 40 mm thick GF/Epoxy composites cured at 70 ℃; (b) ΔT_{max} in a 32 mm thick GF/Epoxy composite cured at70, 80 and 90 ℃, respectively.

6.5.2 Comparison with the numerical simulation

6.5.2.1 Numerical solutions

As mentioned in the Chapter 5, numerical studies were used to simulate the temperature distributions. Here COMSOL Multiphysics® Modeling Software 4.4 is used to model and simulate this heat transfer and cure kinetic system. In order to obtain the proper results, a set of predefinitions are required. For the entire experimental process, it mainly consists of three steps:

- Preheat dry fibers and resin.
- Resin infusion.
- Curing reaction.

This preheating step is to heat up the materials to a certain temperature, as the curing temperature for the glassfiber laminate and 40 ℃ for the epoxy resin. Normally the glassfiber will be heated first, because it needs a long time to heat

up this thick and low thermal conductivity laminate. Once they reach the setting temperatures, and then infuse the resin. In this thesis, the main purpose is to simulate the curing reaction but not the stage of preheating the dry fibers and resin. Thus the preheating process was not included in this numerical analysis.

For the resin infusion step, the resin is infused into the glassfiber laminate, flowing from the inlet to the outlet. The infusion process is finished when the resin reached the outlet. During this period, it is not only a physical phenomenon of the liquid flow but also includes cure kinetic activities which generates a certain amount of heat. Here the mass transfer is not included in our study. Instead, a term called infusion time factor is used to calculate the heat generated during the infusion process.

6.5.2.2 Infusion time factor

For a thick laminate, the process of the resin infusion takes a period time until it is fully infused. For the different thick laminates, the infusion times are different as shown in Figure 6.5. Once considering about the infusion time, the infusion process can be described as shown in Figure 6.10.

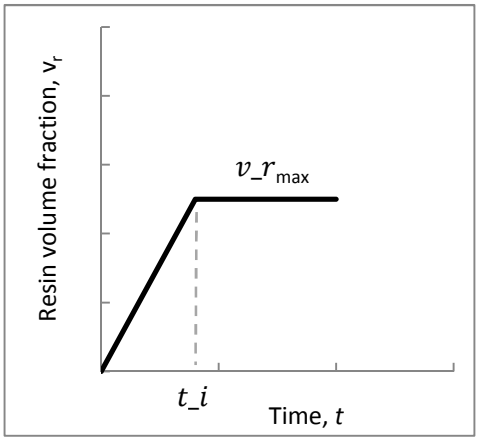

Figure 6.10 Resin volume fraction changes with the infusion time factor.

The resin infusion starts from opening the inlet and ends when the laminate is fully infused, in the time scale from zero to t_{in} as shown in Figure 6.10. The

parameter t_{in} is defined as the infusion time. Within the infusion time, the volume of the resin in the laminate is increasing from zero to $v_{r_{max}}$. After time t_{in}, it keeps constant. Thus, it can be written by a linear piecewise function as Equation 6.1:

$$v_r = \begin{cases} \frac{v_{r_{max}}}{t_{in}} \cdot t, & 0 \le t \le t_{in}; \\ v_{r_{max}}, & t \ge t_{in}. \end{cases} \tag{6.1}$$

When using the infusion time factor for the calculation, note that the resin volume changes in a different mode in the COMSOL modeling compared to the situation in a realistic experiment. In the Comsol model, v_r changes evenly throughout the whole laminate. However, in the experiment, the resin front is moving from the bottom to the top (see also Figure 6.3). This difference may cause the deviation during the numerical simulation.

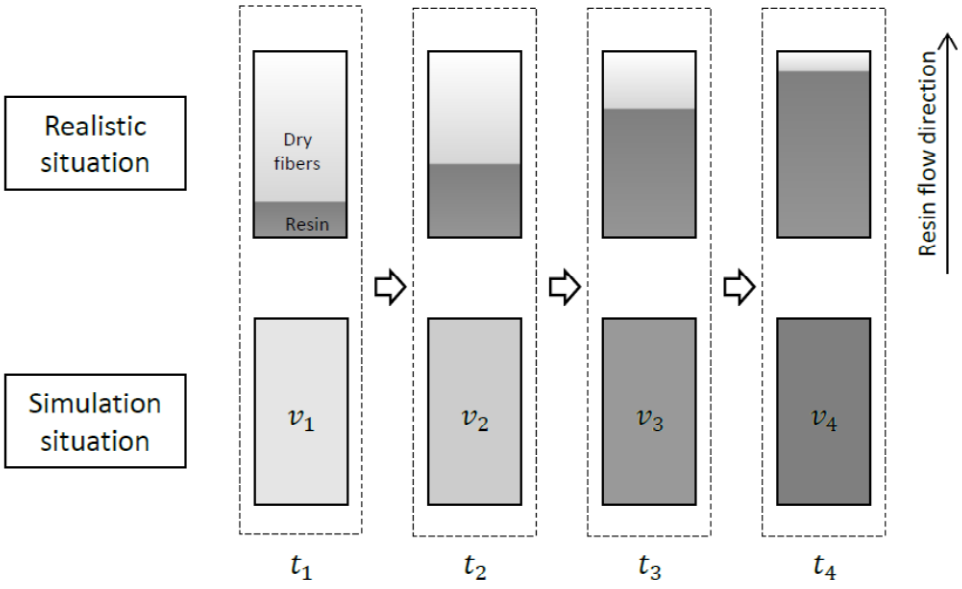

Figure 6.11 Schematic diagram of the resin infusion process for the realistic and simulation situations (cross-section view). Here it presents four stages at time t_1, t_2, t_3 and t_4 ($v_1 < v_2 < v_3 < v_4$, $0 \ll t_1 < t_2 < t_3 < t_4 \ll t_{in}$).

6.5.2.3 Comparison between numerical and experimental results

For the numerical study, it also follows the standard thickness and standard curing temperature. The experimental and numerical results are shown below.

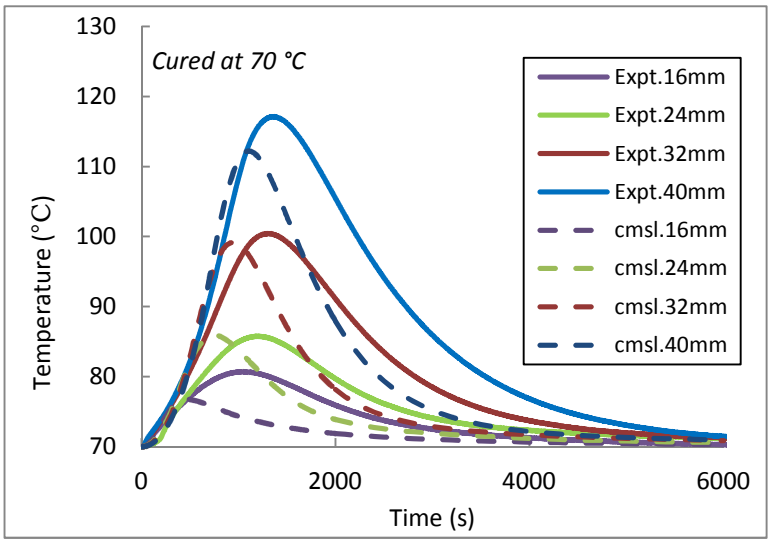

Figure 6.12 Temperature curves during cure simulated by COMSOL models and experimental results cured at 70 ℃ using 16, 24, 32 and 40 mm thick GF/Epoxy composites.

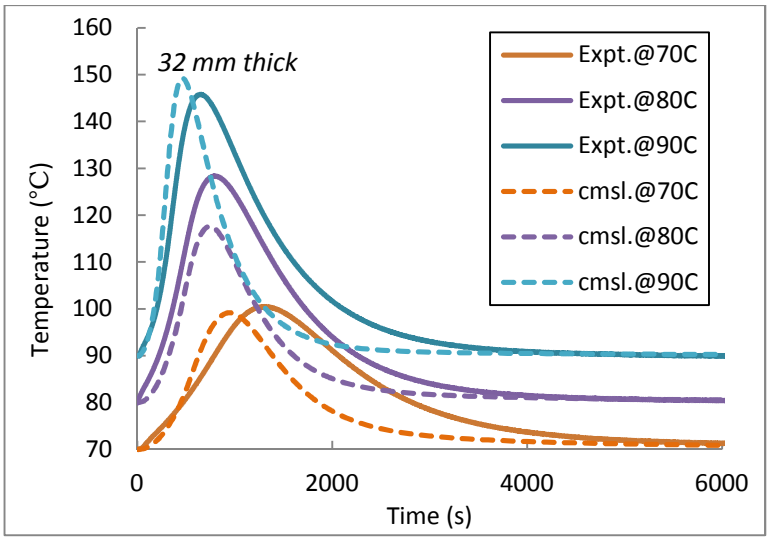

Figure 6.13 Temperature curves during cure simulated by COMSOL models and experimental results using 32 mm thick GF/Epoxy composites cured at 70, 80 and 90 ℃, respectively.

From the Figure 6.12 and 6.13, it shows that the temperature peak positions are slightly shifted to the left in numerical solutions compared to the experimental results. It means in the numerical simulation, the heat is generated more concentrated in the beginning than in the experiment. It also shows that the peak temperature always happen after the infusion (see Figure 6.14).

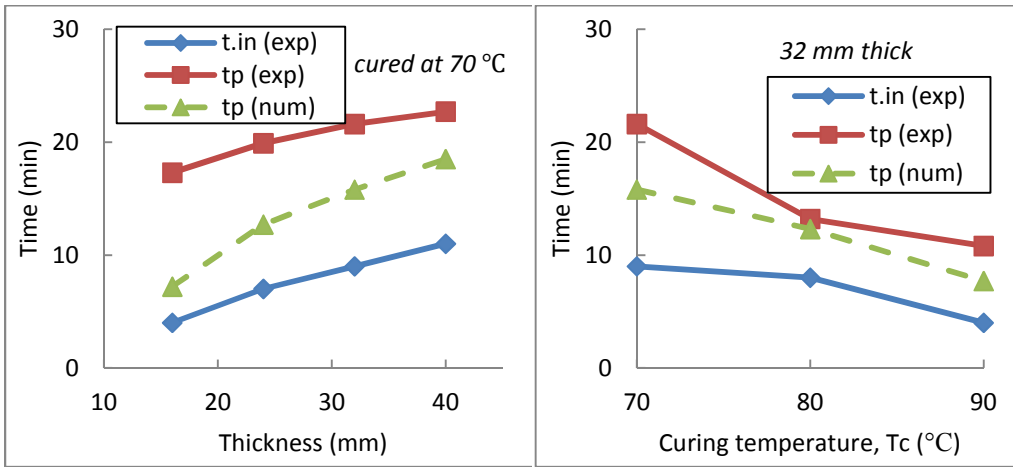

(a) (b)

Figure 6.14 Results of the infusion time $t_{in}(exp)$ and the time reaching ΔT_{max} in the experiments $t_p(exp)$ and numerical solutions $t_p(num)$. (a) Time for the 16, 24, 32 and 40 mm thick GF/Epoxy composites cured at 70 ℃; (b) Time for a 32 mm thick GF/Epoxy composite cured at70, 80 and 90 ℃, respectively.

The maximum temperature values compared between the numerical and experimental results are shown in Figure 6.15 and 6.16.

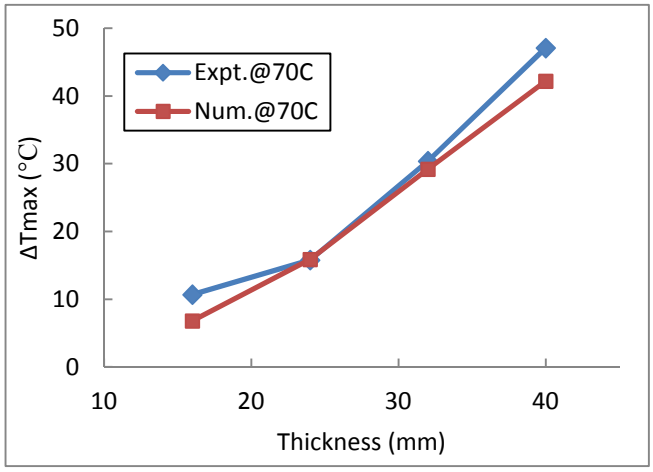

Figure 6.15 Maximum temperature difference compared between numerical and experimental results in the GF/Epoxy composites with the thickness of 16, 24, 32 and 40 mm at the curing temperature70 ℃.

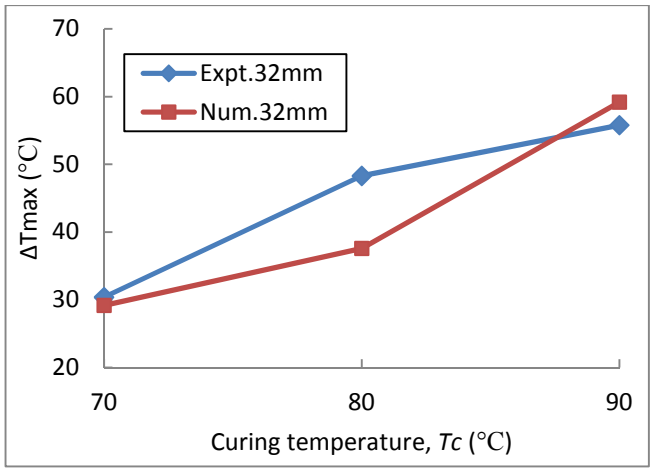

Figure 6.16 Maximum temperature difference compared between numerical and experimental results in the 32 mm thick GF/Epoxy composites at the curing temperature70, 80 and 90 ℃, respectively.

As shown in Figure 6.15 and 6.16 that the biggest deviation of the maximum difference happens at the curing temperature 80 ℃ in a 32 mm thick laminate that has 10.7 ℃ difference. The average of the absolute deviations of ΔT_{max} between the experimental and numerical results are about 1.9 ℃ and 5.2 ℃ in Figure 6.15 and 6.16, respectively.

6.6 Conclusions

In this chapter, experiments are carried out to verify the numerical solutions. By introducing the standard curing temperature and standard thickness, two groups of the experiments were chosen: at the standard curing temperature 70 ℃, 16, 24, 32 and 40 mm thick laminates are selected for the experiments; for a standard 32 mm thick laminate, 70, 80 and 90 ℃ are selected as the curing temperature. Vacuum infusion process was used for manufacturing the composites. The results show that the infusion time increases with the laminate thickness but decreases with the curing temperature which may last from 4 to 11 minutes in our cases.

In addition, comparisons were made between the numerical and experimental results. In the numerical modeling, the infusion time factor was added into the

thermo-chemical model in order to simulate the heat generation during the infusion process. The results show that the numerical solution of ΔT_{max} agrees well with the experimental results and the average of the absolute deviation is less than 5.2 ℃. The experimental results show that the temperature overshoot increases both with the curing temperature and laminate thickness. The temperature overshoot in the core can be 30.4 ℃ in a 32 mm thickness cured at 70 ℃, however if cured at 90 ℃, then it will increases to 55.8 ℃. As mentioned in previous references, in another experiment a 31 ℃ temperature overshoot was found in a 50.4 mm thick pipes cured at 80 ℃ and a temperature overshoot up to 60 ℃ can be created in a 25.4 mm thick glassfiber epoxy-based composite and [4, 5]. These values agree well with our experimental results.

References

[1] A. B. Strong, *Fundamentals of Composites Manufacturing - Materials, Methods, and Applications*: Society of Manufacturing Engineers, 2008.

[2] W. P. Benjamin and S. W. Beckwith, "Resin transfer molding," presented at the SAMPE, 1999.

[3] E. Broyer and C. W. Macosko, "Heat Transfer and Curing in Polymer Reaction Modeling," *AIChE Journal,* vol. 22, pp. 268-276, 1976.

[4] D. J. MICHAUD, A. N. BERIS, and P. S. DHURJATI, "Thick-Sectioned RTM Composite Manufacturing: Part 1: In Situ Cure Model Parameter Identification and Sensing," *Journal of Composite Materials,* vol. 36, pp. 1175-1200, 2002.

[5] K. S. Olofsson, "Temperature Predictions in Thick Composite Laminates at Low Cure Temperatures," *Applied Composite Materials,* vol. 4, 1997.

7

Conclusions and Recommendations

The purpose of this thesis was to study the thermal behavior in thick thermoset composites during manufacturing. Based on the heat transfer theory, a thermo-chemical model was proposed for the simulations of the curing reaction. Both analytical and numerical solutions were obtained and validated by experiments.

7.1 Conclusions

Firstly, based on the energy balance principle, a governing equation was established for the heat transfer coupled with cure kinetics in a thick composite. The heat generated by the curing reaction was defined as an internal heat source. During the manufacturing of glassfiber reinforced epoxy composites, the heat generated during the curing process cannot be conducted to outside immediately because of the low thermal conductivity, which leads to a serious temperature overshoot in the core. The topic of work is therefore to study this temperature overshoot and find analytical and numerical solutions.

In this research, we used an Airstone® infusion resin system as the matrix of the composite, and an AGY® triaxle E-glass fabric as the reinforcement. In order to solve the thermo-chemical model, the material properties such as the density, thermal conductivity and heat capacity of the epoxy resin and composite, as well as the cure kinetic parameters were determined by a series of dedicated experiments and calculations.

For the uncured epoxy resin, the density was determined as 1.10 g/cm^3 and for the uncured composite, it turned out to be 1.92 g/cm^3. The experimental densities of the cured epoxy resin and composite were found to be 1.16 g/cm^3

and 1.98 g/cm^3, respectively. Furthermore, the volumetric cure shrinkage of the epoxy resin and composite were calculated as 5.2% and 3%, respectively.

Both of an analytical model and the experimental measurements were carried out to determine the thermal conductivity. As an anisotropic material property, the thermal conductivity of the composite at parallel and perpendicular (to the fiber orientation) directions are different. The predicted results showed that $k_{\parallel} = 0.84\ W/(m \cdot K)$ and $k_{\perp}$ was in a range from 0.39 to 0.64 $W/(m \cdot K)$. The experimental results showed that the values of the thermal conductivity were 0.75, 0.69 and 0.54 $W/(m \cdot K)$ at x, y and z directions, respectively. For the epoxy resin, the measured thermal conductivity was 0.27 $W/(m \cdot K)$.

Similarly, we found that the heat capacity of the cured epoxy resin was $1164\ J/(kg \cdot K)$, where the value for the composite was $803\ J/(kg \cdot K)$ experimentally and 902 $J/(kg \cdot K)$ from the rule of mixtures.

Moreover, the resin volume fraction and weight fraction were determined as 0.444 and 0.260 for the composite, respectively.

An n^{th} order autocatalytic cure kinetic model was applied for the epoxy resin. Isothermal DSC measurements were carried out to determine the heat flow at 60, 70, 80, 90, 100 and 110 ℃. The results showed that the final degree of cure was 0.77 when it was cured at 60 ℃ and it increased to 0.96 when cured at 110 ℃. Dynamic DSC measurements were used to determine the total heat of reaction during cure which is 440 J/g. By using a global fitting method, the cure kinetic parameter were found to be: $A_1 = 0.001\ s^{-1}$, $E_{a_1} = 13000\ J/mol$, $A_2 = 32000\ s^{-1}$, $E_{a_2} = 50000\ J/mol$, $m = 0.19$ and $n = 1.8$.

In order to find a simple relation between the maximum temperature and the processing and material parameters, an approximate analytical solution of the coupled heat transfer and cure kinetic equation was derived. We therefore first rewrote the equation in a dimensionless expression and assumed that it reached the maximum temperature in the core when the reaction rate was at its peak value. Finally, this resulted in a direct relation between the dimensionless

maximum temperature difference ΔT_{max} and the dimensionless number N_c. The expression of N_c showed that it was related to the composite thickness, curing temperature and cure kinetic parameters. When N_c increased, ΔT_{max} also increased.

A critical thickness for thick thermoset composites was defined as the thickness above which it will create an incontrollable temperature overshoot in the core.

Finally, the analytical solutions of the maximum temperature in the core were verified by a numerical model at different curing temperatures and different thicknesses. The analytical predictions were always about 4 °C higher than the numerical solutions, which was attributed to the approximations made in the analytical model.

Here are the conclusions of the analytical solutions:

- The dimensionless number is (Equation 4.12):

$$N_c = \frac{L^2 c}{e^c k_{zz} T_c} \rho_r v_r H_r A f(\alpha)_{max}$$

- The critical thickness is (Equation 4.17):

$$L_c = \sqrt{\frac{e^c N_{cc} k_{zz} T_c}{c \rho_r v_r H_r A f(\alpha)_{max}}}$$

- The relation between the dimensionless number and dimensionless maximum temperature in the core is (Figure 4.4):

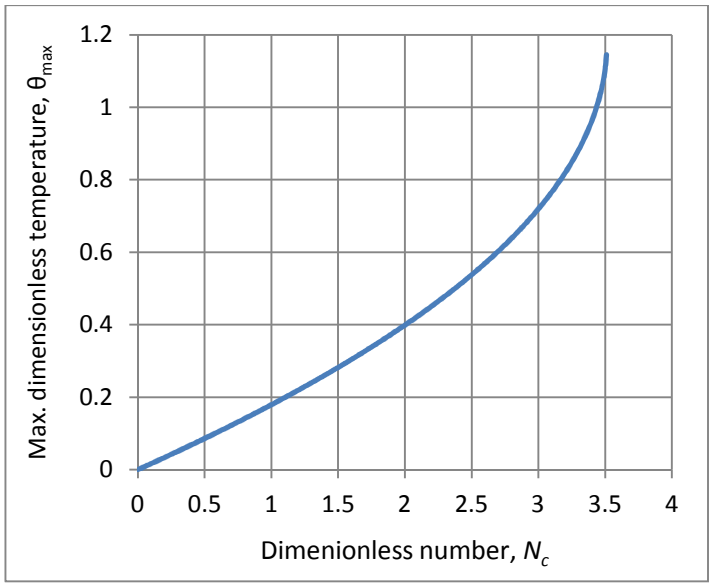

Figure of the analytical solution of maximum dimensionless temperature θ_{max} vs. dimensionless number N_c.

A 3D transient heat transfer model was established for the simulation of the temperature and degree of cure distributions in the thick composites. Though it was a 3D model, the study still focused on the thickness direction. In order to couple the cure kinetics with the heat transfer model, a coefficient form partial differential equation (PDE) was used to add the parameter of the degree of cure as a global variable, similar to the temperature variable. The results showed that the temperature in the composite was increasing until it reached the maximum temperature, and the core always had the maximum temperature values. The temperature curves showed that the core of the composite can be heated up quickly by the curing heat. It also showed that it always reached the maximum temperature just a little bit after the maximum reaction heat appeared.

Due to the temperature gradient, it also created a degree of cure gradient through the thickness resulting in a difference from the core to the surface of about 11%. The results also showed that the degree of cure in the core increased much faster than at the surface. This large gradient through the thickness may result in residual stresses in the cured composites.

The numerical and analytical models for the maximum core temperatures were then compared with a series of dedicated measurements. By using the vacuum infusion set-up, the GF/Epoxy composites were manufactured at curing temperature 70, 80 and 90 ℃, and with thicknesses of 16, 24, 32 and 40 mm, respectively. The experimental results showed that ΔT_{max} in the composites cured at 70 ℃ with the thicknesses of 16, 24, 32 and 40 mm were 10.7, 15.8, 30.4 and 47.1 ℃, respectively. Also, ΔT_{max} in the composites cured at 70, 80 and 90 ℃ with a thickness of 32 mm were 30.4, 48.3 and 55.8 ℃, respectively. The results indicated that the maximum temperatures in the core increased both with the thicknesses and curing temperatures. Furthermore, it was found that the infusion time was related to the thickness of the laminate and the temperature of the resin. In order to improve the accuracy of the numerical solutions, a modified numerical model was built up by adding an infusion time factor for the simulations of the resin volume change during the infusion. Thus, the approximated convection heat during the infusion was taken into account. The results showed that the temperature curves simulated by the modified model fit well with the experimental results and their average deviation was less than 5.2 ℃.

7.2 Recommendations for the future work

In this thesis, the infusion process was not modeled directly, but approximated by an infusion time factor. In that way, the heat generated during infusion deviated from the real situation. Though this convection heat effect is small, it can be useful to include this effect in a more rigorous way and improve the model to obtain more accuracy results.

In this work, constant material properties such as the density, the thermal conductivity and the heat capacity were used for the heat transfer modeling. However, these thermal material properties in reality are all temperature and degree of cure dependent. Thus, in order to improve the accuracy of the simulation, the temperature and degree of cure dependent material properties could be taken into account.

Using the numerical solutions of the degree of cure, it is possible to optimize the cure cycle by setting the peak temperature during cure at a value below the critical temperature and then changing the curing process in an optimized loop. For example, it can be done by changing the curing temperature stepwise from a low pre-cure temperature to a higher value, or by programming a temperature ramp for the cure cycle to achieve a more uniform temperature and degree of cure distributions in the composites.

Acknowledgements

This research was carried out in the Structural Integrity & Composites (SI&C) group, Faculty of Aerospace Engineering (AE) of TU Delft. The accomplishment of this thesis would be impossible without the assistance and support of many people. Here I would like to thank all of those who contributed to this thesis.

First and foremost, I want to thank my promotor Prof. Rinze Benedictus who gave me the opportunity to carry on my research in this group and approved the funding to finish my work. I also very appreciated his precious judgments and guidance during my PhD research. I would like to show my sincere gratitude to my copromotor Prof. Kaspar M.B. Jansen who showed a deep insight into my research, providing me with valuable guidance in every stage of the writing of this thesis. I was so pleasure that we had so many times face-to-face talk, discussing every details in my models and experiments. His patience and deep academic background always can help to take over the dark side of my work. Thank you so much, Kaspar.

At the meanwhile, I want to give my thanks to Dr. Harald Bersee for offering me a PhD position in the DPCS group and supported me at the beginning of my research. Furthermore, this research could not have been accomplished without the scholarship of China Scholarship Council (CSC). I gratefully thanks to their support.

My appreciation also goes to the support from Suzlon Ltd., and its staff. My experiments could not be carried on without their materials. I would like to express my gratitude to Nico van der Mark who always can bring me the materials from Suzlon and shared his experiences with me. Special thanks to Dr. Hans Luinge and Dr. Kapileswar Nayak who contributed a lot of technical support of building up the DSC tests, and for the meetings in Suzlon and TUD, giving me valuable suggestions during my research. Although I cannot count all the members that helped me in Suzlon, I would like to thanks for their help.

Thanks sincerely for all committee members who contributed their time to review this thesis and participated in the defense. Special thanks to Dr. Hans Luinge for his suggestions to improve the thesis.

The five years study at TUD gave me so many precious memories and fun. First I want to thank the group secretary Gemma for all the paper work and organizing all the wonderful group events. I shall extend my thanks to some of my colleagues whom I learned a lot from. Thanks to Julie Teuwen who can share her experience with me on the knowledge of composites and polymers, giving me a lot of advices that helped me to start my research. I would like to thank Jordy Balvers who taught me how to setup the vacuum infusion process which I used for the experiments during my whole PhD life, sharing many tips I will never learn from the books. Shafqat, Didier, Natch and Nat, thank you for all the support and fun, accepting me as your new friend. Jarret grout, your posters and the movie night were really impressive. Thanks to you I started to love the wall climbing and camping. My thanks also goes to Ilias, we had a lot of happiness in the dairy life and getting to know about your favorite football team. Huajie, I was so pleasure that we can work together since our Bachelor study. I really appreciate your continued kindness and help during these years and congratulation to you and Lu that you got a so lovely son, Lucas. I am also very grateful to Paola, for the help during my research and the invitation to your house for the real Italian food, especially the wonderful wedding ceremony in Italy. Many thanks to my new officemates: Morteza, Maria, Maro, Tian, Fabricio, so enjoyable atmosphere in the office. I also want to give the thanks to the colleagues: Adrian F., Adrian L., Bernhard, Gnevieve, Dimitrios, Sofia, Derek, Mayank, Zahid, Nikos, Yao, Ping, Leila, Andriei, Marcelo, Pedro, John-Alan, Konstantin, Niels, Freek, Wandong, zhinan, Chunsen, thank you for all your support and fun. I am deeply thankful to Niels for the translation of my thesis summary and propositions. Thanks also go to Mayank for organizing the wonderful sports and dinners. Adrian Lara and Ilias, thanks for your time and patience for managing the GS meeting, I got a lot of benefits from it.

I want to thank Prof. Adriaan Beukers, Roger, Jos, Irene, Lisette, Marianne, for your great cooperation during my research. I appreciate the support from the lab technicians, Frans, Lijing, Berthil, Hans, and the staff in the workshop, helping me with your very professional skills.

So many thanks to my Chinese friends, making the life so happy and enjoyable. Many years passed, I still remembered my first night in Delft. My three lovely roommates, Ye, Fengnian, Lei Cheng, I really enjoyed the time we spend in our department, starting our new life in the Netherlands, travelling to new places, cooking together. My thanks also go to Pan, Jing, Xiangrong and Ke for your companion in Delft. Thanks for your invitation, Huajie and Lu, I love your Shanxi noodles so much. Ping and Yan, I met so many friends in your department in 'Professor' street. Moreover I cannot forget the happy time with Chongxin, Lei Zu, Hao Cui, Xiaoyu, Mo Li, Lingfeng, Wandong, Tian, having parties in the 'Doctor' Building or the BBQ around Delft Lake. Your friendship is a treasure in my whole life.

My last but not least thank goes to my family. Thanks for the understanding and support from my parents, grandparents, every time I feel so warm and relaxed talking with you. My lovely cousins, I was so happy with you during my holidays in China. My deepest love goes to my girlfriend Weiwei, so lucky that I met you here. We both like the nature and travelling. Now we have so many ideas for the decoration of our new house. My thanks also go to Liying and Hans for your taking care of me as one of your family member, so appreciated.

About the Author

Lei Shi was born on September 15, 1984, in Zhangjiagang, Jiangsu province, China. In 2003, after graduating from the high school, he entered the Faculty of Mechanical Engineering in the Northwestern Polytechnical University in Xi'an, China. He got this Bachelor degree of Aircraft Manufacturing Engineering in 2007. After that, he continued his master study in the same faculty under the supervision of Prof. Gengzheng Sun and Prof.Zhongqi Wang, on the topic "Technology of mold design for composite forming processes" which was aimed to reduce the thermal deformations of the large sandwich-structural composite products. He got his Master Degree of Aeronautical and Astronautical Manufacturing Engineering on March 2010. In September 2010, he was invited by Dr.ir. H.E.N. Bersee to the Netherlands and started his PhD research in TU Delft, which was funded by the Chinese Scholarship Council (CSC). Then he worked with the composite materials in the Faculty of Aerospace Engineering, Design and Production of Composite Structures (DPCS) group, currently the Structural Integrity & Composites (SI&C) group. Under the supervision of promotor Prof.dr.ir. R. Benedictus and copromotor Prof.dr.ir. K.M.B. Jansen, he finished his PhD research on "Heat transfer in the thick thermoset composites". The results of this work are presented in this thesis.